

DISSERTATION

CHROMATIN ORGANIZATION AS A POSSIBLE FACTOR IN THE CONTROL OF
SUSCEPTIBILITY TO RADIATION-INDUCED AML IN MICE

Submitted by

David G. Maranon

Department of Environmental and Radiological Health Sciences

In partial fulfillment of the requirements

For the degree of Doctor of Philosophy

Colorado State University

Fort Collins, Colorado

Fall 2010

Doctoral Committee

Department Head: Jac A. Nickoloff

Advisor: Joel S. Bedford

Susan Bailey

Michael Weil

Jonathan Carlson

Copyright by David Gustavo Maranon 2010
All Rights Reserved

ABSTRACT

CHROMATIN ORGANIZATION AS A POSSIBLE FACTOR IN THE CONTROL OF SUSCEPTIBILITY TO RADIATION-INDUCED AML IN MICE

The studies described in this dissertation involve the use and comparison of two mouse strains: one sensitive (CBA/CaJ) and another resistant (C57BL/6J) to radiation-induced acute myeloid leukemia (AML).

The purpose of these studies was to identify factors that may account for the large difference in the susceptibility of these strains to radiation-induced AML. Both have a near-zero lifetime spontaneous incidence of AML. The CBA/CaJ mice display a radiation dose dependent increase in AML incidence while C57BL/6J mice do not develop AML after any radiation dose.

Deletion of a specific region, known as the minimal deleted region (mdr), of mouse chromosome 2 containing the *PU.1* gene is a virtual requirement for development of AML. Additionally, there are two regions surrounding the mdr, which contain grouped breakpoints defining large breakpoint clusters.

The breakpoint cluster in the proximal region is 10 Mb while the cluster in the distal region is 3 Mb of length. Most of the breakpoints surrounding the *PU.1* deletions occur in these regions.

Murine strains susceptible to radiation-induced AML show about a two-fold hypersensitivity of mouse chromosome 2 relative to chromosomes 1 or 3, whereas in the resistant mouse strains; chromosomes 1, 2, and 3 are similar in radiosensitivity. Differences in global DNA repair processes cannot explain this chromosomal hypersensitivity.

Possible explanations include differences in the interphase structure, geometry or organization of chromosome 2 in the different strains.

The present study was initiated to determine whether the distances between breakpoint clusters on chromosome 2 are in closer proximity in the bone marrow cells of the CBA/CaJ mouse strain than in the C57BL/6J strain which could explain the differences mentioned above. Bacterial artificial chromosomes (BACs) were selected as markers of the central portion of the proximal and distal deletion breakpoint clusters as well as *mdr* on chromosome 2, where the preponderance of breaks occurs. Distance measurements were made by three dimensional fluorescent in situ hybridization (3D-FISH) image analysis of hundreds of cells using Metamorph and ImageJ for data collection and Autoquant software for deconvolution and reconstruction of the three dimensional cell nuclei. Comparing bone marrow cells of CBA/CaJ and C57BL/6J mice, no differences were found between the proximity of the two regions represented for the selected markers compared in both murine strains. Further comparisons were made for other specific cell types. For the markers chosen the distribution of the distances showed similarities between the same cell types from both mouse strains; namely, fibroblasts, whole bone marrow (WBM), and hematopoietic stem cells (HSC).

However, there was not found a change in the distance distributions toward the closer distances expected between the clusters in HSC and WBM compared with fibroblasts in both mouse strains.

There was; however, a tissue-dependent distance distribution between the markers. Specifically, the average distances of the clusters in fibroblasts (2.55 μm for CBA/CaJ and 3.09 μm for C57BL/6) were larger than the distance in blood cells (1.74 μm in BM and 1.53 μm in HSC for CBA/CaJ; and 1.79 μm in BM and 1.77 μm in HSC for C57BL/6).

This tissue-dependency is consistent with the concept of tissue predisposition to certain kind of cancers, in which, for instance blood cells contain specific characteristics or nuclear organization not present in fibroblasts that could lead to AML.

Although the hypothesis that closer interphase proximity of chromosome 2 *PU.1* deletion breakpoints in CBA/CaJ versus C57BL/6J mice was not upheld, a very interesting observation has emerged. The distance between breakpoint markers and the whole organization of the chromosome 2 homologs was different within each cell defining a small domain and a large domain with short and long distances respectively between the markers. This was true not only for bone marrow but for hematopoietic stem cells and fibroblasts of both strains.

This observation of a difference in chromosome 2 domain sizes for the two homologs within each individual cell led to the question whether the *PU.1* deletion that appears many months later in AML cells might have occurred preferentially or systematically in the small or large domain of the original radiation-initiated cell.

Using AML cells from actual radiation-induced tumors, the measurements done within the intact chromosome 2 from these AML samples showed a high proportion of cells with distances between the clusters markers that were similar to the distances seen for the small domain from normal BM cells. Therefore, from our data, deletion of chromosome 2 seemed to occur mainly in a non-random fashion because the PU.1 gene was deleted from the large domain in 8 out of 10 cases in an average proportion of ~74% of the analyzed cells considering all AML cases.

The problem here is that chromosome domains may reorganize during the considerable time and lengthy periods of proliferation involved in the development of an AML. Could the domain organizations develop differently due to the radiation? If there were no such changes it would imply that the AML process resulted in the domain structure differences and not to the initial radiation deletion process. Nevertheless, the deletion in the large domain may suggest that a mechanism through which a preferential deletion is not the result of initial breakpoints proximity resulting from a simple loop formation, but perhaps may be due to the transcriptional activity differences in the two homologs. Such a difference could arise as a result of genomic imprinting.

To explore and test the possible effect of the genomic imprinting on the structure and organization of the chromatin in both small and large domain from mouse chromosome 2, a different mouse model was used that allowed us to differentiate the parental origin of each chromosome 2 inherited after fertilization for the hybrid offspring (F1) obtained from crosses between a C3H/HeNCr1 and Tirano/EiJ mouse strain.

The latter has a Robertsonian translocation that involved chromosome 2 and 8, which allows tracking of a paternal or maternal copy of chromosome 2 in the F1 mice.

Although such a CBA strain was not available, the C3H mouse strain is similarly sensitive to AML induction after radiation treatment, and chromosome 2 in this mouse model is hyper-radiosensitive as well. Then, if the small or closed and large or open configuration of the chromatin that was observed in the interphase is due to the genomic imprinting, we should be able to determine its parental origin. Thus, the expected result was to observe that the most active copy of chromosome 2 would show an open conformation; therefore, a high proportion would be expected to be associated with the large domain. Conversely, the transcription of the less active copy of chromosome 2 should be more silenced and have a closed or more condensed conformation of the chromatin. In other words, a high proportion might be expected to be associated with small domains. In addition, the high proportion of either small or large domain has to be present in either copy of chromosome 2, maternal or paternal, but not in both.

The question was whether the small or large domain conformation of the chromatin is influenced by the parental origin of chromosome 2 or whether it is a random event.

The experimental data did not show evidence of any influence in the chromosomal domain conformation in relation to the genomic imprinting occurring in mouse chromosome 2. No difference was seen for the maternal and paternal copies of chromosome 2 within interphase cells. All chromosome 2 domains from C3H/HeNCR1 showed breakpoint clusters distances and organization of the domains similar to the small domain in both maternal and paternal copies.

Therefore, it was concluded that the suggested preferential deletion of the large domain does not seem to be influenced by genomic imprinting. However, one explanation discussed for the observed frequency was that the fusion of chromosomes 2 and 8 in the Tirano mice might alter the imprinting pattern on the attached chromosome 2, and consequently, the whole organization within the nuclei.

In summary, a clear difference in the chromatin organization in both chromosome 2 homolog domains was observed in interphase cells; where the different distances of the breakpoint clusters is associated to the different organization of the homologs. In addition, the description and classification of the chromosomal territories as small and large domain is a feature that could be used for future research. The bimodal distribution of the distances showed closer distances of the breakpoint clusters within the small domain compared to the large domain suggesting the probability to be consider as the region involved in the rearrangement that lead to the deletion. The distance between the clusters is important because the only way an interstitial deletion can occur is by having a close proximity of the breakpoint clusters to allow for interaction between them. A different conformation of the chromatin could explain the deletion in only one homolog but not in the other homolog; the utilization of the small and large domain could give some clues if the domains are analyzed short after irradiation to accurately determine whether there is any preferential deletion of small or large domain or not. It remains to be seen whether analysis of the nuclear matrix and the matrix attachment region could be involved in the different conformation of the chromatin within both the small and large domain.

The possibility of a dynamic reorganization of the chromatin in radiation-induced AML samples is a question that remains to be answered. The analysis of BM samples right after irradiation would either confirm or reject the observation that showed higher proportion of cells with the large domain deleted.

The complex interaction between the bone marrow and HSCs and the response to ionizing radiation is key to identifying the events leading to the development of AML.

Therefore, not only the effect of IR in the HSC (the target cell) but also in the microenvironment (non-target cells) surrounding the HSC are important in understanding the factors and players involved in the onset and establishment of the conditions needed to allow the potentially leukemic cells to appear.

David G. Maranon
Department of Environmental and
Radiological Health Sciences
Colorado State University
Fort Collins, CO 80523
Fall 2010

ACKNOWLEDGEMENT

This is the final section of my dissertation that I am taking care of, and it is amazing thinking back; and remembering many people who was behind all this work in both sense professional and personally taking care of me and my work; I am always surprised and consider myself so lucky of having all these people crossing the path of my life.

First, I want to acknowledge my mom, who is always with me, in my heart and in every step I make. She is in everything I made, in every thing I built, She made the person I am. And I know she is taking care of me in each moment good and bad she is here; with me.

Always, there is a mixture of feelings and sensation that come across many different thoughts but definitely when things in my life were really bad; one person, my mentor, my friend, a second mother to me, who always pursued my success in life and in science, She taught me that it is still possible to believe in people and that there are still people who wants to do the right things for other people. All this work is dedicated to the memory of Dr Maria Muhlmann, my mentor; my friend and responsible for my experience here in USA and for finishing my whole PH.D. Thank you.

Extraordinary people makes life a better experience and by extension work with extraordinary people in science makes sciences the most exciting experience of all. I

want to thank Dr Joel Bedford, an extraordinary scientist, with a huge passion for science that represent for me the personification of how a real scientist must be.

Meeting people here at CSU was an enrichment experience sometimes, and of course, I could never forget one of the kindest person I ever met. To me she is the person who takes the next step in my career for being a scientist ... Always there when I needed to show a good FISH picture... Dr Susan Bailey, thank you for being there every time I needed. I really expect to work with you during my next steps of my scientific life.

Day to day life in the lab sometimes is miserable, even more when you face some failure with most of the experiments, it feels like it is 99.9% of failure and only 0.01% of success when you start working in optimizing protocols, running experiments....but, of course, lab mates are the right people to make that balance to change to the opposite side, that is why I feel really lucky to met and work with Dr Jennifer Devitt, my lab mate and my coffee partner. She has been always involved with my project, specially by being my personal editor for the most part of my dissertation.

I want to acknowledge to the most important support in my life: my family; and specially the person who is key in supporting me in all situations, supporting me in my depressions and worst moments ... always there, Noelia, my partner in the path of life. She was an important part of this whole project since she was a huge help in analyzing and processing of data and hours of science talks about hypothesis, analysis and results of the project.

As an imminent thought to the future, my kids, Franco and Abril, who are my little shinny treasures...facing sometimes my lack of time to expend with them for my

crazy obsession with science... I dedicate all my efforts to them, and hopefully in a near future I could be their guidance and help them to make a better future for them and for future generations.

Finally, I want to dedicate this work to all the people that died fighting to make a better reality, a better future for all the people without having any personal interest other than help and make the right things in a world where every thing seems to be wrong and unfair.

Dedicated to the Memory of My Mom...and Maria.

I miss you.

TABLE OF CONTENTS

Page

CHAPTER I

GENERAL INTRODUCTION. 1

1.1: Carcinogenic Effects of Ionizing Radiation in Human Populations 1

1.2: Radiation-Induced AML in Mouse Models 3

1.3: Features of the Nuclear Organization and Chromatin Structure that May
 Influence Radiation Response 7

REFERENCES. 13

CHAPTER II

**COMPARISON OF DISTANCES BETWEEN THE BREAKPOINT
CLUSTER REGIONS ASSOCIATED WITH THE RADIATION-
INDUCED DELETIONS IN CHROMOSOME 2 IN INTERPHASE
BONE MARROW FROM MICE THAT ARE SENSITIVE OR
RESISTANT TO RADIATION-INDUCED AML.**

Introduction

2.1-Radiation-induced AML: Molecular and Cytogenetic features. 18

2.2-Hypothesis. 24

2.3-Specific Aims. 24

2.4-Experimental Approach. 25

2.5-Materials and Methods. 26

 2.5.1: Mice

2.5.2: Cells	
2.5.3: BAC-clones	
2.5.4: Fluorescence in situ Hybridization	
2.5.5: Microscopy	
2.5.6: Determination of clusters proximity: criterion of proximity	
2.6-Results	
2.6.1-Measurements of Distances.	32
2.6.2-Breakpoint Cluster Distances Measurements in Fibroblasts:	
CBA/CaJ vs C57BL/6J Mouse Strains.	34
2.6.3-Breakpoint Cluster Distances Measurements in Bone Marrow:	
CBA/CaJ vs C57BL/6J Mouse Strains.	37
2.6.4-Breakpoint Cluster Distances Measurements in Hematopoietic	
Stem Cells (CD117 positive cells): CBA/CaJ vs C57BL/6J	
Mouse Strains.	40
2.7-Discussion.	41
2.8-Conclusions.	51
REFERENCES.	53

CHAPTER III

THE ORGANIZATION OF MOUSE CHROMOSOME 2: INTERPHASE CELL DOMAINS.

Introduction	
3.1-Chromosome Domains Organization.	57
3.2-Hypothesis.	64
3.3-Specific Aims.	64
3.4-Results	
3.4.1-Chromosomal Territories: Features of Chromosome 2 Domains in	
Interphase Cells.. . . .	65

Determination of Distances within Small and Large Domains	
3.4.2-Chromosomal Territories: Features of Chromosome 2 Domains in Fibroblasts, BM and Stem Cells from CBA/CaJ and C57BL/6J.	67
3.4.3-Normalization Values of Small and Large Domain Ratio of Distance Values for Large vs Small Domains.	68
3.4.4-Breakpoint Cluster Distances Measurements in Fibroblasts CBA/CaJ vs C57BL/6J.	73
3.4.5 Breakpoint Cluster Distances Measurements in Bone Marrow CBA/CaJ vs C57BL/6J.	76
3.4.6-Breakpoint Cluster Distances in Hematopoietic Stem Cells (HSC) CBA/CaJ vs C57BL/6J.	80
3.5-Discussion.	82
3.6-Conclusions.	86
REFERENCES.	87

CHAPTER IV

CYTOGENETIC ANALYSIS OF INTERPHASE CELLS FROM RADIATION-INDUCED AML CASES WITH LOSS OF PU.1 THROUGH 3D-FISH.

Introduction	
4.1-Background	89
4.2-Hypothesis	90
4.3-Specific Aims	91
4.4-Experimental Approach	92
4.5-Materials and Methods.	94
4.5.1-Mice and Treatment	
4.5.2-Cells	

4.5.3-Bacteria Artificial Chromosome Clones and Fluorescence In Situ Hybridization	
4.6-Results	
4.6.1-Chromosomal Domains and BAC-Markers Organization.	95
4.6.2-Chromosomal Domain Preferentially Deleted.	106
4.7-Discussion	
4.7.1-Interphase Cells: Dominant deleted cells in each sample cells . . .	113
4.7.2-Domain Preferentially Deleted (Revisited)	116
4.8-Conclusions	118
REFERENCES	120

CHAPTER V

GENETIC ANALYSIS OF THE GENOMIC IMPRINTING INFLUENCE AS POSSIBLE EXPLANATION FOR THE DELETION OF ONE COPY OF PU.1 AFTER IONIZING RADIATION

5.1-Introduction	
5.1.1-Analogies Between Mouse Chromosome 2 and X-chromosome	123
5.1.2-Genomic Imprinting.	125
5.2-Hypothesis	129
5.3-Specific Aims.	129
5.4-Experimental Approach	132
5.5-Materials and Methods	137
5.5.1-Mice	
5.5.2-Cells	
5.5.3-BAC-clones, FISH, and Image Acquisition	
5.6-Results	140

5.7-Discussion	145
5.8-Conclusions	148
REFERENCES	149

CHAPTER VI

GENERAL DISCUSSION AND CONCLUSIONS

6.1-Deletions and Breakpoint Clusters Distance Measurements	152
6.2-Chromatin Conformation	158
6.3-Epigenetic Changes Occurred After Ionizing Radiation	166
6.4-The Role of apoptosis in Radiation-Induced AML Mouse Models Implications in Radiation Sensitivity	168
6.5-Microenvironment, Target Cells, and Radiation Exposure.	170
6.6-A Model of Events Leading to Radiation-induced AML	176
6.7-General Conclusions	181
REFERENCES	184

APPENDIXES

SUPPLEMENTARY INFORMATION

I-Measurements of breakpoint cluster distances	190
I.1-Fibroblasts	
I.2-Bone Marrow	
I.3-Hematopoietic Stem Cells	
I.4-Normalization Values for Small and Large domains	
II-Radiation-induced AML (Spleen Samples) analysis	199
III-Genomic Imprinting (Tirano Project)	208

CHAPTER I

GENERAL INTRODUCTION

1.1-Carcinogenic Effects of Ionizing Radiation in Human Populations

Numerous reports during the first half of the 20th century repeatedly pointed to a strong association between ionizing radiation (IR) exposure and an increased incidence of various cancers⁽¹⁾. Interestingly, these early reports related to observations in humans or human populations, rather than in surrogate animal systems. Exposures largely involved individuals who used x-ray machines or radioactivity in their occupations, or people who were exposed in connection with medical diagnosis or treatment.

After World War 2 and the dawn of the age of atomic energy, a large comprehensive epidemiological project was undertaken to study the relationship between radiation dose and the incidence of cancers in the survivors of the atomic bombings of Hiroshima and Nagasaki in August of 1945^(2,3).

Myeloid leukemia, especially acute myeloid leukemia (AML), was one of the major cancers for which a striking dose-dependent increase was seen among the exposed survivors. This cancer predominated in the earlier years of the study, with the increased incidence reaching a peak at around 5 to 7 years after the bombings.

While the total lifetime excess incidence of other cancers such as thyroid, breast, lung, and bone were eventually seen to be greater than for these leukemias, AML still added a significant contribution to radiation induced cancers, and the disease occurs much earlier after exposure.

More recent combined epidemiological studies of cancer incidence among nuclear radiation workers from several countries including the USA, Canada, and several European countries have added a large population base and involved more individuals in the lower dose category, and these data largely agree with projections from the A-bomb survivor study, but truly adequate epidemiological data are not available that would resolve the issues of major concern regarding quantitative risks of low dose or low dose rate radiation exposure^(4,5).

Further, it seems unlikely that the enormous numbers of humans with precisely known doses will ever become available to directly settle the issues with adequate statistical resolution.

The alternative approach is to address problems that lead to a better understanding of the basic process involved.

Studies along these lines have aimed at understanding purely molecular processes and pathways, as well as cellular and tissue factors known to be associated at least indirectly with carcinogenesis.

However, clear connections between cellular and molecular effects likely to be involved in the actual carcinogenic process initiated by ionizing radiation is not yet available.

1.2-Radiation-Induced AML in Mouse Models

Mouse models of radiation leukemogenesis are perhaps the most relevant systems to date that may help satisfy the need to bridge molecular, chromosomal, cellular, and tissue factors leading to the development of AML. These share some important features with human radiation-induced AML. Use of these mouse model systems are aimed at identification of the role of some of the various steps in the processes leading to AML after irradiation and how they quantitatively influence the eventual expression of the disease in humans as a function of radiation dose, dose-rate, and radiation quality.

Brother-sister mating over many generations result in mouse strains that are homozygous at every genetic locus, and development of different strains that have different susceptibilities to radiation-induced cancers facilitate further genetic analyses of loci conferring or contributing to the various susceptibility phenotypes. The differences in susceptibilities among these strains can be vast, and are correspondingly important for dissecting the important genetically controlled processes involved.

The studies described in this dissertation involve the use and comparison of two mouse strains; CBA/Ca, and C57BL/6. Both have a near-zero lifetime spontaneous incidence of AML.

The CBA/Ca strain shows a dose dependent increase in AML incidence where up to 20 to 30% of these mice have been reported to develop AML after x-or gamma-ray doses of 3 Gy^(6,7). The C57BL/6 strain do not develop AML after any radiation dose, though they do develop some other tumors⁽⁸⁾.

Strains sharing a susceptibility to radiation induced AML include CBA/H, C3H⁽⁹⁾, SJL⁽¹⁰⁾, RFM⁽¹¹⁾, and BALB/c⁽¹²⁾, while no radiation induced AML has been documented in C57BL/6, NON, NOD, A, AKR, or DBA/2 strains⁽¹³⁾.

While a defect associated with the non-homologous end joining (NHEJ) of DNA double-strand breaks has been identified in BALB/c mice^(14,15) (a polymorphism in the *Prkdc* gene), no similar genetic defects in DNA repair systems have been reported for the other AML susceptible strains. The BALB/c strain is also more sensitive to induction of breast cancer by radiation^(16,17), and is more radiosensitive with respect to radiation-induced hematopoietic death than many other strains, especially following low dose-rate irradiation⁽¹⁸⁾.

With time after gamma-irradiation of CBA and C57BL/6 mice, Peng and co-workers in this laboratory followed the frequency of bone marrow cells with a deletion of a region of chromosome 2 containing the *PU.1* gene and in summary, found the following⁽¹⁹⁾:

- 1) Although neither mouse strain develops AML spontaneously, without any radiation about 1% of bone marrow cells of both mouse strains show loss of the *PU.1* gene region, as measured by loss of hybridization of a fluorescent labeled 237 kb BAC containing the gene.
- 2) At 24 hours after irradiation there was a dose-dependent increase in the frequency of cells with *PU.1* loss and the induced loss per unit dose was about twice as high for CBA than C57BL/6 mice (about 4% induced after 3 Gy gamma rays for CBA, and about 2% induced after the same dose for C57BL/6 mice).

One month later, the frequency of cells with *PU.1* loss after 3 Gy was 8% for CBA bone marrow, nearly double the value at 1 day, while for the 3 Gy irradiated C57BL/6 bone marrow the frequency had returned to background levels. In the same communication, which involved a collaboration with Bouffler and his colleagues at Harwell in England the results of independent tracking of the frequency of cells with *PU.1* loss showed a similar pattern, both for spontaneous levels and levels with time in the two strains after irradiation.

One possible explanation for these observations would be that there was a strong selection against the cells with radiation induced (but not spontaneous) *PU.1* deletions in the C57BL/6 mice during the one month period of repopulation of the depleted bone marrow, but an actual growth advantage of the cells with radiation induced (but not spontaneous) *PU.1* loss in the CBA mice.

No remarkable differences in gross radiation sensitivity measured by differences in LD50 or in cell killing between the CBA versus the C57BL/6 strains have been documented. It is known, however, that a deletion of a region of mouse chromosome 2 containing the *PU.1* is a virtual requirement for development of AML⁽²⁰⁻²⁴⁾, and the breakpoints surrounding the deletions cluster in two regions^(25,26). Further, evidence has been reported showing a differential chromosomal hypersensitivity to radiation of mouse chromosome 2 relative to chromosomes 1 or 3 in the AML sensitive vs. the resistant mouse strains^(13,27).

It is also known that in about 87% of tumors that eventually develop, a point mutation in the DNA binding domain of the protein is found in the other allele of *PU.1*.

In some 86% of these the mutation altered a single CpG suggesting a deamination of dC as the origin of the mutation⁽²⁸⁾. Mutation affecting the arginine 235 (Arg235) residue in the protein that is usually involved in these cases is essential for DNA binding by the protein⁽²⁹⁾.

Another interesting finding from the investigators at Harwell is the mapping of the breakpoints of the deletions in chromosome 2 in CBA mice. Silver and Finnon and their colleagues have reported a non-random clustering of breakpoints located proximal and distal to the centromere surrounding the region containing the *PU.1* gene^(26,27). The *PU.1* gene lies within a 1 Mbp region of chromosome 2 located at around 50 centiMorgan (cM) on the genetic map, or around 91 Mbp from the centromere. The proximal breakpoint cluster lies within a 10 Mbp region between about 29 cM and 39 cM on the genetic map, and the distal cluster within a 3 Mbp region at around 55 cM on the genetic map. The physical distance, in Mbp, between the breakpoint clusters ranges up to about 60 Mbp.

In view of the hypersensitivity of chromosome 2 relative to chromosomes 1 and 3 in mice susceptible to radiation-induced AML, with no such differential sensitivity for mouse strains that are not susceptible, and in light of the clustering of the breakpoints around the *PU.1* deletion on chromosome 2 observed for radiation induced AMLs, it was thought one possibility to explain this would involve features of the interphase structure, geometry or organization of chromosome 2. Further, this might differ in ways that could possibly account for the difference in sensitivity of the different mouse strains to radiation induced AML.

1.3-Features of the Nuclear Organization and Chromatin Structure that May Influence Radiation Response

Chromosome organization within the nucleus as well as the chromatin structure and transcriptional activity are known to affect radiation-induced chromosomal rearrangements, including deletions, inversions and translocations.

With regard to transcriptional activity, for example, Barrios and colleagues, and Holmquist reported that radiation induced translocation breakpoints occur predominantly in G-light band regions^(30,31), where labeled cDNA predominantly hybridizes⁽³²⁾, and Muhlmann-Diaz and colleagues showed both that the frequency of radiation induced translocations between autosomes and supernumerary inactive X-chromosomes of cells from Klinefelter's syndrome variants was much lower than that observed between autosomes and active X chromosomes⁽³³⁾.

She also found differences involving other chromosomes known to differ in transcriptional activity⁽³⁴⁾. Regarding deletions, she found that an artificial mosquito chromosome consisting of an amplified plasmid containing a gene conferring resistance to hygromycin⁽³⁵⁾, and which was very active or potentially active as judged by its sensitivity to attack by DNaseI, was 3-to 4-fold more sensitive to radiation induced interstitial deletions than the less active mosquito chromosomes^(36,37).

Finally, another example that was a key observation for the work described in this dissertation was made by Nikiforova and colleagues in connection with a radiation-induced inversion that can bring the H4 and RET genes on human chromosome 10 into juxtaposition and can result in thyroid cancer⁽³⁸⁾.

They found that the breakpoints involving H4 and RET were in much closer proximity to each other in the interphase nuclei of thyroid cells than expected based on their 30 Mb physical distance between them, and they did not see this close proximity in breast epithelial cells. The reason this may result in a greater radiosensitivity for the production of such an inversion stems from the fact that:

- 1) Two breaks within the chromosome are required to produce an inversion, an interstitial deletion or any exchange between or within a chromosome, and
- 2) to the extent that the regions where breaks must occur are to produce the desired rearrangement are very close together, there is a much higher probability that both breaks can be produced by the same electron track (dose from x- or gamma-rays is delivered along electron tracks), and a correspondingly greater chance the rearrangement rather than a simple restitution of the two breaks, whereas if the break regions are much further apart it is more likely that the breaks will require breakage by two independent electron tracks, and more importantly the greater distance decreases the chance that the breaks can interact and mis-rejoin to form the rearrangement, in this case the inversion.

Transcriptional activity⁽³⁹⁻⁴⁷⁾ or gene expression is well known to be associated with nuclear architecture a chromatin positioning within the interphase nucleus. An interesting example is provided by human chromosomes 18 and 19. Both chromosomes have almost the same amount of DNA, however, the gene-poor chromosome 18 is located toward the periphery and the gene-rich chromosome 19 is typically located toward the nuclear interior⁽⁴⁵⁾.

Folle 1998 showed that chromatin from G-light bands were more prone to radiation damage than heterochromatin. According to this study after treatment with different agents such as DNase I, gamma-rays and restriction enzymes the distribution of breakpoints were preferentially found in euchromatic region compared to heterochromatic region. So, it seems reasonable that nuclear organization, will have an important influence on the frequency and location of the breakpoints of particular chromosomal rearrangements within the normal cell nucleus.

From the information outlined regarding the differences in susceptibility of different mouse strains to radiation-induced AML and factors pertaining to the involvement of chromosome 2 deletions, as well as our knowledge of how chromatin structure has actually been shown to affect radiation responses, the following general hypothesis was formulated. Corollaries associated with the general hypothesis or proposition can be tested by four specific aims.

“The architectural features of the interphase nuclei from mouse bone marrow cells show a unique chromatin organization that could contribute to the conditions needed to produce the deletions necessary (but not sufficient) for the development of radiation-induced AML in these AML-susceptible mouse models. Conversely the chromatin organization facilitating the necessary radiation induced deletions in chromosome 2 will be less favorable to the formation of the deletions in AML resistant mice and/or in tissues other than bone marrow.”

The approach to examining and testing aspects of the general hypothesis is, first, to determine whether the proximal and distal breakpoint regions surrounding the *PU.1* gene on chromosome 2 are closer together in bone marrow interphase nuclei in susceptible CBA/CaJ mice than in C57BL/6 mice and/or closer than expected in cells from other tissues.

Preliminary data already suggests that there is closer proximity in the domain of one chromosome 2 homolog in CBA/CaJ bone marrow cells than in the other, therefore:

1. The first aim is to measure interphase distances between the proximal and distal breakpoint cluster region probes within chromosome 2 of CBA/CaJ vs C57BL/6 bone marrow cells, and the distances in nuclei of fibroblast cells as well.
2. The second aim is to determine quantitatively whether the different organization of both chromosome 2 domain in interphase cells can be demonstrated. Previous observations showed a short distance between the breakpoint clusters in one domain but a larger distance within the other domain in the same cell. Therefore, quantitative demonstration of a bimodal distribution of the distances will support the existence of a differential organization of the two homologs in interphase cell. Initial experiments have shown closer proximity of the breakpoint cluster region probes within the smaller chromosomal domain. Considering preliminary result indicating a different size of chromosome 2 domains: it was named: small domain to the domain presenting short distances of the markers and large domain to the domain presenting the large distances between the breakpoint cluster markers.

3. The Third aim is to determine whether the *PU.1* deletion, seen in virtually all AML cells in mice which have developed AML after irradiation, occurs predominantly in one of the chromosome 2 domain. The initial experiments have shown to display closer proximity of the breakpoint cluster region probes (within the smaller chromosomal domain).

4. The fourth aim is to measure the chromosome 2 domain sizes and compare maternal versus paternal copies chromosome 2. This would use an entirely different mouse model, namely, F1 hybrid offspring of crosses between C3H/HeNCrl mice and a Tirano/EiJ sub-strain Rb(2.8)2Lub; which carries a Robertsonian translocation between chromosomes 2 and 8, to allow identification of maternal or paternal copies of chromosome 2 in the heterozygotes depending on the matings. The idea behind this experiment is to detect whether the small and large domains are influenced by the genomic imprinted inherited in the maternal and paternal copy of chromosome 2.

The experimental approaches for each of the above specific aims are outlined below with the following headings:

Chapter II (Comparison of distances between the breakpoint cluster regions associated with the radiation-induced deletions in chromosome 2 in interphase bone marrow cells from mice that are sensitive or resistant to radiation-induced AML); Chapter III (The organization of mouse chromosome 2: Interphase cell domains); Chapter IV (Cytogenetic analysis of interphase cells from radiation-induced AML with loss of PU.1 through 3D-

FISH); and finally, Chapter V (Genetic analysis of the genomic imprinting influence as possible explanation for the deletion of one copy of PU.1 after IR), with “sub-hypotheses” stated within the narrower focus areas of the general hypothesis. Further points involving particularly pertinent background material and rationale are also included regarding the experimental approach as parts of each chapter.

References:

- [1] A. Upton, "Cancer research 1964: Thoughts on the contributions of radiation biology," *Cancer research*, Jan 1964.
- [2] D. Pierce and D. Preston, "Radiation-related cancer risks at low doses among atomic bomb survivors," *Radiation Research*, vol. 154, no. 2, pp. 178–186, 2000.
- [3] D. Preston, D. Pierce, Y. Shimizu, H. Cullings, S. Fujita, S. Funamoto, and K. Kodama, "Effect of recent changes in atomic bomb survivor dosimetry on cancer mortality risk estimates," *Radiation Research*, vol. 162, no. 4, pp. 377–389, 2004.
- [4] E. Cardis, M. Vrijheid, M. Blettner, E. Gilbert, M. Hakama, C. Hill, G. Howe, J. Kaldor, C. Muirhead, and M. Schubauer-Berigan, "Risk of cancer after low doses of ionising radiation: retrospective cohort study in 15 countries," *British Medical Journal*, vol. 331, no. 7508, p. 77, 2005.
- [5] E. Cardis, M. Vrijheid, M. Blettner, E. Gilbert, M. Hakama, C. Hill, G. Howe, J. Kaldor, C. Muirhead, and M. Schubauer-Berigan, "The 15-country collaborative study of cancer risk among radiation workers in the nuclear industry: estimates of radiation-related cancer risks," *Radiation Research*, vol. 167, no. 4, pp. 396–416, 2007.
- [6] I. Major and R. Mole, "Myeloid leukaemia in x-ray irradiated cba mice," *Nature*, vol 272, pp.455-456, March 1978.
- [7] R. Mole and D. Papworth, "The dose-response for x-ray induction of myeloid leukaemia in male cba/h mice.," *British Journal of Cancer*, vol. 47, no. 2, p. 285, 1983.
- [8] J. Storer, T. Mitchell, and R. Fry, "Extrapolation of the relative risk of radiogenic neoplasms across mouse strains and to man," *Radiation Research*, vol. 114, no. 2, pp. 331–353, 1988.
- [9] I. Hayata, "Partial deletion of chromosome 2 in radiation-induced myeloid leukemia in mice.," *Progress and Topics in Cytogenetics[PROG. TOP. CYTOGENET.]*. ..., Jan 1984.
- [10] P. Resnitzky, Z. Estrov, and N. Haran-Ghera, "High incidence of acute myeloid leukemia in sjl/j mice after x-irradiation and corticosteroids," *Leukemia Research*, vol. 9, no. 12, pp. 1519–1528, 1985.

- [11] R. Ullrich, M. Jernigan, G. Cosgrove, L. Satterfield, N. Bowles, and J. Storer, "The influence of dose and dose rate on the incidence of neoplastic disease in rfm mice after neutron irradiation," *Radiation Research*, vol. 68, no. 1, pp. 115–131, 1976.
- [12] R. Mole, "Radiation-induced acute myeloid leukemia in the mouse: experimental observations in vivo ...," *Leukemia Research*, Jan 1986.
- [13] F. Darakhshan, C. Badie, J. Moody, M. Coster, R. Finnon, P. Finnon, A. A. Edwards, M. Szluinska, C. J. Skidmore, K. Yoshida, R. Ullrich, R. Cox, and S. D. Bouffler, "Evidence for complex multigenic inheritance of radiation aml susceptibility in mice revealed using a surrogate phenotypic assay," *Carcinogenesis*, vol. 27, pp. 311–8, Feb 2006.
- [14] R. Okayasu, K. Suetomi, Y. Yu, A. Silver, and J. Bedford, "A deficiency in dna repair and dna-pkcs expression in the radiosensitive balb/c ...," *Cancer research*, Jan 2000.
- [15] Y. Yu, R. Okayasu, M. Weil, A. Silver, and M. McCarthy, "... polymorphism of the prkdc (dna-dependent protein kinase catalytic subunit) gene," *Cancer research*, Jan 2001.
- [16] R. Ullrich, "Tumor induction in balb/c female mice after fission neutron or gamma-irradiation," *Radiation Research*, Jan 1983.
- [17] R. Ullrich and R. Preston, "Radiation induced mammary cancer," *Journal of Radiation Research*, Jan 1991.
- [18] R. Kallman and G. Silini, "... : I. kinetic aspects and the relationship with conditioning dose in c57bl ...," *Radiation Research*, Jan 1964.
- [19] Y. Peng, N. Brown, R. Finnon, C. Warner, X. Liu, P. Genik, M. Callan, F. Ray, T. Borak, and C. Badie, "Radiation leukemogenesis in mice: Loss of *PU.1* on chromosome 2 in cba and C57BL/6 mice after irradiation with 1 gev/nucleon ⁵⁶Fe ions, x-rays or gamma-rays. part i. experimental observations," *Radiation Research*, vol. 171, no. 4, pp. 474–483, 2009.
- [20] A. Silver, W. Masson, J. Adam, G. Breckon, R. Cox, and E. Wright, "Chromosome-2 encoded genes in radiation-induced murine acute myeloid-leukemia," Jan 1988.
- [21] G. Breckon, D. Papworth, and R. Cox, "Murine radiation myeloid leukaemogenesis: A possible role for radiation-sensitive sites on chromosome 2," *Genes*, Jan 1991.

- [22] G. Breckon, A. Silver, and R. Cox, "Radiation-induced chromosome 2 breakage and the initiation of murine radiation acute myeloid leukaemogenesis," *Journal of Radiation Research*, Jan 1991.
- [23] S. D. Bouffler, G. Breckon, and R. Cox, "Chromosomal mechanisms in murine radiation acute myeloid leukaemogenesis," *Carcinogenesis*, vol. 17, pp. 655–9, Apr 1996.
- [24] K. Rithidech, V. Bond, E. Cronkite, and M. Thompson, "A specific chromosomal deletion in murine leukemic cells induced by radiation with different qualities," *Experimental Hematology*, vol. 21, pp. 427-431, Mar 1993.
- [25] A. Silver, J. Moody, R. Dunford, D. Clark, and S. Ganz, "... localizes a putative tumor suppressor gene to a 1.0 cm region homologous to human chromosome segment ...," *Genes Chromosomes and Cancer*, Jan 1999.
- [26] R. Finnon, J. Moody, E. Meijne, J. Haines, D. Clark, A. Edwards, R. Cox, and A. Silver, "A major breakpoint cluster domain in murine radiation-induced acute myeloid leukemia," *MOLECULAR CARCINOGENESIS*, vol. 34, pp. 64–71, Jun 2002.
- [27] S. D. Bouffler, E. I. Meijne, D. J. Morris, and D. Papworth, "Chromosome 2 hypersensitivity and clonal development in murine radiation acute myeloid leukaemia," *Int J Radiat Biol*, vol. 72, pp. 181–9, Aug 1997.
- [28] W. D. Cook, B. J. McCaw, C. Herring, D. L. John, S. J. Foote, S. L. Nutt, and J. M. Adams, "PU.1 is a suppressor of myeloid leukemia, inactivated in mice by gene deletion and mutation of its dna binding domain," *Blood*, vol. 104, pp. 3437–44, Dec 2004.
- [29] R. Kodandapani, F. Pio, C. Ni, G. Piccialli, and M. Klemsz, "A new pattern for helix-turn-helix recognition revealed by the pu. 1 ets-domain-dna complex," *Nature*, Jan 1996.
- [30] L. Barrios, R. Miró, M. Caballin, and C. Fuster, "Cytogenetic effects of radiotherapy breakpoint distribution in induced chromosome aberrations," *Cancer Genetics and Cytogenetics*, vol. 41, pp. 61-70, Jan 1989.
- [31] G. Holmquist, "Chromosome bands, their chromatin flavors, and their functional features," *American Journal of Human Genetics*, vol. 51, pp. 17-87, Jan 1992.

- [32] J. Yunis, M. Kuo, and G. Saunders, "Localization of sequences specifying messenger rna to light-staining g-bands of human chromosomes," *Chromosoma*, vol. 61, pp. 335-344, Jan 1977.
- [33] M. Muhlmann-Diaz and J. Bedford, *A comparison of radiation-induced aberrations in human cells involving early and late replicating X chromosomes*. In *Chromosomal Alterations*; ed. Obe, G and Natarajan, AT-Springer Verlag, New York, pp 125-131, 1994.
- [34] M. Muhlmann-Diaz and J. Bedford, "Breakage of human chromosomes 4, 19 and y in G0 cells immediately after ...," *International journal of Radiation Biology*, Jan 1994.
- [35] T. Monroe and M. Muhlmann-Diaz, "Stable transformation of a mosquito cell line results in extraordinarily high copy ...," *Proceedings of the National Academy of Sciences*, Jan 1992.
- [36] M. Muhlmann-Diaz, "Ionizing radiation induced chromosome aberrations and chromatin structure," 1993.
- [37] J. Bedford and M. Muhlmann-Diaz, "Damage selectivity in chromosomes," *In Radiation Research: A Twentieth Century Perspective (W. C. Dewey, M. Edington, R. J. M. Fry, E. J. Hall and G. F. Whitmore, Eds.)*, pp. 212-216, Academic Press, San Diego 1992.
- [38] M. Nikiforova, J. Stringer, R. Blough, M. Medvedovic, J. Fagin, and Y. Nikiforov, "Proximity of chromosomal loci that participate in radiation-induced rearrangements in human cells," *Science*, vol. 290, pp. 138-141, Oct 2000.
- [39] L. Parada, S. Sotiriou, and T. Misteli, "Spatial genome organization," *Experimental Cell Research*, vol. 296, pp. 64-70, Jan 2004.
- [40] H. Neves, C. Ramos, M. da Silva, A. Parreira, and L. Parreira, "The nuclear topography of abl, bcr, pml, and raralpha genes: evidence for gene proximity in specific phases of the cell cycle and stages of hematopoietic differentiation," *Blood*, vol. 93, no. 4, p. 1197, 1999.
- [41] L. Parada, P. McQueen, and P. Munson, "Conservation of relative chromosome positioning in normal and cancer cells," *Current Biology*, vol. 12, pp. 1692-1697, Oct 2002.
- [42] G. Folle, W. Martínez-López, E. Boccardo, and G. Obe, "Localization of chromosome breakpoints: implication of the chromatin structure and nuclear ...," *Mutation Research-Fundamental and Molecular Mechanisms of ...*, Jan 1998.

- [43] W. Martínez-López, G. Folle, G. Obe, and P. Jeppesen, “Chromosome regions enriched in hyperacetylated histone h4 are preferred sites for endonuclease and radiation-induced breakpoints,” *Chromosome Research*, vol. 9, pp. 69-75, Jan 2001.
- [44] N. Mahy, P. Perry, S. Gilchrist, and R. Baldock, “Spatial organization of active and inactive genes and noncoding dna within chromosome territories,” *Journal of Cell Biology*, Jan 2002.
- [45] T. Cremer and C. Cremer, “Chromosome territories, nuclear architecture and gene regulation in mammalian cells,” *Nat Rev Genet*, vol. 2, pp. 292–301, Apr 2001.
- [46] T. Cremer, K. Kupper, S. Dietzel, and S. Fakan, “Higher order chromatin architecture in the cell nucleus: on the way from structure to function,” *Biol Cell*, Jan 2004.
- [47] T. Cremer, M. Cremer, S. Dietzel, S. Müller, I. Solovei, and S. Fakan, “Chromosome territories—a functional nuclear landscape,” *Current Opinion in Cell Biology*, vol. 18, pp. 307–16, Jun 2006.

CHAPTER II

COMPARISON OF DISTANCES BETWEEN THE BREAKPOINT CLUSTER REGIONS ASSOCIATED WITH RADIATION-INDUCED DELETIONS IN CHROMOSOME 2 WITHIN INTERPHASE BONE MARROW FROM MICE THAT ARE SENSITIVE OR RESISTANT TO RADIATION INDUCED AML.

INTRODUCTION

2.1-Radiation-induced AML: Molecular and Cytogenetic Features.

Some strains of mice, such as CBA and C3H, are sensitive to the induction of acute myeloid leukemia (AML) by radiation while others, such as the C57BL/6 strain, do not show any measurable induction of AML by radiation⁽¹⁻³⁾. The spontaneous incidence of AML is virtually zero for both strains. Additional studies have identified a strong relationship between the initial production of chromosome 2 deletions in bone marrow cells and the eventual appearance of AML⁽⁴⁻¹³⁾. Further, analysis of the breakpoints surrounding the deletion found in the AML cells always include a small “common deleted region (cdr)” or “minimally deleted region (mdr)” that is present whatever other regions

may also be deleted, and the breakpoints surrounding the deletions are not located randomly on either side of the *mdr*. The deletion breakpoint locations have been mapped and found to occur in clusters; one, the proximal breakpoint cluster (*pb*) is located on the centromere side of the *mdr* and the other, the distal breakpoint cluster (*db*) is beyond the *mdr* with respect to the centromere^(14,15).

A map of chromosome 2 showing the location of the *mdr* and the breakpoint clusters is shown in figure 2.1, along with the fluorescent hybridization probes used in this study to mark a region in the proximal, distal, and *mdr* region that were derived from bacterial artificial chromosome (BAC) library that will be discussed further below.

There are various genes within this minimally deleted region, but a number of reports have focused on the loss of one of these, known as the *PU.1* gene in humans, also known as the *Sfpi-1* gene in mice⁽¹⁶⁾. The gene is essentially the same in mice and humans, so we have used the human gene nomenclature in the present studies. The vast majority of cells involved in radiation induced AML in mice have experienced a large deletion involving *PU.1*, followed later by a point mutation in the other allele. *PU.1* gene is thought to operate in the manner of a “tumor-suppressor-like” gene. *PU.1* codes for a transcription factor that has a key role in hematopoietic cell lineage development, including differentiation and self-renewal activities of HSCs and it is involved in the progression of myeloid and lymphoid progenitors to the differentiated state⁽¹⁶⁾.

This chapter addresses a question relating to the nature and relevance of the breakpoint cluster regions surrounding the initial loss of the *PU.1* gene on mouse chromosome 2.

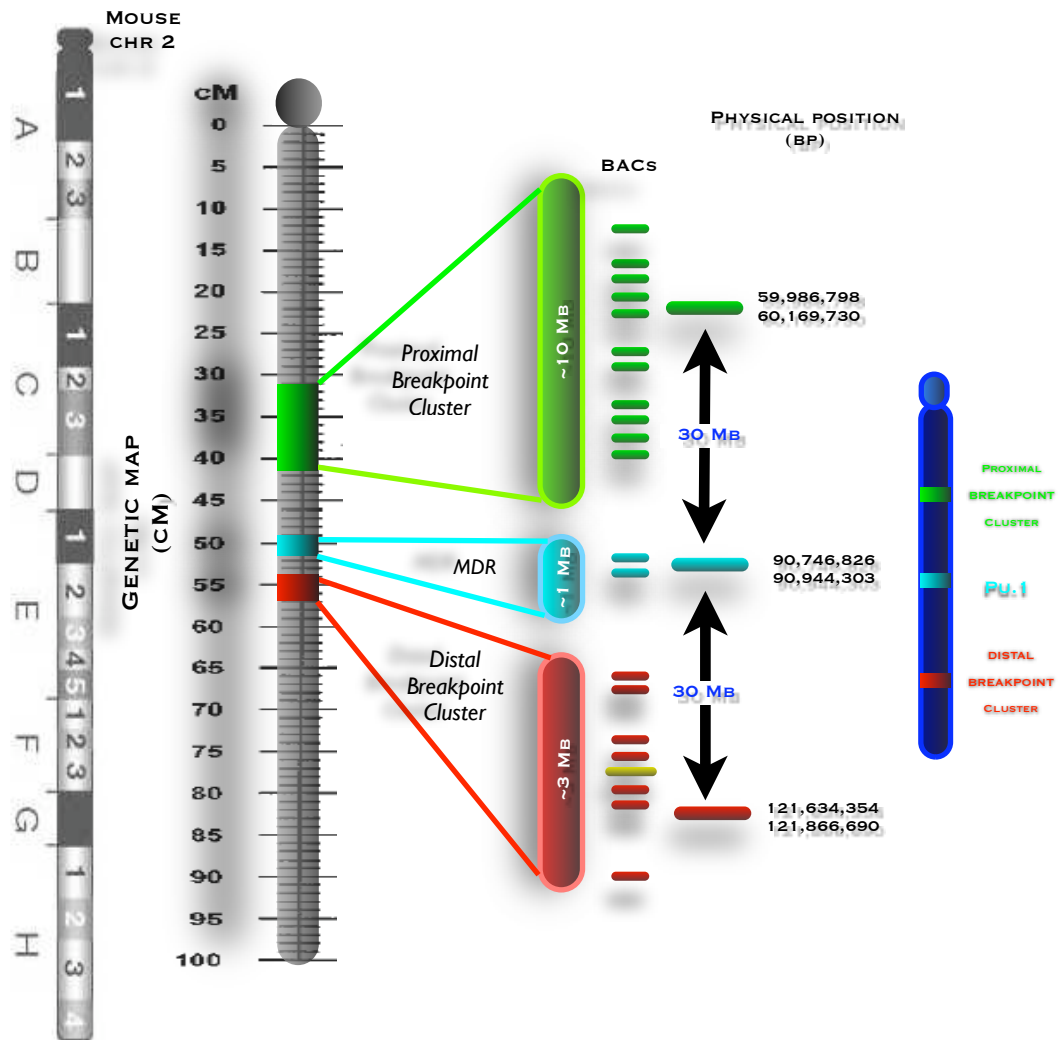


Figure 2.1: Schematic representation of the chromosome 2 showing the location of breakpoint clusters and the minimal deleted region. BACs selected at 30 Mb from PU.1 distal and proximal within each cluster.

The potential relevance stems from a report by Nikiforova and colleagues in connection with radiation induced thyroid cancer initiated from an inversion on human chromosome 10 that results in the fusion of the H4 and RET genes located 30 Mb apart on this chromosome⁽¹⁷⁾.

Using fluorescent labeled hybridization probes to identify their location, they reported a high proportion of interphase normal human thyroid cells had a much closer proximity between H4 and RET genes on chromosome 10 than would be expected based on their 30 Mb separation. This close proximity was seen in some 35% of normal human thyroid cells, in 21% of peripheral blood lymphocytes, but in only 6% of normal mammary epithelial cells.

The suggestion from this finding is that when two breakpoints involved in a particular radiation induced chromosomal rearrangement are very close together, the probability that a radiation dose will produce two independent breaks and that the two broken ends will mis-rejoin to form an inter-or intra-change will be much greater than if the two breakpoints are far apart. While the chromosome rearrangement involved in the *P.U.1* loss associated with AML is an interstitial deletion, but not an inversion, which is the alternate outcome of an exchange process that is essentially the same.

The only difference is whether mis-rejoining due to interaction of two nearby chromosome breaks is symmetrical or asymmetrical. In the first case the result is an inversion and in the second, an interstitial deletion. The latter is the process underlying the early radiation-induced *P.U.1* loss on chromosome 2. This is illustrated in figure 2.2 below.

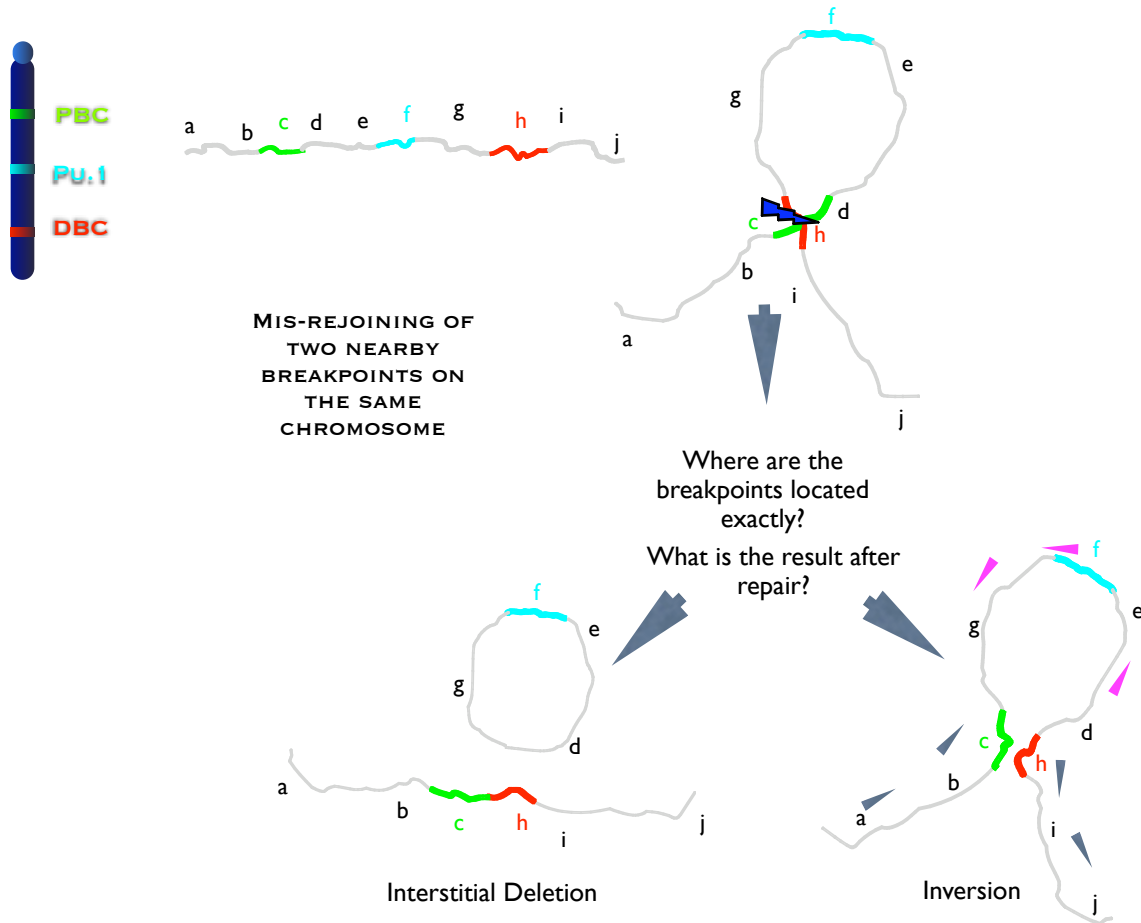


Figure 2.2: hypothetical outcome after mis-rejoin due to the interaction of two nearby chromosome breaks. Results of this mis-rejoin could be an inversion (symmetrical interaction) or an interstitial deletion (asymmetrical interaction). In terms of this study, the location of the breakpoints and the result of DNA repair mechanism was key for the determination of the work hypothesis.

This is certainly not the only example of a non-random arrangement of genes and chromosomes or chromosome segments within the cell nucleus.

The architecture and organization of the chromatin in the nucleus is tissue-specific and is closely related to the transcriptional activity of genes that may be functioning to different extents or not at all depending on the tissue context of the cell (see for example, reviews and reports of T. Cremer and co-workers and others⁽¹⁸⁻²⁴⁾).

In other words, the set of genes that are actively transcribed in one cell type in one tissue are different from those needed in another cell in another tissue, location of these genes within the nucleus differs accordingly.

Beyond the importance of the nuclear location of breakpoints involved in radiation induced chromosomal aberrations, the structure of chromatin itself, with respect to transcriptional activity or potential activity, is well known to be an important factor influencing breakpoint locations, such that radiation induced exchanges and deletions occur far more frequently in transcriptionally active or potentially active chromatin than in inactive chromatin or regions of chromosomes⁽²⁵⁻²⁹⁾.

With the above considerations in mind the first aim of this project was to determine whether a difference in nuclear localization of the proximal and distal breakpoint cluster regions may differ in interphase bone marrow cells between the radiation induced AML-susceptible CBA/CaJ and the AML-resistant C57BL/6 mouse, and whether there may be a tissue dependence of any such difference.

These observations helped to complete the first part of the research to test the hypothesis of this chapter.

2.2-Hypothesis

Thus, the following hypotheses formed the basis of this first project:

H1a: The proximal and distal breakpoint clusters leading to the initial deletion of the PU.1 gene on chromosome 2 are in closer proximity in the hematopoietic interphase nuclei of the AML-susceptible CBA/CaJ mice than in the AML-resistant C57BL/6J mice.

A second corollary hypothesis was

H1b: The proximal and distal breakpoint clusters regions are tissue-dependent; so, they are in closer proximity within the CBA/CaJ interphase nuclei of hematopoietic cells compared with fibroblasts from CBA/CaJ and C57BL/6J mice.

2.3-Specific Aims

Specific Aim 1: The first aim was to measure the physical projected distances between labeled chromosome 2 BAC-probes used as markers of the “proximal breakpoint cluster” (pbc) and “distal breakpoint cluster” (dbc) in interphase bone marrow cells from CBA/CaJ (AML-susceptible) and C57BL/6J (AML-resistant).

Specific Aim 2: perform the same measurements in mouse fibroblast interphase cells to compare differences between different cell types showing

distinct arrangement of the interphase nuclei architecture in both CBA/CaJ and C57BL/6J mouse strains.

The comparison was made following the same procedure applied by Nikiforova et al. in studies of H4/RET inversions in chromosome 10 in human thyroid cells.

The distribution of distances measured between the markers were used to show difference in the proximity of breakpoint cluster regions, which presumably would reflect differences in chromatin organization between the CBA/CaJ (AML-susceptible) and C57BL/6J (AML resistant) mice and within different cell types.

2.4-Experimental Approach

The first aim was to measure the physical distances between labeled chromosome 2 BAC probes used as markers lying within the proximal breakpoint cluster (pbc) and distal breakpoint cluster (dbc) described above. These two markers were selected to be near the mid-point of the pbc and dbc respectively and the selection resulted in the Mb distances between them to be approximately 60 Mb and both at approximately 30 Mb distance from the *PU.1* gene.

The physical shortest 3D distances between the probes were measured in interphase nuclei obtained from the cells of CBA/CaJ or C57BL/6 mice.

The comparison was made following the same general procedure used by Nikiforova and co-workers⁽¹⁷⁾ for studies of H4/RET inversions in chromosome 10 in human thyroid cells but the microscopy and image reconstruction analysis was technically different as described below. The distributions of distances measured between the markers were used to determine whether any differences were apparent in the proximity of breakpoint cluster regions, in different proportion of cells which presumably would reflect differences in chromatin organization between the CBA/CaJ (AML-susceptible) and C57BL/6J (AML resistant) mice.

By chance, the distance may be very close or very far, in occasional cells, but follow a distribution of “expected” distances among cells based on the physical base-pairs separation along the DNA that tethers the probes together, as described by Nikiforova and co-workers⁽¹⁷⁾. The distances of the two markers were also measured in mouse fibroblast interphase cells to compare differences between different cell types that may show distinct arrangement of the interphase nuclei architecture in both CBA/CaJ and C57BL/6J mouse strains.

2.5-Materials and Methods

2.5.1-Mice

All CBA/CaJ and C57BL/6J mice used in these experiments were obtained from Jackson laboratory along with the NASA-supported NSCOR Leukemogenesis studies carried out in this department during the past five years.

Animals were approximately two months of age when they arrived and these were used to obtain bone marrow and fibroblast cells.

2.5.2-Cells

Whole bone marrow (BM): The femurs were obtained from the mice and the bone marrow was flushed out with a syringe and a 30-gauge needle. The collected bone marrow in PBS is then centrifuged at 1,000 rpm and resuspended in 8 ml of KCl 7.5 mM and 1.5 ml trypsin-EDTA. The addition of trypsin dissolved the connective tissue characteristic from the bone marrow tissue. After incubation at 37C the sample is filtered through cell strainer mesh of 40 um allowing to obtain a single cell suspension preparation.

The cell suspension is then fixed with methanol: acetic acid glacial (3:1). After dropping the cell suspension onto the slides it was air-dried and aged for at least 3 days.

Hematopoietic Precursors: After bone marrow extraction a separation of stem cells was carried out according to instructions specified by Miltenyi Biotec (Bergisch Gladbach, Germany) which uses a magnetic bead approach to enrich the cell populations for the stem cells. The procedure involve a two-selection steps. The first step is the lineage positive depletion (Lineage Cell Depletion Kit No. 130-090-858) consist in the selection of all the differentiated cell sub-populations present in this tissue, such as T cells, B cells, monocytes/macrophages, granulocytes and erythrocytes and their committed precursors from bone marrow of adult mice.

This step allows a pre-enrichment of stem cells and progenitor cells from the bone marrow. The second selection step is the positive selection of CD117 (c-Kit) cells (CD117 MicroBeads No. 130-091-224) to obtain the HSC. CD117 also known as c-Kit or Stem Cell Factor Receptor (SCF-R) is a cell surface protein that is expressed on hematopoietic stem cells. Thus, this positive selection through magnetic beads allowed the isolation of HSC from bone marrow. After obtaining the hematopoietic stem cells the fixation procedure was the same applied for whole bone marrow cells.

Fibroblasts: Punch biopsies from ears from each individual mouse were disaggregated into small pieces and cultured in RPMI containing 12% fetal bovine serum. After 4 days of culture the fibroblasts attached to the culture surface started migrating away from the pieces of tissue and growing, spreading out to occupy the petri dish. Fibroblasts were grown until the cultures became confluent. Cells were then resuspended by trypsin treatment, harvested and fixed following the procedure previously described. After drops of the cell suspensions were placed on slides and air dried they were aged at room temperature for 3 days before the fluorescence in situ hybridization procedures.

2.5.3- Bacterial Artificial Chromosomes Clones

The Bacterial Artificial Chromosomes (BAC) clones were selected and ordered from the BACPAC resources center <http://bacpac.chori.org/> at Children's Hospital Oakland Research Institute in Oakland, California.

The cloned bacterial cultures separately containing the five BAC clones were grown and the DNA was isolated and purified using alkaline lysis and according to instructions accompanying the QIAGEN filter Plasmid Maxi kit (Qiagen, Valencia, CA) used.

Then the different BAC-DNA were labeled using a Nick Translation Kit (Roche Applied Science, Indianapolis, IN) to incorporate nucleotides that were directly labeled with the fluorochromes.

The first BAC-probe [RP23-90A5](#) located in the Proximal Breakpoint Cluster (pbc) at position 59,986,798 and was labeled with Spectrum Green (Abbott, Abbott Park, IL).

The second BAC-probe [RP23-263H8](#), which contains the *Sfpi-1* or *PU.1* gene at position 90,746,826 was labeled with DEAC (PerkinElmer, Waltham, MA).

Finally, the third BAC-probe [RP23-409P4](#) that map at position 121,634,354, is located within the Distal Breakpoint Cluster (dbc) on chromosome 2 labeled with Spectrum red (Abbott).

An additional probe was a whole chromosome 2 paint and was incorporated in the experiments in order to allow visualization of each chromosome 2 within the interphase nucleus of the different cell types. This whole chromosome 2 paint was biotin-labeled (Star-FISH®, Cambio, Cambridge, UK) and was visualized with Streptavidin-Alexa-647 (Invitrogen, Carlsbad, CA).

All BAC clone names used as probes, the chromosome 2 (physical map) binding locations and fluorescent labels used are summarized in table 2.1 below.

BAC's name	Label	Location on Chr2 (bp)	Notes
RP23-90A5	S. Green	59,986,798 - 60,169,730	<i>Proximal Breakpoint Cluster</i>
RP23-20F9	DEAC	90,746,826 - 90,944,303	<i>PU.1 Gene</i>
RP23-34E24	S. Red	121,634,354 - 121,866,690	<i>Distal Breakpoint Cluster</i>
Chr2 painting	Alexa-647	0-180,000,000	<i>Whole chr2 Territories</i>

Table 2.1: This table is showing BAC's name, fluorochromes used for labeling and physical location within mouse chromosome 2

2.5.4-Fluorescent In Situ Hybridization

0.5 ul of labeled BAC-probes were applied at a concentration of about 1 ng/ul to the slides. The slides were cover-slipped and sealed with rubber cement. Co-denaturation of probes and target DNA occurred at 80°C in hybridization mix (proprietary solution designed to optimize hybridization of multiple probes) for 5 minutes followed by incubation at 37°C overnight. The coverslips were removed and the slides washed in 50% formamide/2X SSC at 43.5°C for 5 minutes followed by 3 washes in 2X SSC at 43.5°C for 5 minutes to remove any mismatched probe. The slides were counterstained with DAPI (4',6-diamidino-2-phenylindole, dihydrochloride) in Anti-Fade Prolong Gold (Invitrogen, Carlsbad, CA), coverslipped, and sealed.

2.5.5-Microscopy

The slides were examined using a Nikon Eclipse 600 epi-fluorescent microscope and scored for probe number and probe order. 3D-deconvolution, reconstruction and measurements were performed using a combination of softwares such as ImageJ Software (<http://rsbweb.nih.gov/ij/index.html> - NIH), Autoquant software (Media Cybernetics, inc; Bethesda, MD) and Metamorph (Molecular Devices, Sunnyvale, CA).

The procedure involved acquisition of 26 image plate stacks of 0.2 um per plane in 5 different wavelength channels. After the acquisition of the stacks a 3D-deconvolution procedure was carried out to be able to make the 3-Dimensional reconstruction and measurements of the absolute physical distances between the BAC-probes in the reconstructed space of every interphase cell.

2.5.6-Determination of clusters proximity

Criterion of proximity: A cutoff distance for measurement of proximity was chosen at 0.2 um similar to the criteria used by Nikiforova, as described above.

By considering that a closer distance between the potential breakpoints will bias the likelihood to produce an illegitimate rejoining of the broken ends generated after ionizing radiation exposure, we considered that a proximity of 0.2 um will be the cutoff distance. The image acquisition was carried out with 0.2 um distance between z-stack image planes and X=Y= 0.065 um/pixel.

2.6-Results

2.6.1-Measurements of Distances

The acquisition of 26 stacks of every individual channel for each assayed cells gave us the possibility of visualizing the 3-dimensional organization by the reconstruction of the positional information of each probe. The dimensional parameters used for the acquisition and reconstruction were define as X=Y=0.0645 um/pixel and Z=0.2 um/pixel. Thus, we performed the measurements using absolute values of the two main markers pbc (in green) and dbc (in red) in micrometers taking into account that all the cells were scored only if they showed the two clusters, PU.1 and the chromosome paint territories as shown in figure 2.3.

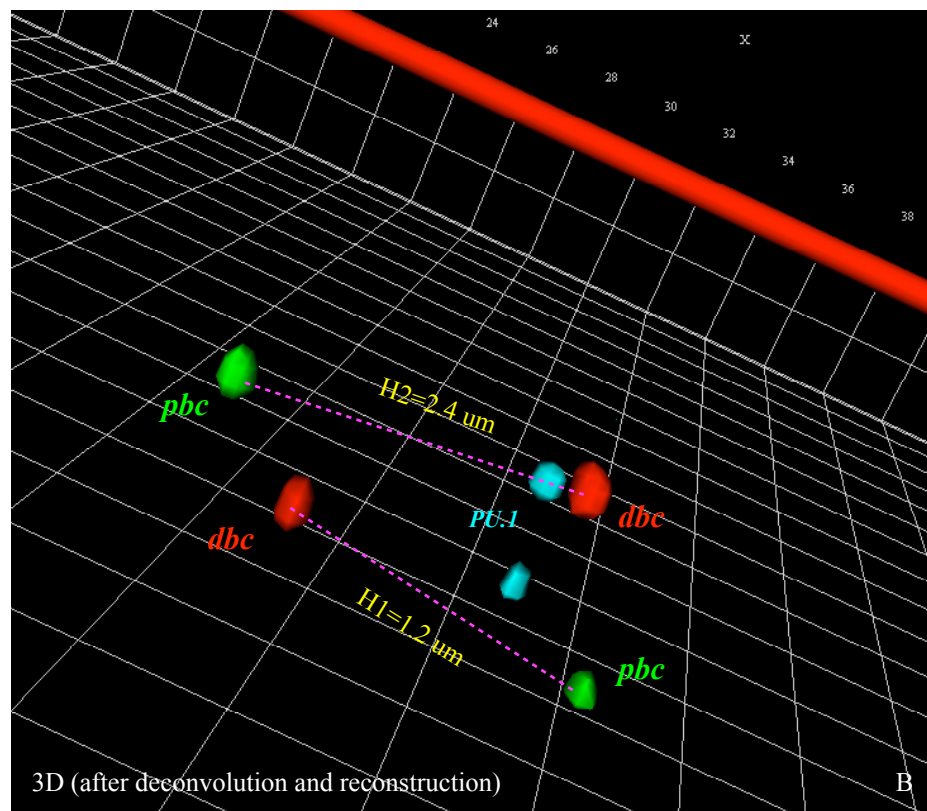
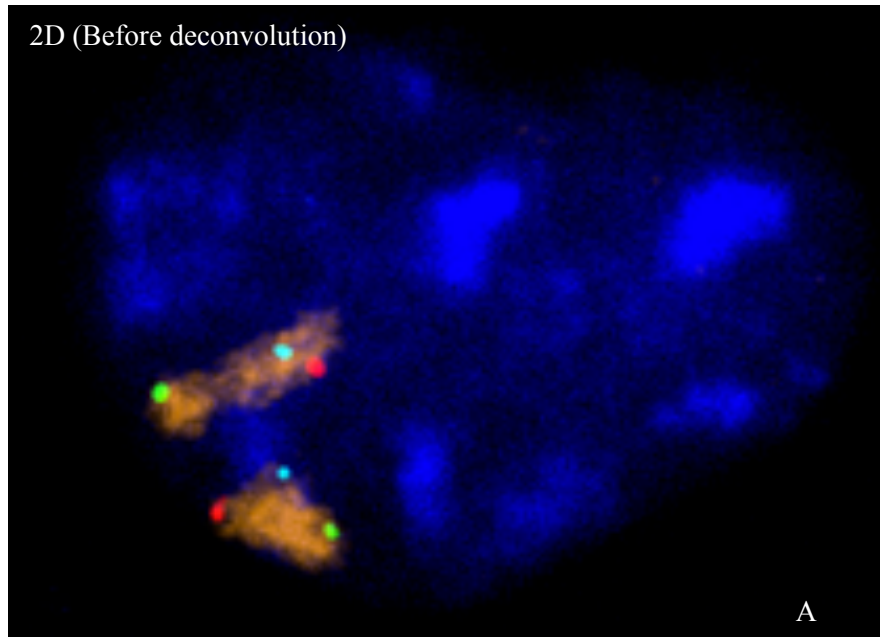


Figure 2.3: HSC cell from CBA showing Chr2 paints and 3 markers. A- 2D before and B- 3D after deconvolution. (Deconvoluted markers and measurements).

Therefore, the inter-marker distances gave us an idea of the distances between the clusters within each interphase cell measured.

2.6.2-Breakpoint Cluster Distances Measurements in Fibroblasts: CBA/CaJ vs C57BL/6J Mouse Strains

Measurements were made in low passage cultured fibroblasts obtained from each mouse strain. By considering the fact this cell type is different from those that belong to the hematopoietic compartment. This set was taken as a negative control for which the expectation would be to find no preponderance of cells having close proximity between the two clusters. For the overall gross comparison between fibroblasts from CBA/CaJ and C57BL/6J mice, Distance measurements for cells from each mouse strain were measured and pooled without regard for any differences within individual cells. This later topic will be discussed at length in chapter 3.

The data were grouped to plot histograms of the proportions of measurements falling within distance ranges and the result for fibroblasts is shown in figure 2.4 and table 2.2. This plot shows a general shift toward the right (the larger distances) of the histogram for C57BL/6 making it appear that the distances in C57BL/6J fibroblasts are greater.

Due to this difference in the distribution of the distances in the two strains the average values for the global measurement are not similar.

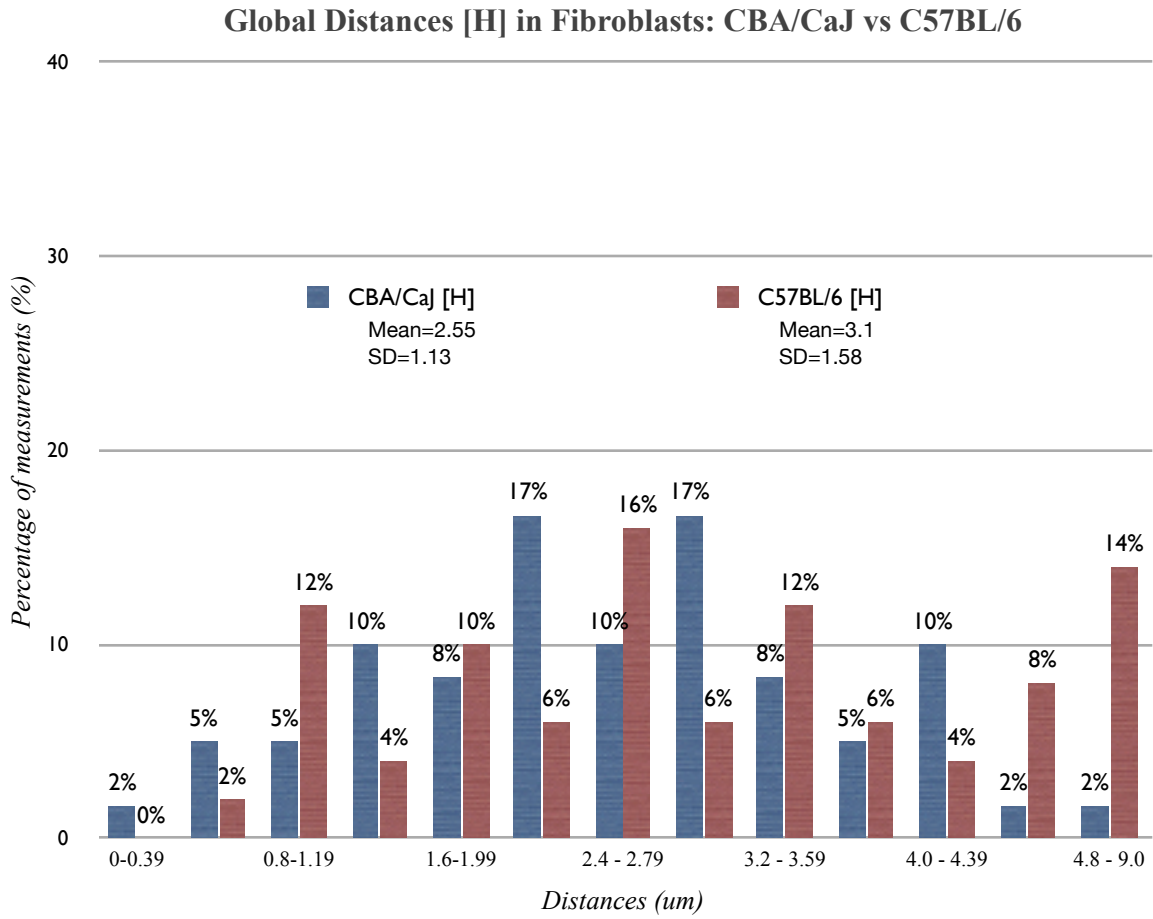


Figure 2.4: Histogram showing pbc-dbc distances distribution obtained from interphase fibroblasts. Comparison between CBA/CaJ and C57BL/6 mouse strains.

Distances (um)	Number of Measurements [Frequency]	CBA/CaJ (FIB) [H] (Percent)	Number of Measurements [Frequency]	C57BL/6 (FIB) [H] (Percent)
0 - 0.39	1	1.7	0	0.0
0.4 - 0.79	3	5.0	1	2.0
0.8 - 1.19	3	5.0	6	12.0
1.2 - 1.59	6	10.0	2	4.0
1.6 - 1.99	5	8.3	5	10.0
2.0 - 2.39	10	16.7	3	6.0
2.4 - 2.79	6	10.0	8	16.0
2.8 - 3.19	10	16.7	3	6.0
3.2 - 3.59	5	8.3	6	12.0
3.6 - 3.99	3	5.0	3	6.0
4.0 - 4.39	6	10.0	2	4.0
4.4 - 4.79	1	1.7	4	8.0
4.8 - 9.0	1	1.7	7	14.0
TOTAL	60	100.0	50	100.0

Table 2.2: Pbc-dbc distances distribution obtained from interphase fibroblasts. Frequency and percentage of measurements fitting in different distance ranges. Comparison between CBA/CaJ and C57BL/6 mouse strains.

Thus, the measurement values for the distances between the markers (pbc-to-dbc) for CBA/CaJ gave an average of [HCBA/CaJ] equal to 2.55 μm and the value for C57BL/6 [HC57BL/6] was equal to 3.09 μm .

The validity of standard statistical tests was uncertain, however, because the distance frequency histograms did not appear to be normally distributed.

As will be discussed in chapter 3, the distributions appear to be bimodal, and the arguments and evidence supporting this will be presented there.

2.6.3-Breakpoint Cluster Distances Measurements in Bone Marrow: CBA/CaJ vs C57BL/6J Mouse Strains

The next measurements were performed in cells obtained from whole bone marrow (BM).

The distribution of distances measured in cells from BM showed a shift in the average distances such that the distances were closer on average when compared with fibroblasts. The distributions for bone marrow for the different mouse strains showed a similar distribution shape, and the mean values were very similar, even though, in C57BL/6 cells, the peak of the distribution was shifted one distance interval to the right toward larger distances between the clusters as shown in figure 2.5 and table 2.3.

Thus, in CBA/CaJ the peak is within the range 0.8-1.19 μm with 23% of the measurements.

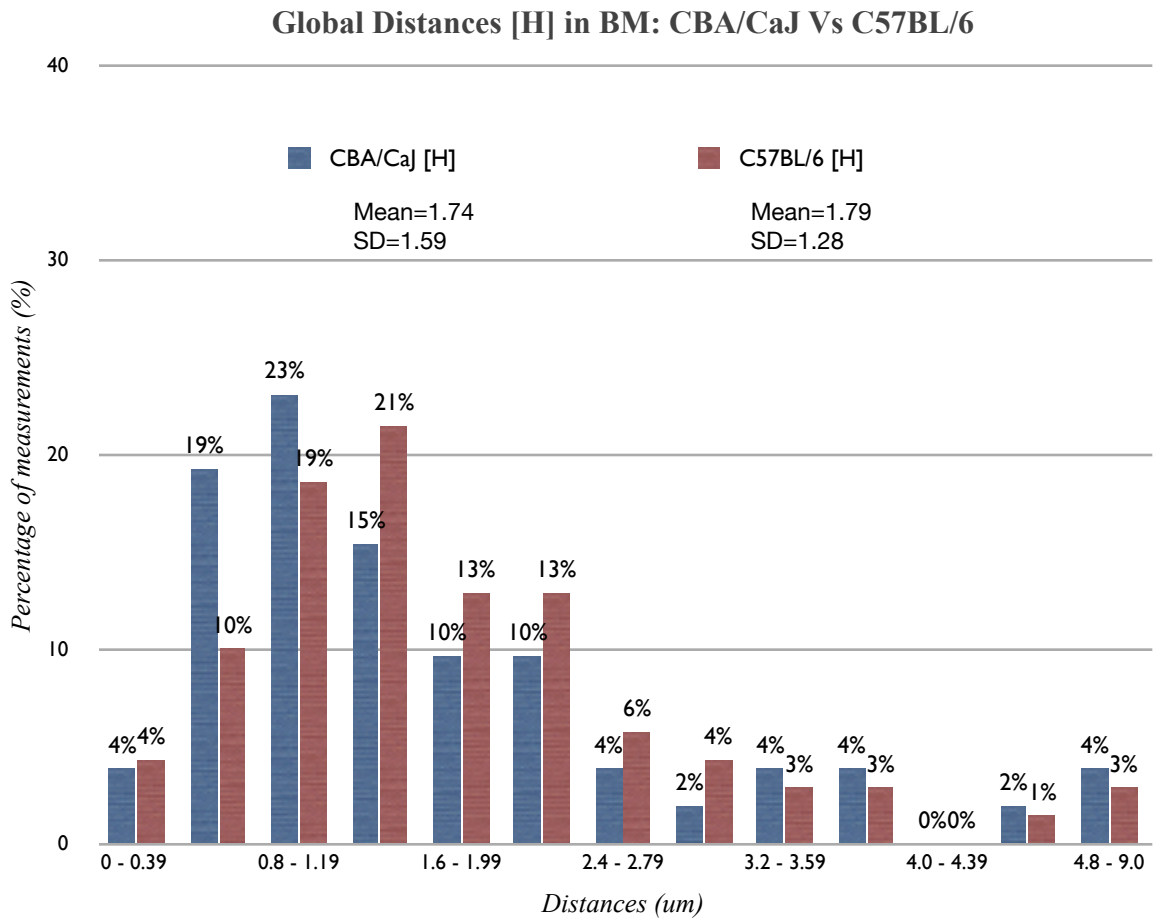


Figure 2.5: Histogram showing distances from pbc to dbc distribution from interphase BM cells. Comparison between CBA/CaJ and C57BL/6 mouse strains.

Distances (um)	Number of Measurements [Frequency]	CBA/CaJ (BM) [H] (Percent)	Number of Measurements [Frequency]	C57BL/6 (BM) [H] (Percent)
0 - 0.39	2	3.8	3	4.3
0.4 - 0.79	10	19.2	7	10.0
0.8 - 1.19	12	23.1	13	18.6
1.2 - 1.59	8	15.4	15	21.4
1.6 - 1.99	5	9.6	9	12.9
2.0 - 2.39	5	9.6	9	12.9
2.4 - 2.79	2	3.8	4	5.7
2.8 - 3.19	1	1.9	3	4.3
3.2 - 3.59	2	3.8	2	2.9
3.6 - 3.99	2	3.8	2	2.9
4.0 - 4.39	0	0.0	0	0.0
4.4 - 4.79	1	1.9	1	1.4
4.8 - 9.0	2	3.8	2	2.9
TOTAL	52	100.0	70	100.0

Table 2.3: pbc-dbc distances distribution obtained from whole bone marrow (BM) cells. Frequency and percentage of measurements fitting in the different distance ranges. Comparison between CBA/CaJ and C57BL/6 mouse strains.

On the other hand, the peak for C57BL/6 is shifted to the range 1.2-1.59 μm with 21% of the measurements.

Then, the average value for the group [H] in CBA/CaJ bone marrow cells was $[\text{H}]\text{CBA/CaJ}_{(\text{BM})} = 1.74 \mu\text{m}$ and assuming a normal distribution the standard deviation was 1.59 μm .

The average value for C57BL/6 was $[\text{H}]\text{C57BL/6}_{(\text{BM})} = 1.79 \mu\text{m}$; standard deviation 1.28 μm .

The distribution of distances between pbc-dbc within bone marrow cells are evidently showing more cells with distances in closer proximity compared with fibroblasts.

Thus, 71% of the measurements in BM from CBA/CaJ and 66% of measurements from C57BL/6 mice showed distances values $< 2 \mu\text{m}$.

These frequencies (values $< 2 \mu\text{m}$) were 28% and 30%, respectively, for fibroblasts from the same strains.

2.6.4-Breakpoint Cluster Distances Measurements in Hematopoietic Stem Cells (CD117 positive cells): CBA/CaJ vs C57BL/6J Mouse Strains

The comparison of the measurement distributions between CBA/CaJ and C57BL/6 hematopoietic stem cells (HSC) were similar to the results for nucleated bone marrow cells.

In both mouse strains there were two peaks: one that represents the most frequent distances measured within the range from 0.8 to 1.19 μm with $\sim 32\%$ and $\sim 29\%$ of the measurements for CBA/CaJ and C57BL/6 respectively (figure 2.6 and table 2.4).

The statistical values for CBA/CaJ in HSC was group average $\text{HCBA/CaJ}_{(\text{HSC})} = 1.53 \mu\text{m}$ and a standard deviation of 1.23 μm , again assuming a normal distribution.

For C57BL/6 the average distance frequency was $\text{HC57BL/6}_{(\text{HSC})} = 1.77 \mu\text{m}$ and standard deviation of 1.34 μm . The distribution showed that 79% of the measurements in CBA/CaJ HSC had distances that were less than 2 μm .

In C57BL/6 HSC there were 69% of measurements showed values that were less than 2 μm .

The remaining 21% of measurements for CBA/CaJ and 31% for C57BL/6 showed distances more than 2 μm . Finally, there were 7% of measurements in CBA/CaJ and 2% in C57BL/6 that were less than 0.39 μm .

2.7-Discussion

The breakpoint clusters within mouse chromosome 2 are classified as areas in which a high frequency of breaks associated with the deletions are located. However, we do not know whether these sites on both homologs have the same so-called hot-spots or high frequency breakpoint regions for radiation-induced deletions.

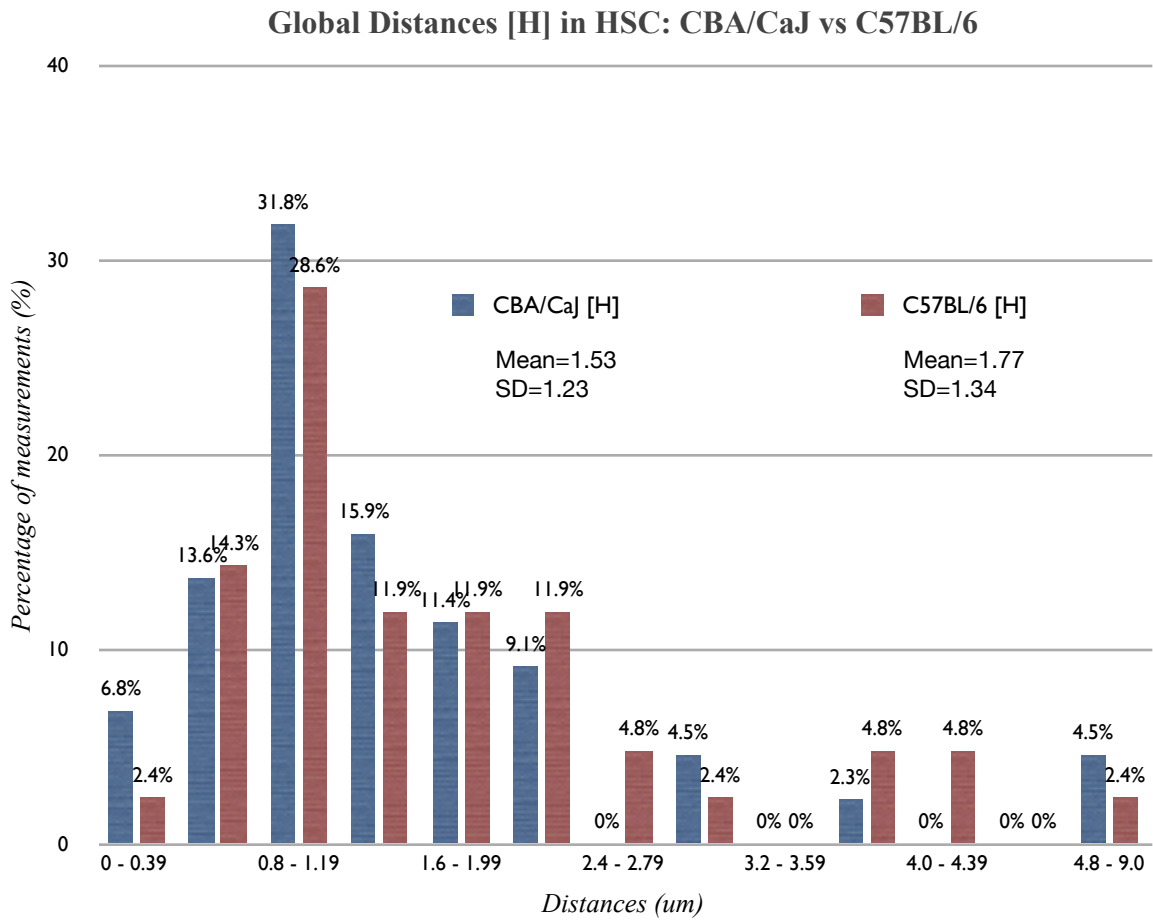


Figure 2.6: Histogram showing distances pbc-dbc distribution from hematopoietic stem cells (HSCs). Comparison between CBA/CaJ and C57BL/6 mouse strains.

Distances (um)	Number of Measurements [Frequency]	CBA/CaJ (HSC) [H] (Percent)	Number of Measurements [Frequency]	C57BL/6 (HSC) [H] (Percent)
0 - 0.39	3	7	1	2
0.4 - 0.79	6	14	6	14
0.8 - 1.19	14	32	12	29
1.2 - 1.59	7	16	5	12
1.6 - 1.99	5	11	5	12
2.0 - 2.39	4	9	5	12
2.4 - 2.79	0	0	2	5
2.8 - 3.19	2	5	1	2
3.2 - 3.59	0	0	0	0
3.6 - 3.99	1	2	2	5
4.0 - 4.39	0	0	2	5
4.4 - 4.79	0	0	0	0
4.8 - 9.0	2	5	1	2
TOTAL	44	100	42	100

Table 2.4: pbc-dbc distances distribution obtained from hematopoietic precursor (HSC). Frequency and percentage of measurements fitting in the different distance ranges. Comparison between CBA/CaJ and C57BL/6 mouse strains.

The global distances from pbc to dbc in CBA/CaJ and C57BL/6 showed essentially the same distribution with no significant differences between these mouse strains for any of the cell types. However, there was a significant difference when comparing distances between the clusters within different cell types, especially for fibroblasts as opposed to whole bone marrow or hematopoietic stem cells.

The proportion of HSCs and bone marrow cells that showed a close (less than 1.79 μm) proximity of the markers in interphase was about 70% leaving the corresponding 30% of cells showing distances greater than 2 μm . In contrast, fibroblasts showed exactly the opposite proportion. Therefore, only 30% of the total measurement in both mouse strains showed distances values that were less than 1.79 μm . Meanwhile, the other 70% showed distances greater than 2 μm suggesting a priori that there is a low probability for two potential double strand breaks within these regions to interact based in the initial distance greater or equal to 2 μm (figure 2.7).

Hypothetically, the interaction of DNA broken-ends generated by ionizing radiation are less likely to rejoin illegitimately to form exchanges or large interstitial deletions and more likely to properly rejoin with the correct broken-end if they are further apart.

On the other hand, despite the closer distance of the markers within HSCs and BM cells it was not found, in any of the mouse strains, a high frequency of cells with distances where the clusters were in very close proximity, such as reported for RET and H4 loci in thyroid cells by Nikiforova and co-workers where there was high frequency of cells with distance values less than 0.2 μm . Figure 2.8 shows distribution of distances for values less than 0.6 μm within fibroblast and blood cells in both mouse strains.

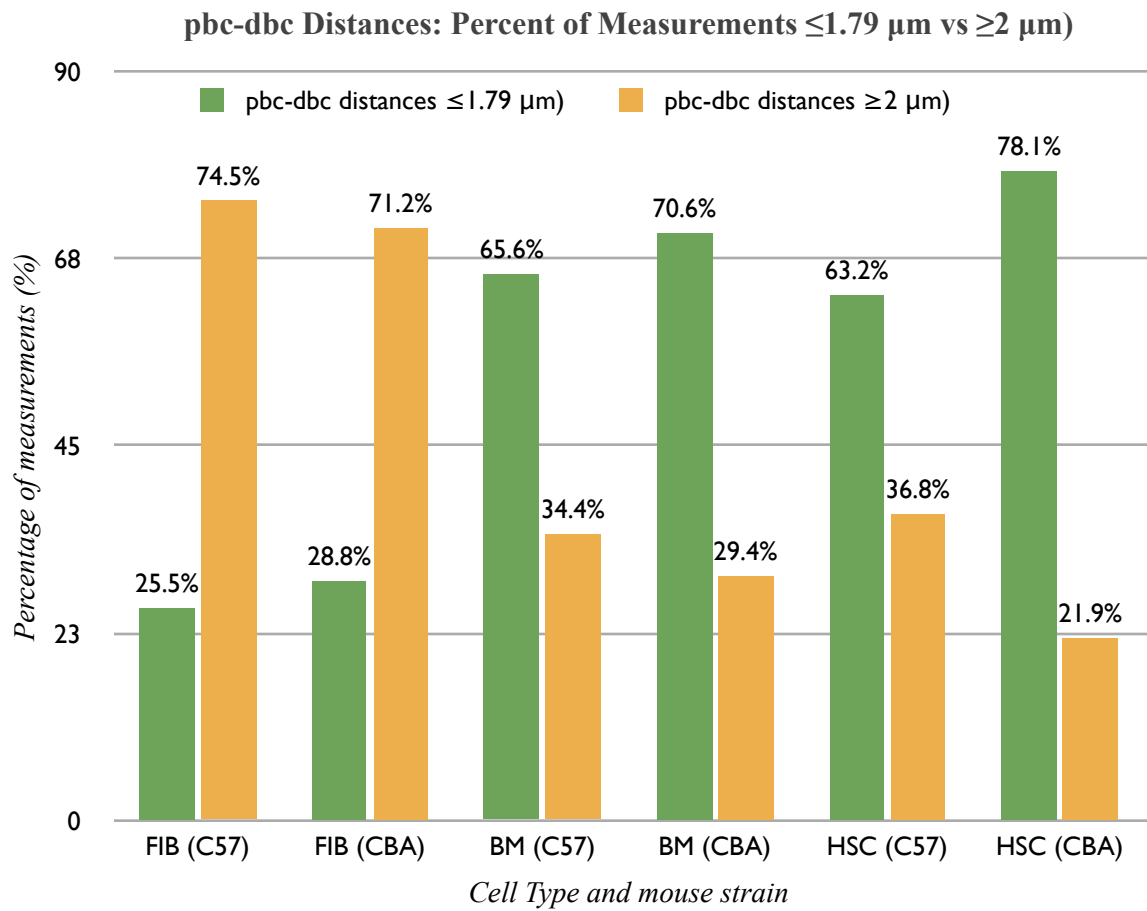


Figure 2.7: Histogram showing percentage of measurements that falls into values $\leq 1.79 \mu\text{m}$ and values that were $\geq 2 \mu\text{m}$ in fibroblasts, BM, and HSC from CBAC/aJ and C57BL/6 mouse strains.

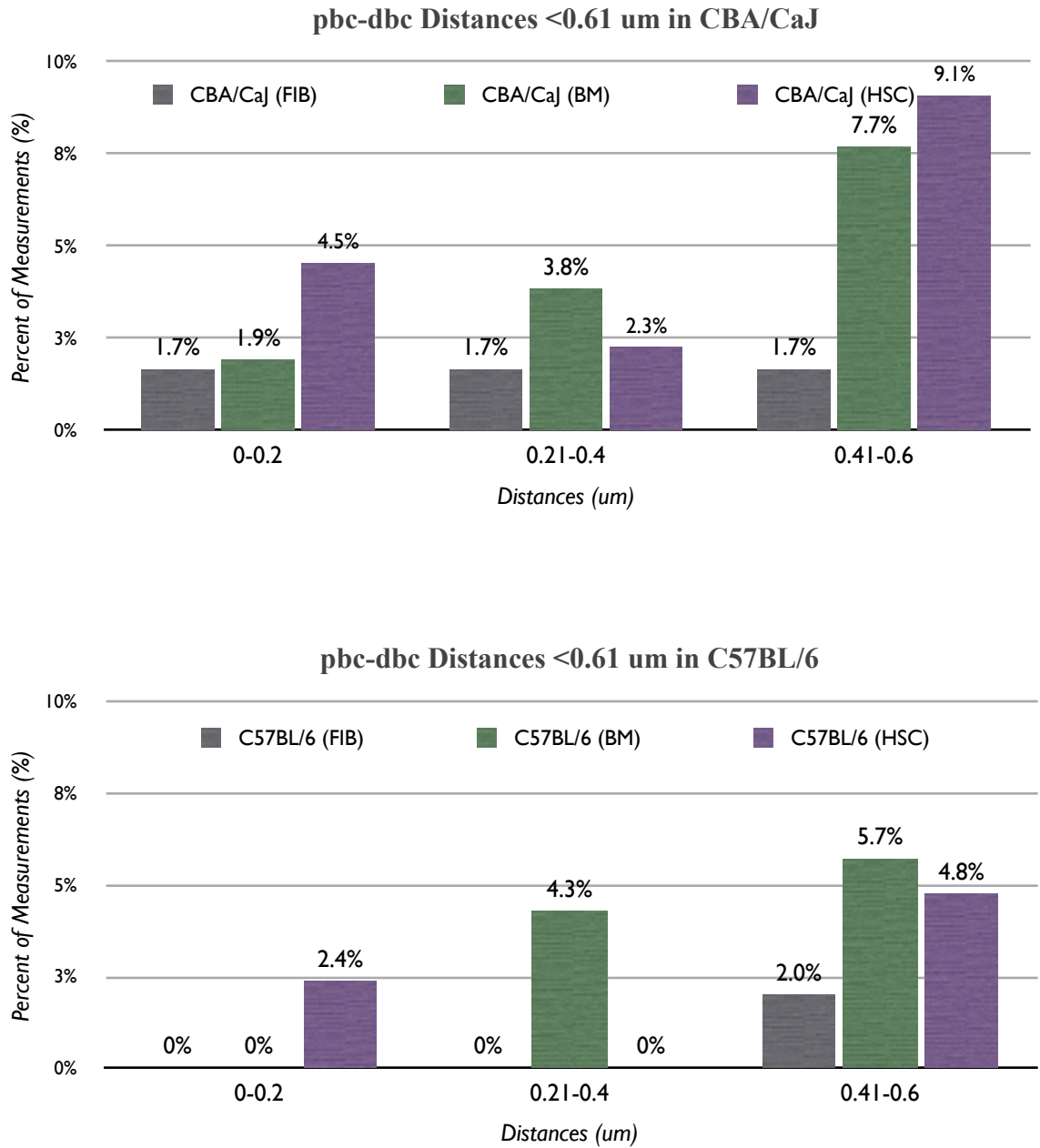


Figure 2.8: Pbc-dbc distances distribution obtained from fibroblasts, bone marrow, and hematopoietic precursor cells. Percentage of measurements fitting within distance ranges <0.61 μm in CBA/CaJ (top) and C57BL/6 (bottom).

In order to compare results from both, we have to consider that in Nikiforova's approach they were concerned with actual breakpoints and not breakpoint clusters as in the hypothesis we tested.

Specifically, the breakpoint in H4 (~118 Kb) gene is within intron 1 (which size is ~53 Kb) and the other breakpoint at RET (~53 Kb) gene is within intron 11 (which size is ~1,800 bp) both in human chromosome 10 and separated by a distance of approximately 30 Mb.

In the situation tested here, the breakpoints are clusters of different sizes where the proximal covers a region of 10 Mb and the distal covers a region of 3Mb.

Additionally, the outcome after irradiation exposure is a deletion (the counterpart of an inversion) after exposure to IR.

The main problem is represented by the large size of the clusters that make it impossible to choose a unique pair of markers that will potentially be involved in the rearrangement after the treatment of mice with IR (figure 2.9).

In fact, since all the breakpoints do not occur within well defined regions of a few 10's of kilobases, the approach here would reveal a generally closer than expected proximity only if all the regions within the clusters were generally nearer each other in the nucleus rather than randomly distributed.

Technically, a set of multiple markers may be needed to be able to cover the whole region of both clusters. However, it is unknown if there is some particular preference for a specific section of the clusters region (clusters within the clusters) to be involved in the breakage and reunion to cause the deletion of *mdr*.

COMPARING APPROACHES

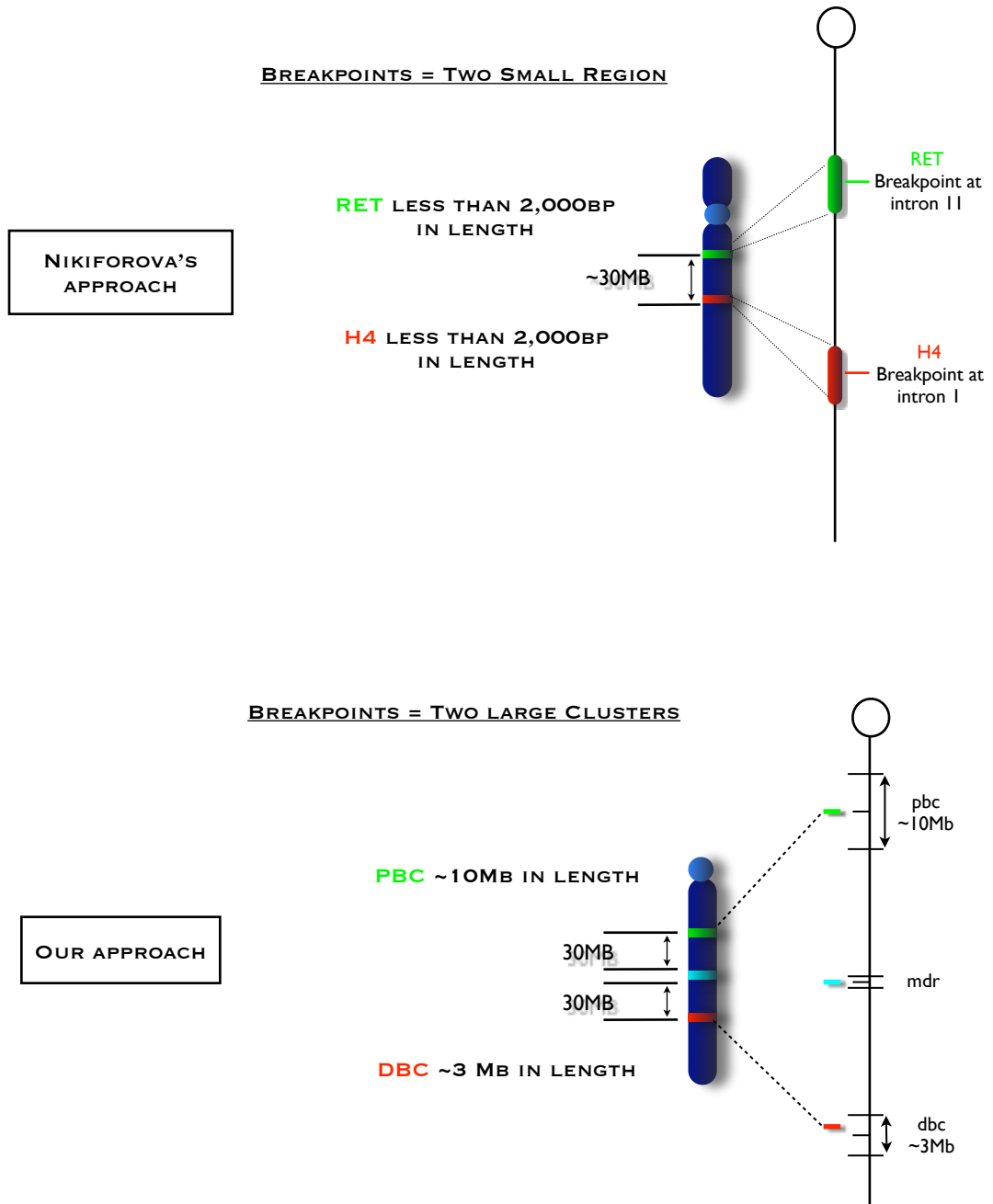


Figure 2.9: Comparison of approaches: Nikiforova's approach (top) and our approach (bottom) for detection of breakpoint clusters.

Nevertheless, the determination of the clusters, characterized by Silver⁽¹⁴⁾ (1999) and Finnon⁽¹⁵⁾ (2002) are not extensive enough to resolve any sub-structure within the general areas of the two breakpoint clusters so the implication would be that unless it is shown otherwise the simplest conclusions based on available data (Occam's Razor) would be that all the regions in both clusters have a similar likelihood of being involved in the rearrangement on chromosome 2.

It would not seem reasonable to expect that breakpoints for exchanges and deletions must only be located at distances less than 0.2 μm in within blood cells, especially since the breakpoint clusters themselves are fairly large.

One might suspect that their sizes would themselves be appreciably larger than 0.2 μm . May distances not be so short ($>0.2 \mu\text{m}$) but close enough ($>1.79 \mu\text{m}$) to allow the broken-ends to interact? Could this evidence show that there is a predisposition for this rearrangement to occur even if the distances are not just less than 0.2 μm but less than 2 μm ? Would it not seem reasonable to suggest that there is no sharp cutoff for interaction distances but that the probability just decreases with distance between the breaks?

As shown in Kozubek⁽³⁰⁾ et al. 1997, the measurements of distances between BCR and ABL genes within lymphocyte interphase cells showed a very close proximity (between 0.2-0.3 μm) but only in a small proportion about 8% of the cell population (perhaps the target cells) which might be responsible for the development of chronic myeloid leukemia. The same result was obtained for the pair c-MYC and IgH, which is one of the three possible rearrangements between c-MYC and an immunoglobulin locus that can lead to Burkitt's lymphoma.

In contrast, the different aberrations could happen within cells in different stages of differentiation or even fully differentiated cells; however, this should not be enough to initiate the disease due to the lack of self-renewal capability of these committed cells in the differentiation pathway.

Therefore, the mutation in these cells may disappear with the death of the cells after they reach the final stage of differentiation or even after they become apoptotic after the treatment.

So far, it is unknown which cell population is more sensitive to IR in bone marrow of these mouse strain, and how much, if there is a difference.

However, there is evidence supporting the idea that HSC are more resistant to IR in general⁽³¹⁻³⁵⁾; therefore, this sub-population seems likely to be the target population of interest in terms of initiation of the disease.

Thus, the undifferentiated state of HSC along with the self-renewal capabilities that are features of all stem cells makes it the candidate cells to suffer and carry the mutations before or even during the clonal expansion leading to the development of AML.

In retrospect, the shorter distances between pbc's and dbc's of blood cells in comparison with fibroblasts may suggest a predisposition for this deletion to occur; however, we do not know what the frequency should be and how short the distance should be considering the sizes of the clusters.

Further, the average distance measurements made above certainly cannot account for the different radiosensitivity for AML induction in CBA/CaJ vs C57BL/6J mice.

However, it still seems reasonable to suppose that the closer the potential breakpoints are the more likely they are to interact with each other after the broken-ends are formed.

I have explored the possibility that there is a different domain organization between the chromosome 2 homologs and that this could have some influence predisposing to the characteristic deletion of one of the homologs.

This predisposition might be increased in cells that present closer distances of the breakpoint clusters as showed for HSC.

Nevertheless, there must be more factors influencing the genetic susceptibility to AML, since the closer distances are present in both AML-sensitive and AML-resistant mouse strain.

Factors such as apoptosis rate after irradiation, gene expression profile changes after irradiation, and methylation pattern after irradiation among others that may better explain the very large difference in radiation susceptibility to AML between CBA/CaJ and C57BL/6J mouse strains.

2.8-Conclusions:

In contrast to the situation reported for papillary thyroid cancer in humans in which a chromosome 10 inversion places H4 and RET in close proximity, there is not a precise location of the breakpoints involved in deletion of the *PU.1* gene in mice leading to AML.

Instead the breakpoints are located in clusters where the preponderance of breaks are found. Therefore, unless the entire cluster regions are in general closer than expected location, it represents a problem for the selection of the markers that best represented the breakpoint clusters, and for the same reason it is difficult to determine the minimal proximity of those markers.

In fact, I did not find differences between the proximity of the two regions represented for the selected markers compared in both mouse strains CBA/CaJ and C57BL/6.

The distribution of the distances showed similarities between the same cell types from both mouse strains: fibroblasts (CBA/CaJ); CBA/CaJ (BM) and C57BL/6J (BM); and CBA/CaJ (HSC) and C57BL/6J (HSC).

However, we did observe a shift in the distance distributions toward the closer distances in HSCs and BM compared with fibroblasts in both mouse strains.

In summary, there is a tissue-dependent distance distribution of the clusters. In other words, the average distance of the clusters in fibroblasts (2.55 um for CBA/CaJ and 3.09 um for C57BL/6) were larger than the distance in blood cells (1.74 um in BM and 1.53 um in HSC for CBA/CaJ; and 1.79 um in BM and 1.77 um in HSC for C57BL/6).

This tissue dependency is in concordance with the concept of tissue predisposition to certain kind of cancers where blood cells showed characteristics that could lead to AML but not present in fibroblasts. Perhaps, the difference would be that *PUI* loss would have no effect on fibroblasts.

References:

- [1] I. Major and R. Mole, "Myeloid leukaemia in x-ray irradiated cba mice," *Nature*, vol. 272, pp. 455–456, Mar 1978.
- [2] R. Mole and D. Papworth, "The dose-response for x-ray induction of myeloid leukaemia in male cba/h mice.," *British Journal of Cancer*, vol. 47, no. 2, p. 285, 1983.
- [3] J. Storer, T. Mitchell, and R. Fry, "Extrapolation of the relative risk of radiogenic neoplasms across mouse strains and to man," *Radiation Research*, vol. 114, no. 2, pp. 331–353, 1988.
- [4] I. Hayata, "Partial deletion of chromosome 2 in radiation-induced myeloid leukemia in mice.," *Progress and Topics in Cytogenetics[PROG. TOP. CYTOGENET.]*. ..., Jan 1984.
- [5] G. Breckon, A. Silver, and R. Cox, "Consistent chromosome changes in radiation-induced murine leukemias.," 1988.
- [6] A. Silver, W. Masson, J. Adam, G. Breckon, R. Cox, and E. Wright, "Chromosome-2 encoded genes in radiation-induced murine acute myeloid-leukemia," Jan 1988.
- [7] R. Cox, G. Breckon, A. Silver, W. Mason, and A. George, "Chromosomal changes: Radiation sensitive sites on chromosome 2 and their role in radiation myeloid leukaemogenesis in the mouse," *Radiation and Environmental Biophysics*, vol. 30, no. 3, pp. 177–179, 1991.
- [8] L. Thompson, D. Mitchell, J. Regan, S. Bouffler, S. Steward, W. Carrier, R. Nairn, and R. Johnson, "Cho mutant uv61 removes (6-4) photoproducts but not cyclobutane dimers," *Mutagenesis*, vol. 4, pp. 140–146, Jan 1989.
- [9] S. D. Bouffler, G. Breckon, and R. Cox, "Chromosomal mechanisms in murine radiation acute myeloid leukaemogenesis," *Carcinogenesis*, vol. 17, pp. 655–9, Apr 1996.
- [10] D. Clark, E. Meijne, and S. Bouffler, "Microsatellite analysis of recurrent chromosome 2 deletions in acute myeloid leukaemia induced by radiation in in f1 hybrid mice.," *Genes, Chromosomes and Cancer*, vol. 16, pp. 238–246, Jan 1998.

- [11] S. D. Bouffler, E. I. Meijne, D. J. Morris, and D. Papworth, "Chromosome 2 hypersensitivity and clonal development in murine radiation acute myeloid leukaemia," *Int J Radiat Biol*, vol. 72, pp. 181–9, Aug 1997.
- [12] F. Darakhshan, C. Badie, J. Moody, M. Coster, R. Finnon, P. Finnon, A. A. Edwards, M. Szluinska, C. J. Skidmore, K. Yoshida, R. Ullrich, R. Cox, and S. D. Bouffler, "Evidence for complex multigenic inheritance of radiation aml susceptibility in mice revealed using a surrogate phenotypic assay," *Carcinogenesis*, vol. 27, pp. 311–8, Feb 2006.
- [13] K. Rithidech, V. Bond, E. Cronkite, and M. Thompson, "A specific chromosomal deletion in murine leukemic cells induced by radiation with different qualities.," *Experimental Hematology*, vol. 21, pp. 427–431, Jan 1993.
- [14] A. Silver, J. Moody, R. Dunford, D. Clark, and S. Ganz, "Molecular mapping of chromosome 2 deletions in murine radiation-induced aml localizes a putative tumor suppressor gene to a 1.0 cm region homologous to human chromosome segment 11p11-12," *Genes Chromosomes and Cancer*, vol. 24, pp. 95–104, Jan 1999.
- [15] R. Finnon, J. Moody, E. Meijne, J. Haines, D. Clark, A. Edwards, R. Cox, and A. Silver, "A major breakpoint cluster domain in murine radiation-induced acute myeloid leukemia.," *MOLECULAR CARCINOGENESIS*, vol. 34, pp. 64–71, Jun 2002.
- [16] W. D. Cook, B. J. McCaw, C. Herring, D. L. John, S. J. Foote, S. L. Nutt, and J. M. Adams, "Pu.1 is a suppressor of myeloid leukemia, inactivated in mice by gene deletion and mutation of its dna binding domain," *Blood*, vol. 104, pp. 3437–44, Dec 2004.
- [17] M. Nikiforova, J. Stringer, R. Blough, M. Medvedovic, J. Fagin, and Y. Nikiforov, "Proximity of chromosomal loci that participate in radiation-induced rearrangements in human cells," *Science*, vol. 290, pp. 138–141, Jan 2000.
- [18] T. Cremer and C. Cremer, "Chromosome territories, nuclear architecture and gene regulation in mammalian cells," *Nat Rev Genet*, vol. 2, pp. 292–301, Apr 2001.
- [19] T. Cremer, K. Kupper, S. Dietzel, and S. Fakan, "Higher order chromatin architecture in the cell nucleus: on the way from structure to function," *Biol Cell*, vol. 96, pp. 555–567, Jan 2004.
- [20] T. Cremer, M. Cremer, S. Dietzel, S. Müller, I. Solovei, and S. Fakan, "Chromosome territories—a functional nuclear landscape," *Current Opinion in Cell Biology*, vol. 18, pp. 307–16, Jun 2006.

- [21] J. Mateos-Langerak, S. Goetze, H. Leonhardt, T. Cremer, and M. Cremer, "Nuclear architecture: Is it important for genome function and can we prove it?," *Journal of cellular Biochemistry*, vol. 102, pp. 1067–1075, Jan 2007.
- [22] R. Zinner, K. Teller, R. Versteeg, T. Cremer, and M. Cremer, "Biochemistry meets nuclear architecture: multicolor immuno-fish for co-localization analysis of chromosome segments and differentially expressed gene loci with various histone methylations," *Adv Enzyme Regul*, vol. 47, pp. 223–41, Jan 2007.
- [23] J. Rouquette, C. Genoud, and G. Vazquez-Nin, "Revealing the high-resolution three-dimensional network of chromatin and interchromatin space: a novel electron microscopic approach to reconstructing nuclear architecture.," *Chromosome Research*, vol. 17, pp. 801–810, Jan 2009.
- [24] D. Koehler, V. Zakhartchenko, L. Froenicke, G. Stone, R. Stanyon, E. Wolf, T. Cremer, and A. Brero, "Changes of higher order chromatin arrangements during major genome activation in bovine preimplantation embryos," *Experimental Cell Research*, vol. 315, pp. 2053–2063, Jan 2009.
- [25] J. Bedford and M. Muhlmann-Diaz, "Damage selectivity in chromosomes," *In Radiation Research: A Twentieth Century Perspective (W. C. Dewey, M. Edington, R. J. M. Fry, E. J. Hall and G. F. Whitmore, Eds.)*, pp. 212–216, Academic Press, San Diego 1992.
- [26] M. Muhlmann-Diaz, "Chromatin structure and ionizing radiation induced chromosome aberrations," 1993.
- [27] M. Muhlmann-Diaz and J. Bedford, *A comparison of radiation-induced aberrations in human cells involving early and late replicating X chromosomes*. In *Chromosomal Alterations*; ed. Obe, G and Natarajan, AT-Springer Verlag, New York, pp 125-131, 1994.
- [28] M. Muhlmann-Diaz and J. Bedford, "Breakage of human chromosomes 4, 19 and y in G0 cells immediately after exposure to gamma-rays," *International journal of Radiation Biology*, vol. 65, pp. 165–173, Jan 1994.
- [29] G. Holmquist, "Chromosome bands, their chromatin flavors, and their functional features," *American Journal of Human Genetics*, vol. 51, pp. 17–37, Jan 1992.
- [30] S. Kozubek, L. Ryznar, M. Kozubek, R. Govorun, E. Krasavin, and G. Horneck, "Distribution of abl and bcr genes in cell nuclei of normal and irradiated lymphocytes," *Blood*, vol. 89, pp. 4537–4545, Jun 1997.

- [31] J. Down, A. Boudewijn, R. V. Os, H. Thames, and R. Ploemacher, "Variations in radiation sensitivity and repair among different hematopoietic stem cell subsets following fractionated irradiation," *Blood*, vol. 86, no. 1, p. 122, 1995.
- [32] D. Bryder, D. Rossi, and I. Weissman, "Hematopoietic stem cells: the paradigmatic tissue-specific stem cell," *American Journal of Pathology*, vol. 169, no. 2, p. 338, 2006.
- [33] I. Shuryak, R. Sachs, L. Hlatky, M. Little, P. Hahnfeldt, and D. Brenner, "Radiation-induced leukemia at doses relevant to radiation therapy: modeling mechanisms and estimating risks," *JNCI Journal of the National Cancer Institute*, vol. 98, no. 24, p. 1794, 2006.
- [34] M. Wicha, S. Liu, and G. Dontu, "Cancer stem cells: an old idea—a paradigm shift," *Cancer research*, vol. 66, no. 4, p. 1883, 2006.
- [35] A. J. Simonnet, J. Nehmé, P. Vaigot, V. Barroca, P. Leboulch, and D. T.-L. Roux, "Phenotypic and functional changes induced in hematopoietic stem/progenitor cells after gamma-ray radiation exposure," *Stem Cells*, vol. 27, pp. 1400–1409, Jun 2009.

CHAPTER III

THE ORGANIZATION OF MOUSE CHROMOSOME 2: INTERPHASE CELL DOMAINS.

INTRODUCTION

3.1-Chromosome Domains Organization

In the previous chapter, I reported results where I measured and compared interphase distances between the proximal (pbc) and distal breakpoint clusters (dbc) surrounding the radiation induced PU.1 gene deletions associated with AML development on mouse chromosome 2 in cells from the bone marrow as well as fibroblasts from CBA and C57BL/6 mice.

The purpose was to test the hypothesis that much closer distances in the location of these regions of chromosome 2 in normal bone marrow from CBA vs C57BL/6 mice might explain or partly account for the radiation susceptibility of CBA mice to AML relative to C57BL/6 mice.

The measurements did not show any such systematic differences in these distances, nor were there any differences between mouse strains for distances measured in fibroblasts. However, an interesting observation that arose from the measurements was that the mean distances between the pbc and dbc were apparently not random but there appeared to be a systematic difference in the interphase distances of the two homologs of chromosome 2.

Examination of organization of chromatin in interphase nuclei has been made possible by whole chromosome painting^(1,2). Chromosome painting has had an important role in the development of the concept of “chromosomal territories” (Cremer, T: *Nat Rev Genet.* 2001 Apr;2(4):292-301)⁽³⁾, because they allow direct visualization of these chromosomal territories and show the boundaries and position of the chromosomal domains in the interphase nuclei.

The conformation and the position of the domains are not random and their organization is partly determined depending on the gene-content of the chromosome⁽⁴⁾. As a clear example, those chromosomes that are gene-rich are located more towards the center of the cell nuclei while, the gene-poor chromosomes are located towards the periphery of the nuclei⁽⁵⁾. Another observation related to the genetic activity of the chromosome has been demonstrated in relation to the X-chromosome in mammals.

In mammalian females there is an inactivation of one of the X-chromosomes inherited from the parents. This inactivation leads to a high degree of silencing of expression of only one of the X-homologs^(6,7). The visualization of the X-active (Xa) chromosome domain and the inactive (Xi) through chromosome painting showed a quite different “organization” in human interphase cells^(3,6-9).

Xa territories or domains are described as “open chromatin” and the geometry of the BAC markers showed a disperse organization. In contrast, the inactive Xi territories or domains are more compact and the organization of BACs markers showed closer proximities between them compared to Xa territories^(3,9), as would be expected from the original observation of the “Barr Bodies”⁽¹⁰⁾ and the association with lack of X-linked gene expression in one X homolog in females by Lyon as mentioned above⁽⁶⁾.

The previous observation described in chapter 2 of the domains revealed by FISH with BAC probes and chromosome domain paints of mouse chromosome 2 in interphase cells that recalls the appearance of Xa and Xi described above. Both the BACs markers organization within each chromosome territory as well as the chromosome painting, which delineated the actual borders of the territories, appears to have a different organization similar to Xa territories and Xi territories.

Thus, the nuclear architecture is highly influenced by the organization of the active and potentially active chromatin and the inactive heterochromatin.

Several authors have reported evidence for the dependence of sensitivity to ionizing radiation on the transcriptional activity and structural status of chromatin in the nucleus⁽¹¹⁻¹⁶⁾. Barrios⁽¹¹⁾, as well as Holmquist⁽¹²⁾ and later Folle⁽¹⁷⁾ 1998 showed that the preponderance of radiation induced exchange breakpoints occurred in chromatin from G-light band regions which are rich in transcriptional activity⁽¹⁸⁾ relative to the less frequent occurrence of breakpoints in G-dark band heterochromatin.

According to the study of Folle, after treatment with different agents such as DNase I, gamma-rays and restriction enzymes the distribution of breakpoints were preferentially

found in euchromatic region compared to heterochromatic region.

Within the same line of research in 2001 Martinez-Lopez published⁽¹⁹⁾ interesting results showing the localization of breakpoints in chromatin with hyper-acetylated histone H4, that represents active chromatin as opposed to the more compact chromatin containing hypo-acetylated histone H4 that occurs predominantly in the inactive heterochromatin.

In addition, in cells from patients with Klinefelter's syndrome, radiation induced exchanges between autosomes and the inactive supernumerary X-chromosomes occur very rarely, if at all, whereas expected numbers of such exchanges occur involving the active X chromosome as reported by Muhlmann-Diaz & Bedford⁽¹⁵⁾.

There is also evidence that asymmetric intrachanges leading to interstitial deletions occur more frequently in highly transcriptionally active artificial chromosomes⁽¹³⁾.

The question that these studies suggests is whether a preferential distribution of breakpoints play any role in the fact that the deletion in mouse chromosome 2 occurs more frequently in one of the homologs?

The spatial arrangement of genes and chromosomes within the nucleus is nonrandom and this generates a pattern. Therefore, the architecture and organization of the chromatin in the nucleus is tissue-specific and determine what set of genes will be sharing some positions in the nucleus to become actively transcribed or actively silenced. Thus, this organization could also affect the probability that certain radiation induced deletions or exchanges would be more or less likely to be produced.

In other words, since the set of genes that are actively transcribed in, for instance, an epithelial cell are different than those needed in a blood cell, then the genes that are active in the one cell type could be inactive in the other affecting the interphase architecture and organization providing unique tissue-specific features; so while the average frequency of all aberrations may be the same or close to the same for two cell types the *particular* yield of certain specific aberrations might be very different.

As already mentioned in experiments of the previous chapter (chapter 2), we measured the physical distances between the two breakpoint clusters in interphase cells and it became immediately apparent that in all the cells, one chromosome 2 domain was considerably smaller than the other and the distances between the markers were smaller in one domain than the other.

The basic observation of a different organization of mouse chromosome 2 domains in interphase cells and the BAC markers within them is illustrated in figure 3.1 below, where the appearance of active and inactive X chromosomes is also shown as a comparative reference.

Panel a is an interphase hematopoietic stem cell (cells enriched from bone marrow) where the signal from the dbc appears in red, the signal from the pbc appears green, and the *PU.1* containing BAC is aqua.

The whole chromosome 2 paint appears orange and the cell is counterstained with DAPI (blue).

Panel b is the same scheme and preparation but is an interphase cell from the unseparated bone marrow.

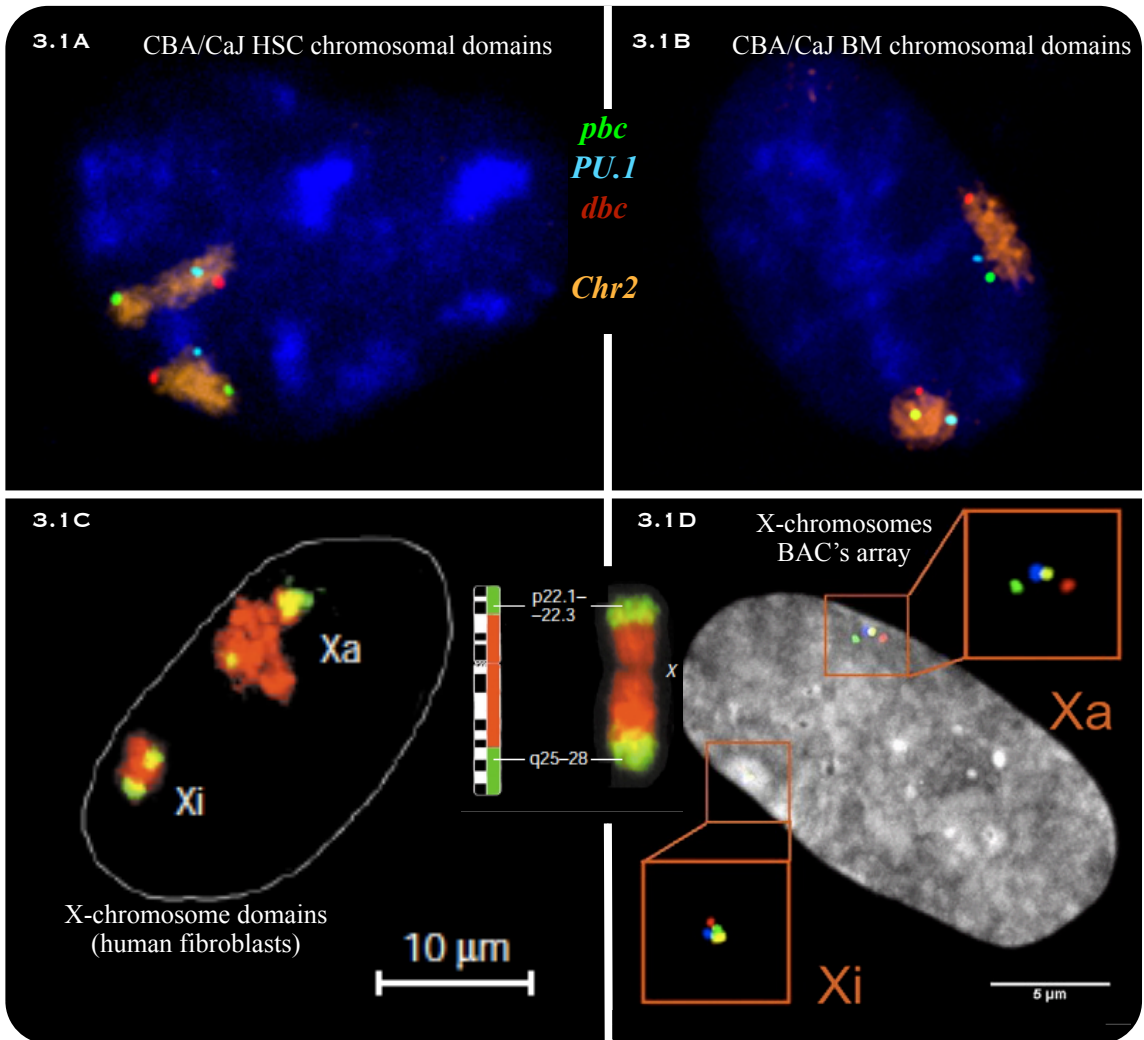


Figure 3.1: Chromosomal Domains: a) Hematopoietic stem cell and b) bone marrow from CBA/CaJ mice showing both large and small chromosome 2 domains. In comparison, c) shows active (Xa) and inactive (Xi) X-chromosome domain from female human fibroblast (Cremer et al 2001); and d) 4 BAC's array showing Xi and Xa from Yang et al 2008. NOTES: *pbc*: proximal breakpoint cluster (Green), *PU.1* (Cyan), *dbc*: distal breakpoint cluster (Red), and chromosome 2 paints (Orange) in a) and b).

Panel c was taken from Cremer et al 2001 showing both active and inactive X-chromosome territories from human female interphase fibroblasts through chromosome paints (red) and distal band (green) from the q- and p-arms.

Panel d: human female interphase nucleus showing the organization of 4 BAC probes within the active (Xa) and inactive (Xi) chromosome X territories (Yang et al 2008).

As a result of the consideration that the distances between pbc's and dbc's may be different for the two homologs of chromosome 2 within the same cell, the data was reanalyzed to determine if such differences between homologs was present, and if so, whether a subset of cells with close proximities might account for the AML differential chromosomal sensitivities might emerge.

Since the distributions of distances appeared to have a bimodal appearance, I decided to separate the measurements of breakpoint cluster markers into two separate sets of data: one for what appeared to be the smaller domain and the other for the larger domain in each cell.

Therefore, CBA/CaJ and C57BL/6J mouse strains in the present chapter are compared in relation to the breakpoint clusters distances in fibroblasts, bone marrow, and progenitor cells. This is outlined in the Specific Aims below.

3.2-Hypothesis

The distance distributions of the breakpoint clusters is associated with the characteristic organization of the two homologs that are referred as small and large domain; therefore, the small domain will shows closer distances of the breakpoint clusters compared to the large domain.

3.3-Specific Aims

Specific Aim 1: Measure the physical projected distances between labeled chromosome 2 BAC-probes used as markers of the “proximal breakpoint cluster” and “distal breakpoint cluster” and analyze them in separate groups designated “small domain group” and “large domain group. This analysis was performed in both CBA/CaJ and C57BL/6J mouse strains.

Specific Aim 2: Determine differences in the distance distributions of the breakpoint clusters within the small and large domain to compare them in all three cell types (fibroblasts, BM and HSC interphase cells) from both mouse strains. The distances of the two markers would reflect differences between different cell types showing distinct arrangement within the interphase nuclei architecture and organization in both CBA/CaJ and C57BL/6J mouse strains.

3.4-Results

3.4.1-Chromosomal Territories: Features of Chromosome 2 Domains in

Interphase. Determination of Distances within Small and Large Domains.

Distance measurements in the XY, YZ, and XZ planes between red (pbc) and green (dbc) signal pairs were then made against a standard calibrated micrometer and distance distribution histograms prepared as described in chapter 2. The image acquisition of the interphase cells makes evident the different organization of chromosome 2 territories described in this chapter. This feature is evident when using chromosome paints probes along with the above mentioned BAC-probes that define the organization of the chromatin domain in regions proximal, central, and distal with respect to the linear chromosome. One chromosome 2 territory was considerably smaller or more compact than the other homolog within the same cell. In addition, the organization of BAC-probes used as markers showed a differential organization within the territories, providing a unique characteristic to recognize the small or large chromosome 2 domain within an interphase nucleus (figure 3.2). The analysis of data from normal non-irradiated cells showed that the small domain was more compact or closed and smaller than its homolog and contained the three markers forming a triangular organization and filling the whole chromosomal domain. In contrast, the large domain showed an elongated shape in which the markers were located along the elongated domain running linearly from centromere to telomere.

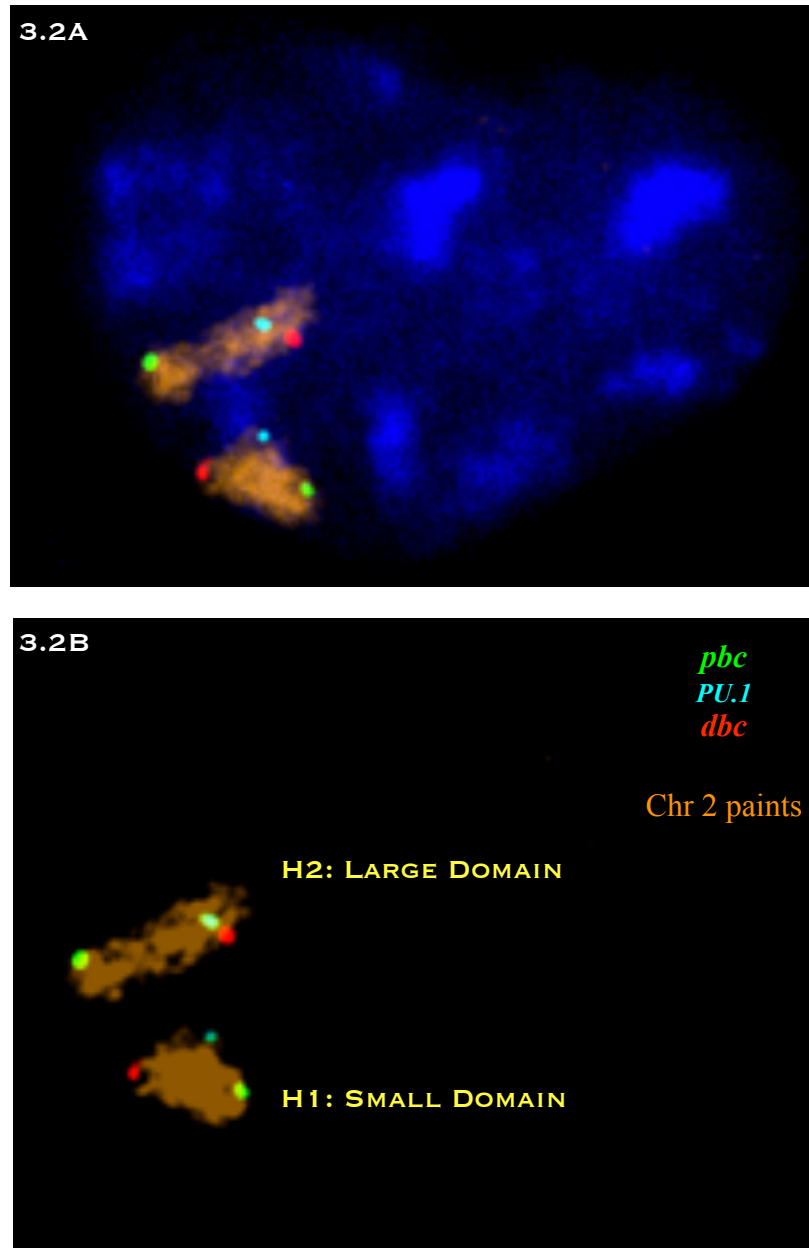


Figure 3.2: Chromosome 2 domains: a) CBA/CaJ interphase HSC cell and b) same cell showing chromosomal domains plus markers organization within the large and small domain.

Thus, within each cell I refer to the chromosomal domain that is more compact and showed the closest proximities of the breakpoint clusters as small domain; whereas, the large domain refers to the domain which is more extended, less compact, and showed the larger distances between the two breakpoint clusters.

3.4.2-Chromosomal Territories: Features of Chromosome 2 Domains in Fibroblasts, BM and Stem Cells from CBA/CaJ and C57BL/6J.

As I mentioned above the analysis of interphase cells showed a differential organization of the homologs was present in all cell types and both mouse strains.

The chromosome territories of both chromosome 2 were different in shape and organization showing the small and large domain is not a characteristic feature of a particular mouse strain or cell type. Thus, this qualitative feature is present in bone marrow, HSC and fibroblasts showing consistency within all cells analyzed in both CBA/CaJ and C57BL/6 mouse strain.

Some of the nuclei that showed overlapping of domains and some other cells showed replication of the markers (implicating the cell cycle progression in those cells) were not taken into the analysis or scoring procedure.

The qualitative similarity of the above feature of two chromosome 2 domains was present in all cell types and in both mouse strain and was also present in cells that acquire additional copies of chromosome 2.

This additional evidence was apparent in polyploid fibroblasts (generally present in cultured fibroblasts). When I analyzed these tetraploid fibroblasts I observed that these fibroblasts still kept the small and large domains (figure 3.3).

Even though there were four copies of chromosome 2, two had the small domain configuration and two had the large domains configuration in the tetraploid interphase cells.

After an average of 25 diploid cells were analyzed per cell type, all the cells showed the same organization where the small domain has a triangular order of the three BAC-probes and the large domain showed a more linear configuration of the probes.

3.4.3-Normalization Values of Small and Large Domain: Ratio of Distance Values for Large versus Small Domains.

The qualitative feature observed for chromosome 2 homologs is represented in a quantitative way as well by the normalization values calculated through the ratio of the cluster distances obtained from both domains (these data tables of the measurements are summarized in appendix I).

In a very high proportion of the measurements, the large domain (H2) showed pbc to dbc distances that were larger than the distances of pbc to dbc in the small domain (H1) within the same cell.

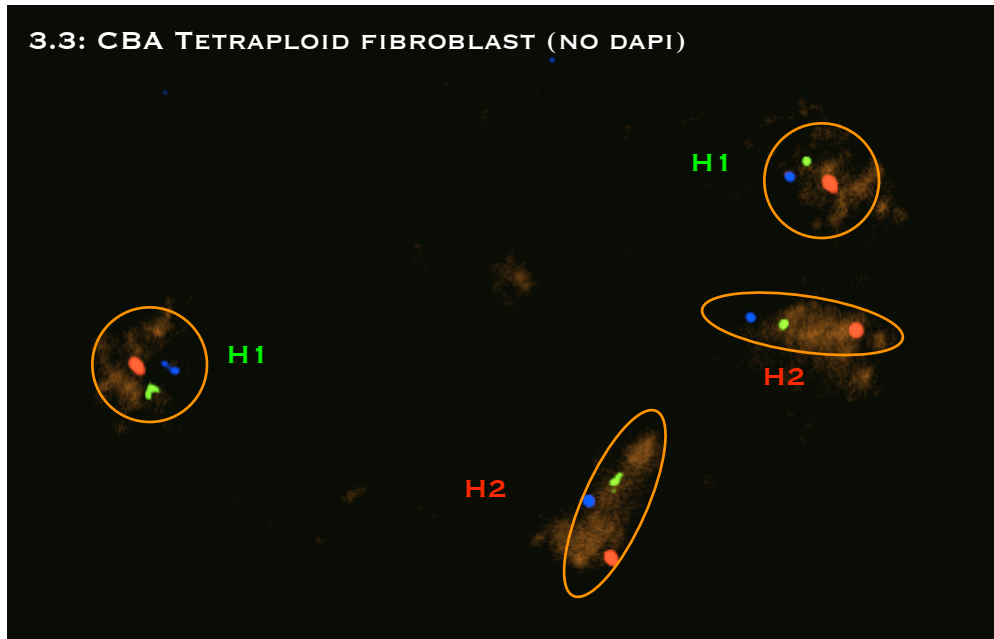
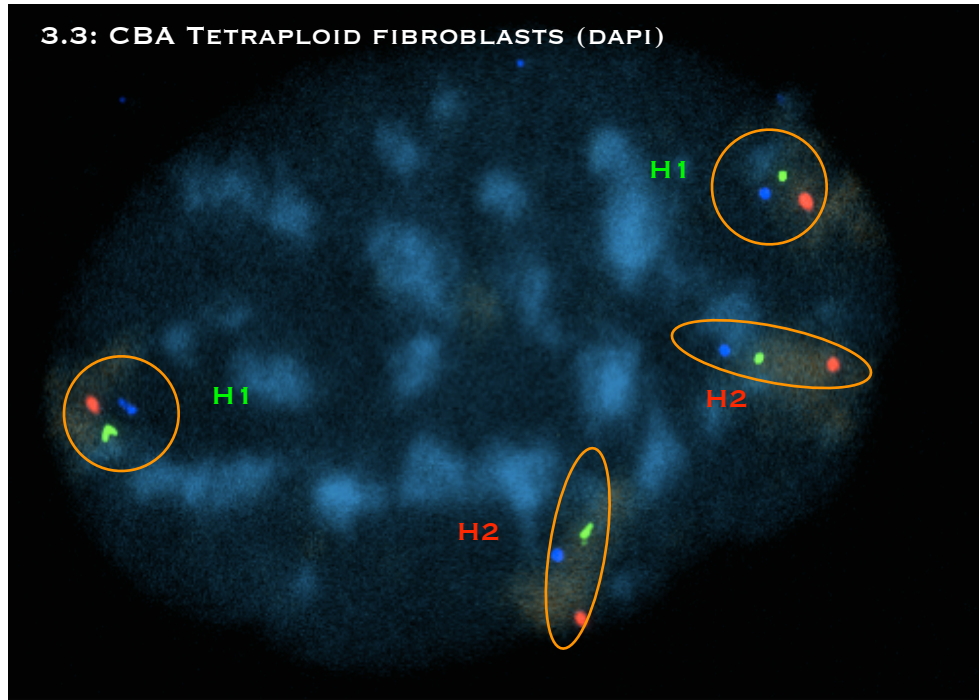


Figure 3.3: Tetraploid fibroblast (from CBA/CaJ) showing the organization of the 4 chromosomal domain (2 small domains and 2 large domains) within the same cell. Green (dbc), blue (PU.1), and red (dbc), orange (chr2 domains). H1: Small domain, H2: Large domain.

Therefore, within a given cell one homolog shows shorter distance (H1) between the clusters when compared with the other homolog that always shows the largest distance (H2) between the two breakpoint clusters. To quantify the qualitative data I normalized the values obtained for the small and large domains by calculating the ratio of the distances measured in the large domain to that for the small domain (L/S) in the same cell.

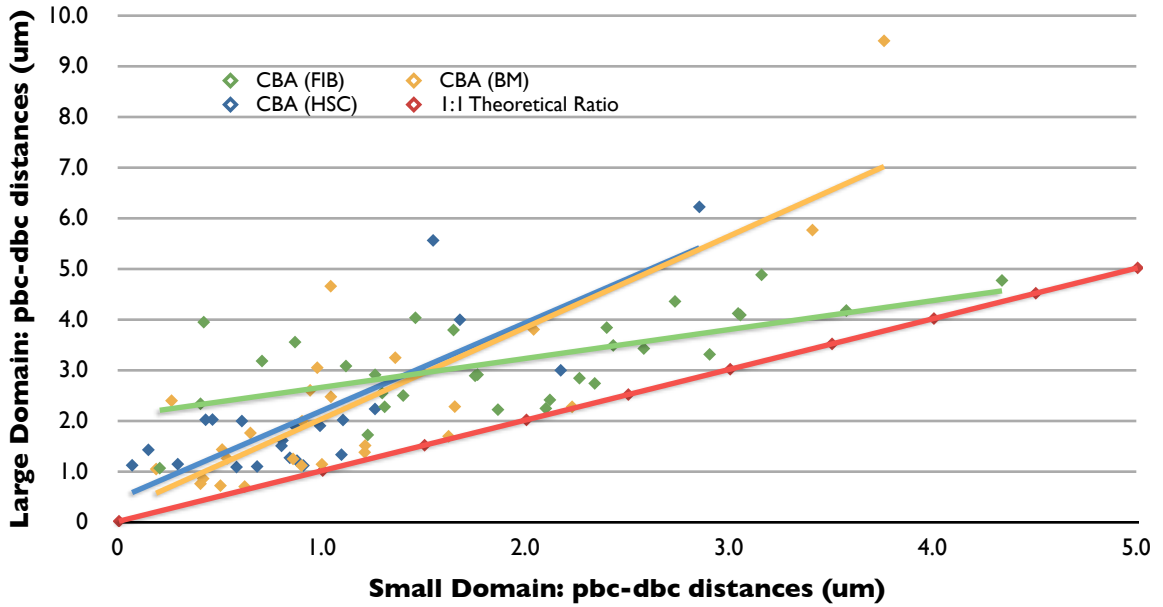
Thus, obtaining a ratio of 1 or ~ 1 indicates that the distances within both the large and small domain are equal.

If the average of the ratio over many cells is around 1 then presumably there is no particular correlation between distances and domain shapes. However, obtaining an average value larger than 1 over many cells, means that the two domains are different within individual cells.

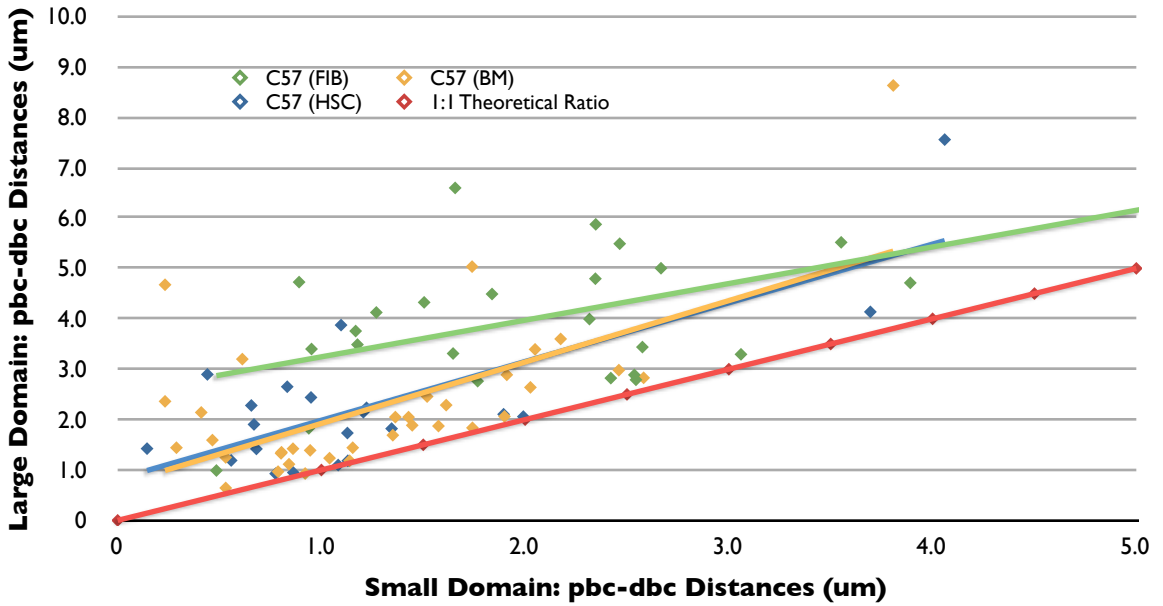
This is a clearer way to present the data, because average pooled measurements made without reference to the cell where measurements were made, could yield some cells with two small distances some with two large distances and some with one small and one large distance with no difference related to a difference in distances within one or another homolog.

The figure 3.4 and figure 3.5 below shows the ratio (L/S) on a cell by cell basis for each cell type from CBA/CaJ and C57BL/6J respectively. In addition, figure 3.6 and figure 3.7 shows the percentage of measurements showing the different range ratio (L/S) taken into consideration all cell type together from CBA/CaJ and C57BL/6J.

3.4 Large Domain vs Small Domain (CBA/CaJ)

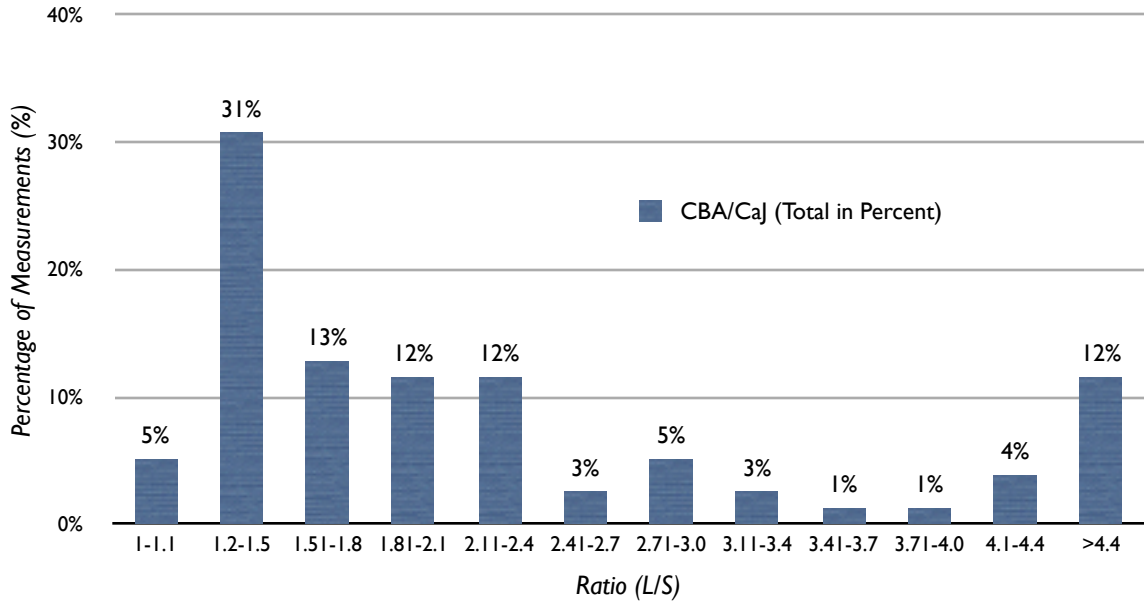


3.5 Large Domain vs Small Domain (C57BL/6J)

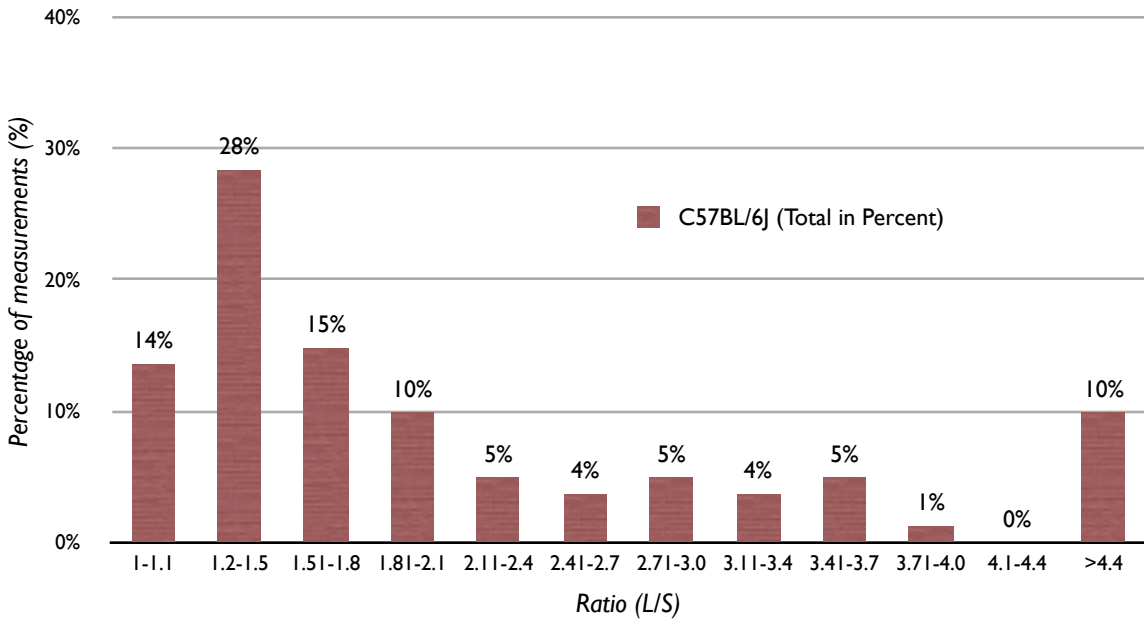


Figures 3.4, and 3.5: Ratio (large/small) calculated in each cell type group in CBA/CaJ (fig. 3.4) and C57BL/6J (fig. 3.5). Fibroblasts (green); bone marrow (yellow); and hematopoietic precursors (blue). Theoretical ratio (red) when small=large=1.

3.6 CBA/CaJ Normalization (L/S) (Percent %)



3.7 C57BL/6J Normalization (L/S) [Percent %]



Figures 3.6 and 3.7: Ratio (L/S) taken all cell types together in CBA/CaJ (figure 3.6) and C57BL/6J (figure 3.7). Percentage of cells.

3.4.4-Breakpoint Cluster Distances in Fibroblasts:

CBA/CaJ versus C57BL/6J Mouse Strains

As shown in figure 3.8, the distances distribution within fibroblast small domains (H1) showed that 20% of the measured distances were between 1.2 to 1.6 μm . In addition, there is a second peak in the distribution that contained 17% of the measured values ranging from 2 to 2.39 μm . The range covered for the distribution within the small domain was from 0.2 to 4.39 μm . Finally, the average value obtained for the small domain (H1) was: $H1_{\text{CBA/CaJ(FIB)}} = 1.92 \mu\text{m}$ and the standard deviation of 0.99 μm .

On the other hand, the large domain (H2) in CBA/CaJ showed values bigger than 1 μm covering a wide range up to about 9 μm of separation. The distances more represented were between 2.8 and 3.19 μm in 20% of the large domains measured. In addition, two more peaks were observed in the ranges of 2-2.39 μm , and 4-4.39 μm ; each with 17% of measurements. The average value calculated for the large domain was $H2_{\text{CBA/CaJ(FIB)}} = 3.17 \mu\text{m}$, and the standard deviation of the measurements for H2 is 0.91 μm (figure 3.8).

By comparison with CBA/CaJ; the values from C57BL/6 showed a shift toward larger values in the distance distribution histogram.

Figure 3.9 shown below, displays the distance distribution for the small domain (H1) in C57BL/6J fibroblasts. The distribution of the values covered a range from 0.4 to 5 μm . Within this set, 24% of distance measurements falls into values between 2.4 to 2.79 μm . Furthermore, a second peak (20%) is observed within the range 0.8-1.19 μm .

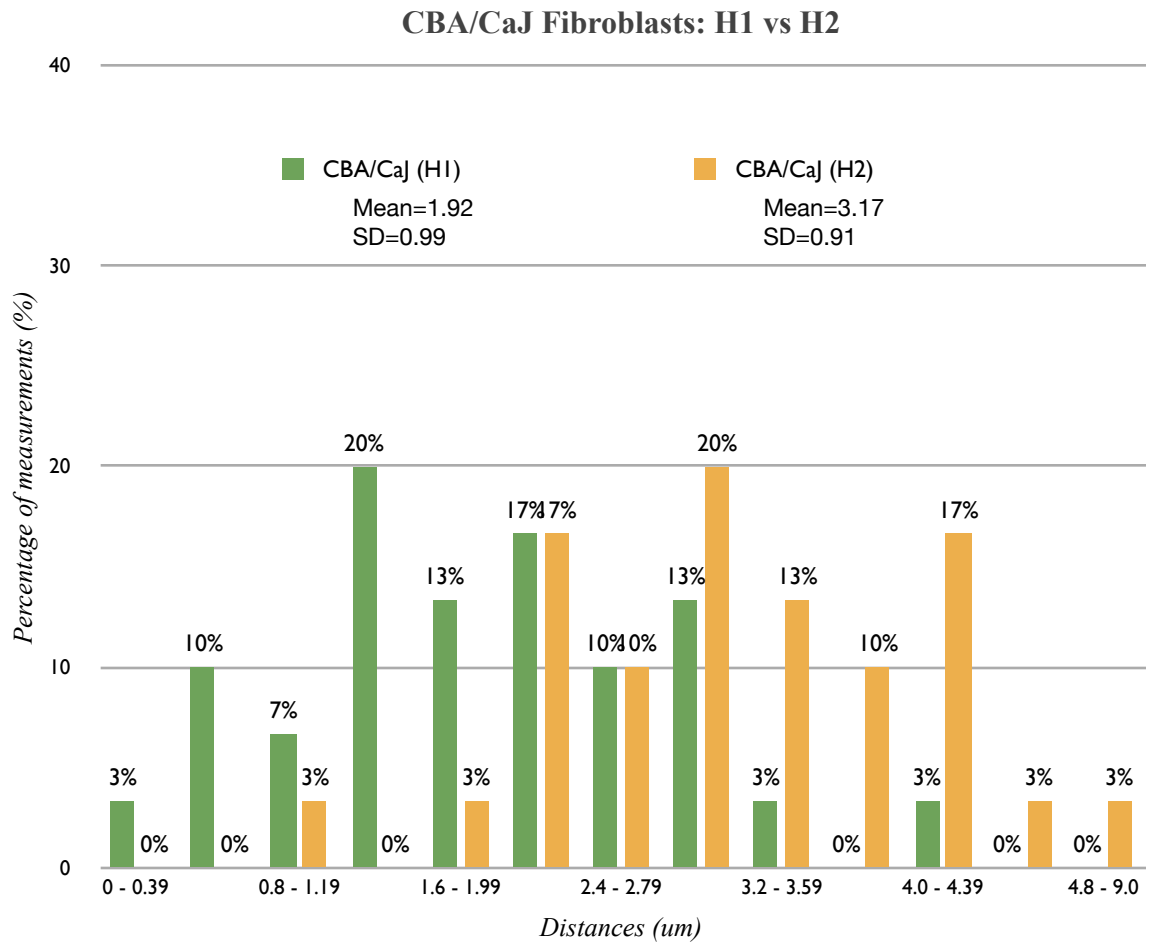


Figure 3.8: Distances distribution from pbc-dbc within the small domain (H1) and large domain (H2) in interphase fibroblasts obtained from CBA/CaJ mouse strain.

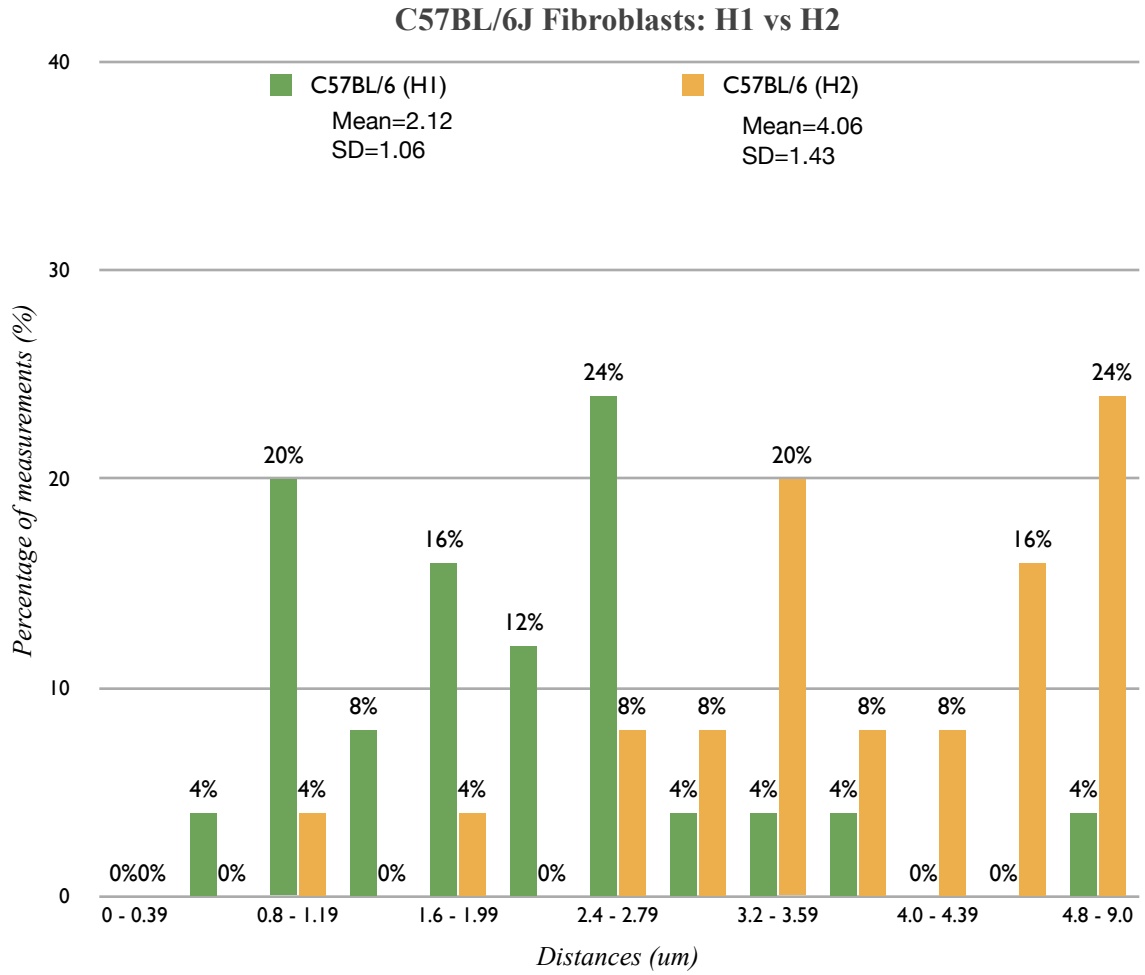


Figure 3.9: Distances distribution from pbc-dbc within the small domain (H1) and large domain (H2) in interphase fibroblasts obtained from C57BL/6J mouse strain.

The corresponding average for the small domain (H1) was $H1_{C57BL/6(FIB)} = 2.12 \text{ um}$ and the standard deviation was 1.06 um. Values of the large domain (H2) have shown separation distances of the clusters up to 7.1 um. Moreover, from all the measurements within the large domain, there were some 24% that showed distances between 4.8 to 7.1 um. Another peak (20%) was observed within the range 3.2-3.59 um. Consequently, the average value of distance distribution for C57BL/6 was $H2_{C57BL/6(FIB)} = 4.06 \text{ um}$ and the standard deviation was 1.43 um.

3.4.5-Breakpoint Cluster Distances Measurements in Bone Marrow:

CBA/CaJ versus C57BL/6J Mouse Strains

As shown in figure 3.10, the average distances measured in these bone marrow cells showed a shift in both small, and large domains showing, in general, shorter distances when compared with the distances of the clusters in fibroblast domains. Thus, the average distance in CBA for the small domain $H1_{CBA/CaJ(BM)} = 1.16 \text{ um}$ and a standard deviation of 0.88 um. In the small domain (H1) some 31% of measurements between pbc and dbc were within a range of 0.8 to 1.19 um apart. A second peak of 27% was observed within the range 0.4-0.79 um. The total distribution showed values from 0.18 to 3.76 um. Finally, only 8% of the measurements were less than 0.39 um. In contrast, the large domain (H2) showed distances within the range of 1.2 to 1.59 um in 19% of the measurements and within 0.8-1.19 um range in 15%. There were no values less than 0.4 um (figure 3.10).

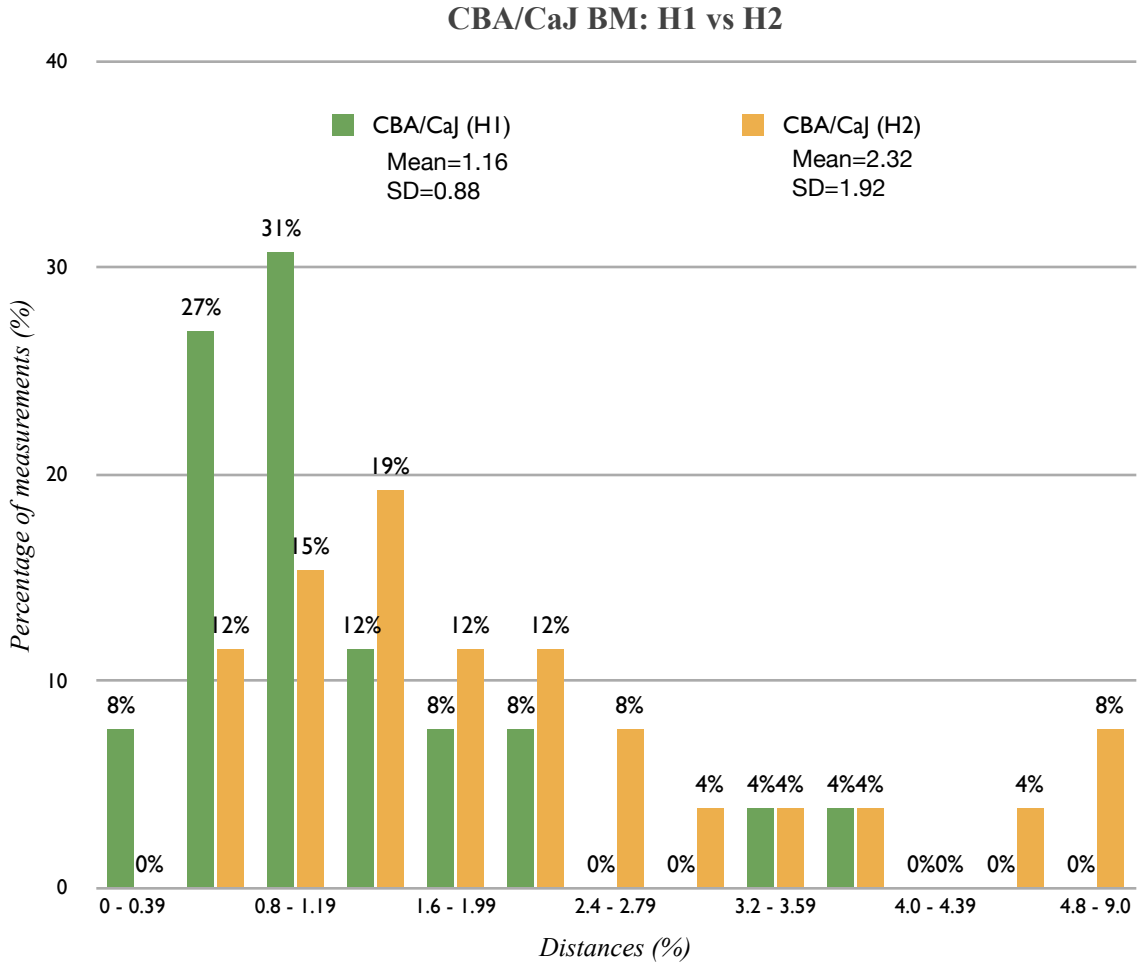


Figure 3.10: Distances distribution from pbc-dbc within the small domain (H1) and large domain (H2) in interphase bone marrow (BM) cells obtained from CBA/CaJ mouse strain.

The total distribution covered values from 0.684 to 9.481 μm and the average for this group was $H2_{\text{CBA/CaJ(BM)}} = 2.32 \mu\text{m}$ and the standard deviation was 1.92 μm .

For C57BL/6 BM the values of the small domain (H1) covered a range from 0.233 to 3.8 μm distance between the two clusters.

The most frequent values were in the range 0.8 to 1.19 in 26% of the measurements. Additionally, two more peaks of 17% each were observed within the ranges 0.4-0.79 μm and 1.2-1.59 μm .

Distance values smaller than 0.4 μm were observed only in 9% of the measurements.

The average value for the small domain was $H1_{\text{C57BL/6(BM)}} = 1.29 \mu\text{m}$ and the standard deviation for the group was 0.78 μm .

The large domain (H2) showed values skewed toward the largest distances compared to the values of the small domains (H1) (figure 3.11).

The grouped data H2 showed values from 0.643 to 8.63 μm having 26% of the measurements represented within the range 1.2 to 1.59 μm and a second peak (17%) within the distance range of 2-2.39 μm .

There were no measurements with values smaller than 0.4 μm .

Consequently, the average value for the large domain in bone marrow from C57BL/6 was $H2_{\text{C57BL/6(BM)}} = 2.28 \mu\text{m}$ and the standard deviation was 1.49 μm .

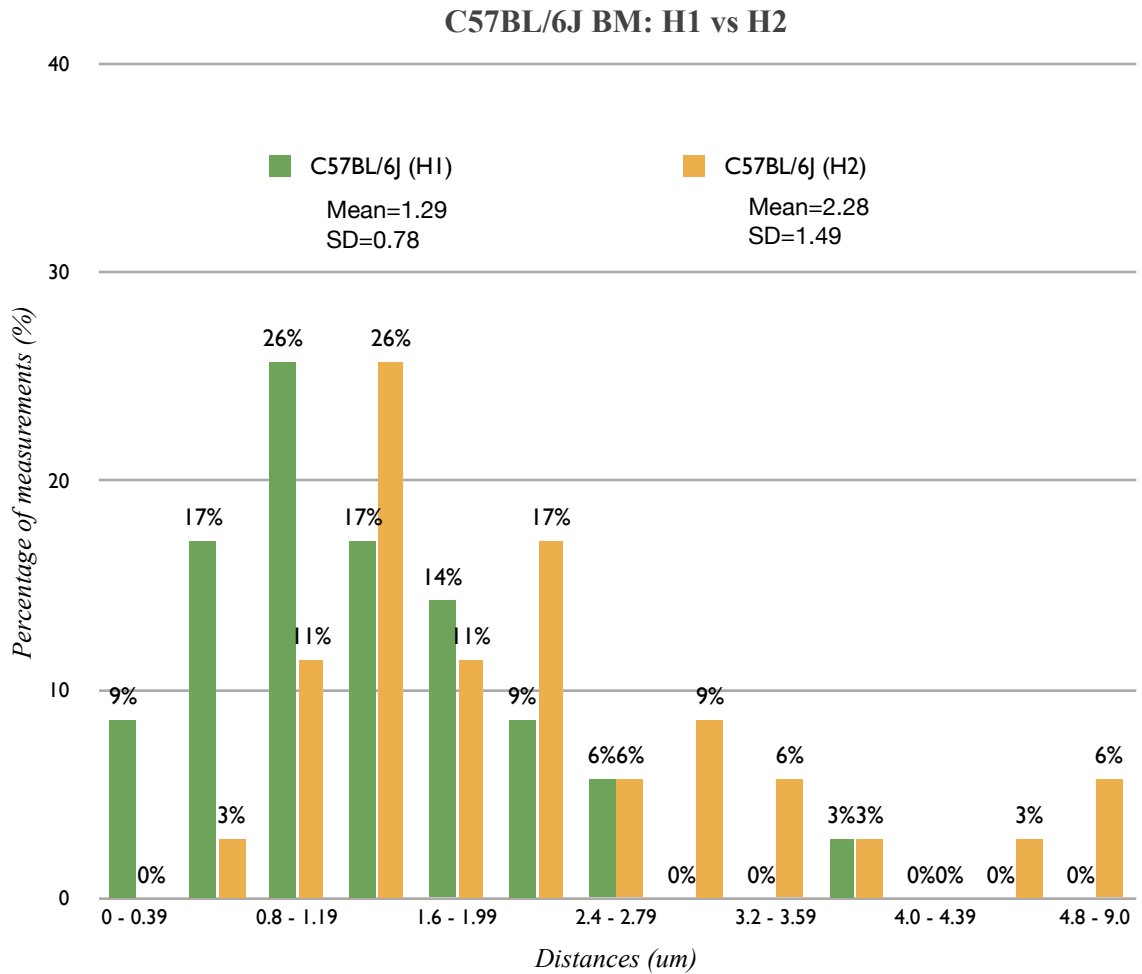


Figure 3.11: Distances distribution from pbc-dbc within the small domain (H1) and large domain (H2) in interphase bone marrow (BM) cells obtained from C57BL/6 mouse strain.

3.4.6-Breakpoint Cluster Distances in Hematopoietic Stem Cells (HSC):

CBA/CaJ versus C57BL/6J Mouse Strains

As shown in figure 3.12, the comparison of the measurements distribution between CBA/CaJ and C57BL/6J hematopoietic stem cells (HSCs) gave no bigger differences between the distances of the two probes within these cells compared to the whole bone marrow cells. The distance distributions appeared to be similar to the distribution seen in bone marrow cells. The average distance for the clusters within the small domain (H1) in CBA/CaJ was $H1_{CBA/CaJ(HSC)} = 0.95$ μm and a standard deviation of 0.65 μm . There were 36% of the measurements within the small domain (H1) that fall within the value range of 0.8-1.19 μm and 27% into the range 0.4-0.79 μm .

Besides, 14% of the measurements were within values < 0.4 μm . The total distribution showed values that covered distances from 0.065 μm to 2.85 μm .

On the other hand, the large domain (H2) from CBA/CaJ showed an average distance value of $H2_{CBA/CaJ(HSC)} = 2.11$ μm and a standard deviation of 1.4 μm .

The distances distribution showed 27% of the measurements fall into the range of 0.8-1.19 μm and a second peak with 23% into the range 1.2-1.59 μm . Values smaller than 1 μm were not observed. Finally, the total distribution within the large domain in CBA/CaJ covered values from 1.07 μm to 6.2 μm (figure 3.12).

The values corresponding to C57BL/6J were very similar to the values obtained from hematopoietic stem cells from CBA/CaJ.

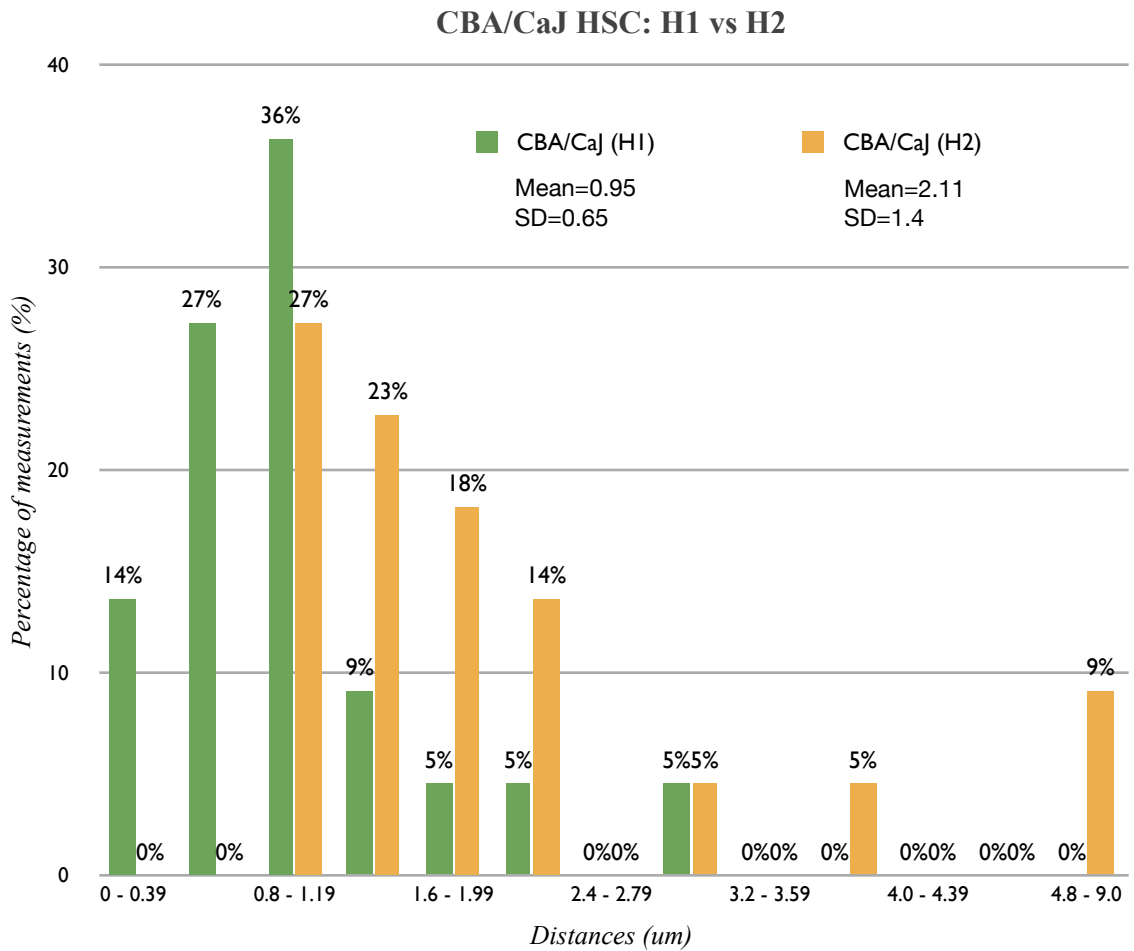


Figure 3.12: Distances distribution from pbc-dbc within the small domain (H1) and large domain (H2) in interphase hematopoietic progenitors (HSC) obtained from CBA/CaJ mouse strain.

Thus, the average distance within the small domain (H1) for HSC in C57BL/6J was $H1_{C57BL/6J(HSC)} = 1.26$ μm and the standard deviation 0.97 μm (figure 3.13).

The distribution within H1 showed a total range that covered from 0.144 to 4.059 μm , presenting 33% of the measurements into the range between 0.8 and 1.19 μm of distance, the second peak (29%) was observed in the range 0.4-0.79 μm . In addition, 5% of the measurements showed values smaller than 0.4 μm .

The large domain (H2) within these cells showed that two peaks with 24% of measurements each within the ranges 0.8-1.19 μm and 2-2.39 μm . The total distribution within H2 covered values from 0.927 to 7.555 μm (figure 3.13). There were no values smaller than 0.4 μm present in the measurements obtained.

Thus, the average value for the large domain (H2) in C57BL/6 was $H2_{C57BL/6(HSC)} = 2.29$ μm and the standard deviation 1.48 μm .

3.5-Discussion

The breakpoint clusters within mouse chromosome 2 are classified as hot-spots for the location of deletion breakpoints. We do not know whether these sites on both homologs have the same sensitivity to radiation-induced aberrations.

From experimental data, it is known that the aberration only occurs in one copy of chromosome 2 but not in the other.

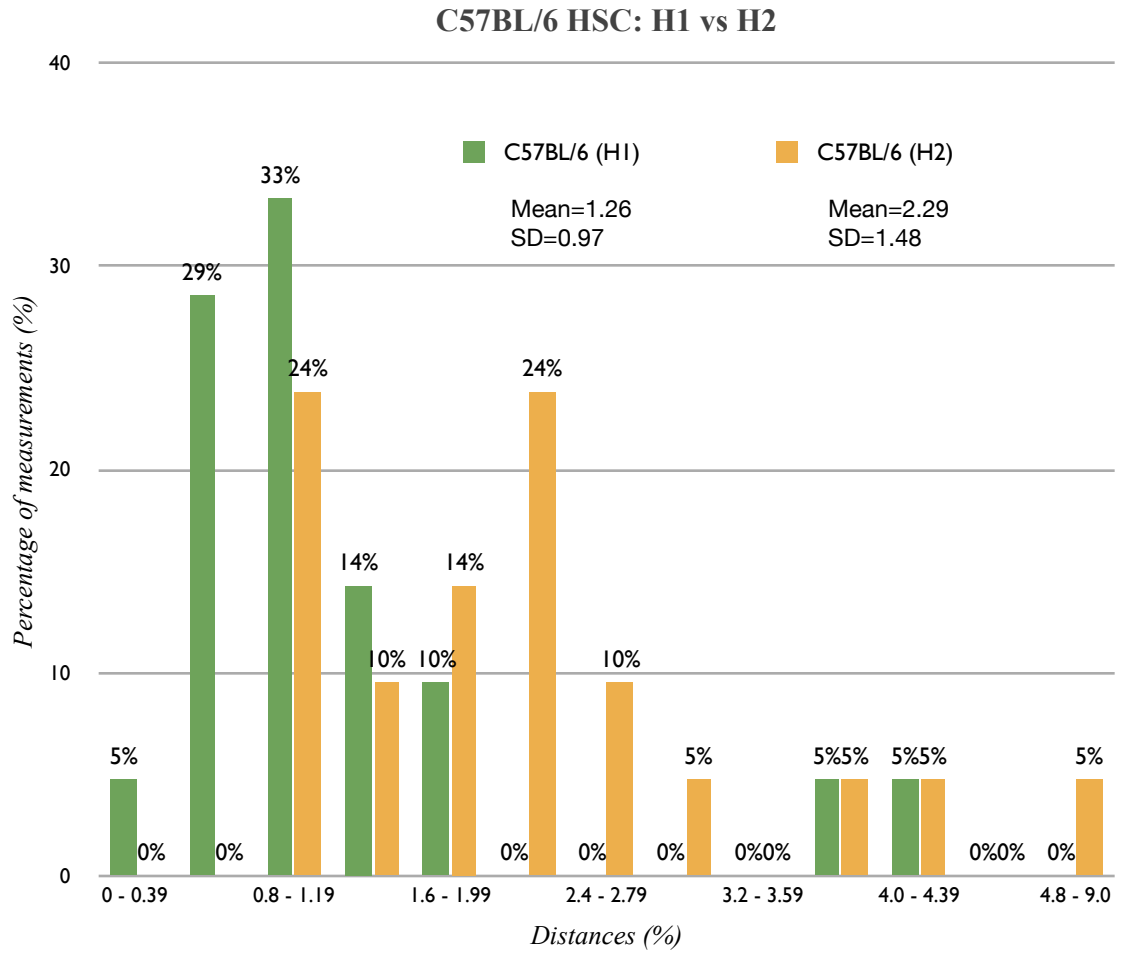


Figure 3.13: Distances distribution from pbc-dbc within the small domain (H1) and large domain (H2) in interphase hematopoietic progenitors (HSC) obtained from C57BL/6 mouse strain.

Interstitial deletion of chromosome 2 is observed in mice that have developed AML after irradiation treatment.

It is not known whether the aberration occurs specifically or preferentially in the maternal or paternal copy or if it is an event that occurs randomly. One possibility to explain this may be that a difference in sensitivity exists between the homologs. In other words, one homolog could be more sensitive than the other due to the different three dimensional organization of the chromatin within each homolog (figure 3.14).

There is a clear difference between both chromosome 2 domain organization observed through the whole chromosome paints where one chromosomal territory is organized in a more compacted or closed configuration; while, the other domain showed an extended or open configuration of the chromatin.

The chromatin within one domain appeared to be arranged in a different conformation compared to the other as demonstrated when we visualized all three BAC-probes used as markers either forming a triangle or a line in the three dimensional space within all cell types analyzed. These features of the chromosomal domains are similar to those observed in mammalian females chromosome X domains.

While it may ultimately turn out that a different organization of both chromosome 2 domains could have some influence predisposing to the characteristic deletion of one of the homologs, this was not obvious from this particular aspect of the study.

This predisposition might be increased in cells that present closer distances of the breakpoint clusters as showed for HSC and in BM cells.

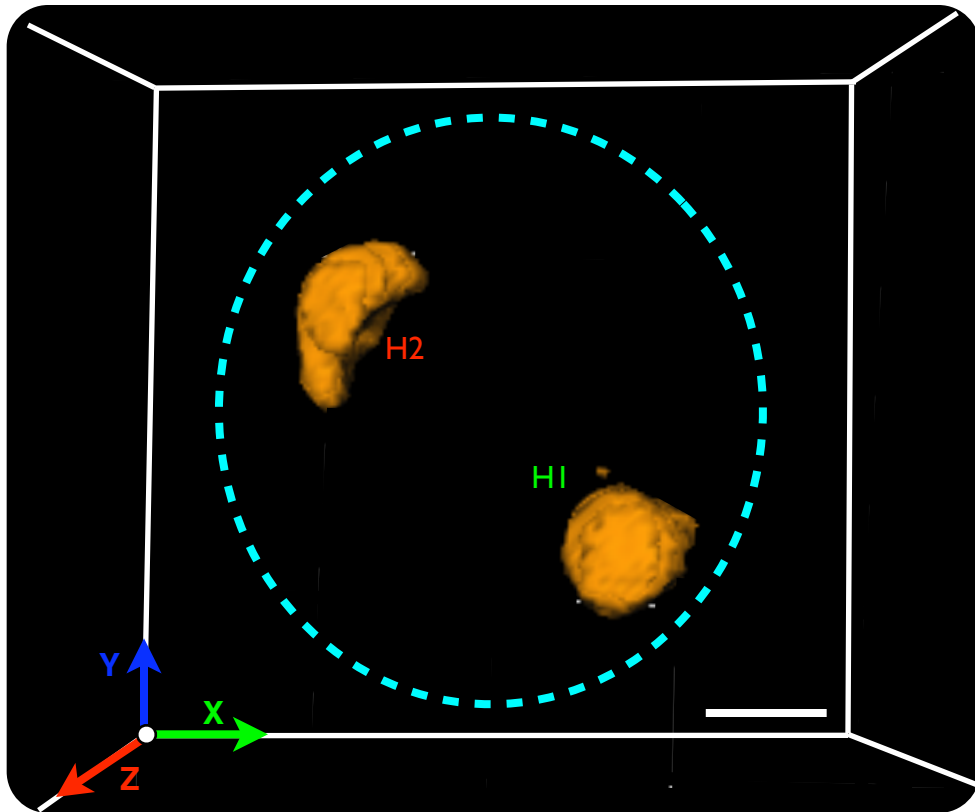


Figure 3.14: Three dimensional reconstruction of the small domain (H1) and large domain (H2) in interphase hematopoietic progenitors (HSC) obtained from CBA/CaJ mouse strain. Chromosome paintings stained with Alexa-647 (Invitrogen)

Nevertheless, there must be other factors influencing AML onset, since the closer distances are present in both AML-sensitive and AML-resistant mouse strain.

Factors such as apoptosis rate, gene expression profile changes, and methylation pattern after irradiation among others have shown to be different comparing CBA and C57BL/6 mouse strains.

3.7-Conclusions

The distribution of distances between the *proximal breakpoint cluster* and the *distal breakpoint cluster* on mouse chromosome 2 appeared to follow a bimodal distribution.

This was not surprising since one homolog in a given cell showed a shorter distance between the markers compared with the distances in the other homolog. This different organization of the markers was a characteristic of all cell types in both mouse strains. Furthermore, through the combination of chromosome paints and at least three markers revealed the closed and open arrangements of the chromatin within both chromosome 2 territories in interphase cells.

Consequently, an open or close conformation of markers and domains might be useful as a tool to test different hypothesis that could lead to or provide hints about the causes of the interstitial deletion in one copy of chromosome 2 observed in AML-sensitive mouse strains after radiation treatment.

References

- [1] D. Pinkel, T. Straume, and J. Gray, "Cytogenetic analysis using quantitative, high-sensitivity, fluorescence hybridization," *Proceedings of the National Academy of Sciences USA*, vol. 83, pp. 2934–2938, Jan 1986.
- [2] P. Lichter, T. Cremer, J. Borden, and L. Manuelidis, "Delineation of individual human chromosomes in metaphase and interphase cells by in situ suppression hybridization using recombinant dna ...," *Hum Genet*, vol. 80, pp. 224–234, Jan 1988.
- [3] T. Cremer and C. Cremer, "Chromosome territories, nuclear architecture and gene regulation in mammalian cells," *Nat Rev Genet*, vol. 2, pp. 292–301, Apr 2001.
- [4] N. Mahy, P. Perry, and W. Bickmore, "Gene density and transcription influence the localization of chromatin outside of chromosome territories detectable by fish," *Journal of Cell Biology*, vol. 159, pp. 753–763, Dec 2002.
- [5] N. Mahy, P. Perry, S. Gilchrist, and R. Baldock, "Spatial organization of active and inactive genes and noncoding dna within chromosome territories," *Journal of Cell Biology*, vol. 157, pp. 579–589, May 2002.
- [6] M. Lyon, "Sex chromatin and gene action in the mammalian x-chromosome," *American Journal of Human Genetics*, vol. 14, pp. 135–148, 1962.
- [7] S. Duthie, T. Nesterova, E. Formstone, A. Keohane, B. Turner, S. Zakian, and N. Brockdorff, "Xist rna exhibits a banded localization on the inactive x chromosome and is excluded from autosomal material in cis," *Human Molecular Genetics*, vol. 8, pp. 195–204, Jan 1999.
- [8] S. Dietzel, K. Schiebel, G. Little, P. Edelmann, G. Rappold, R. Eils, C. Cremer, and T. Cremer, "The 3d positioning of ant2 and ant3 genes within female x chromosome territories correlates with gene activity," *Experimental Cell Research*, vol. 252, no. 2, pp. 363–375, 1999.
- [9] S. Yang, D. Illner, K. Teller, I. Solovei, R. van Driel, B. Joffe, T. Cremer, R. Eils, and K. Rohr, "Structural analysis of interphase x-chromatin based on statistical shape theory," *Biochim Biophys Acta*, vol. 1783, pp. 2089–99, Nov 2008.

- [10] M. Barr, "Sexual dimorphism in interphase nuclei," *American Journal of Human Genetics*, vol. 12, pp. 118–127, Jan 1960.
- [11] L. Barrios, R. Miró, M. Caballín, C. Fuster, F. Guedea, A. Subias, and J. Egozcue, "Cytogenetic effects of radiotherapy breakpoint distribution in induced chromosome aberrations," *Cancer Genetics and Cytogenetics*, vol. 41, pp. 61–70, Jan 1989.
- [12] G. Holmquist, "Chromosome bands, their chromatin flavors, and their functional features," *American Journal of Human Genetics*, vol. 51, pp. 17–37, Jan 1992.
- [13] J. Bedford and M. Muhlmann-Diaz, "Damage selectivity in chromosomes," In *Radiation Research: A Twentieth Century Perspective* (W. C. Dewey, M. Edington, R. J. M. Fry, E. J. Hall and G. F. Whitmore, Eds.), pp. 212–216, Academic Press, San Diego 1992.
- [14] M. Muhlmann-Diaz, "Chromatin structure and ionizing radiation induced chromosome aberrations," 1993.
- [15] M. Muhlmann-Diaz and J. Bedford, *A comparison of radiation-induced aberrations in human cells involving early and late replicating X chromosomes*. In *Chromosomal Alterations*; ed. Obe, G and Natarajan, AT-Springer Verlag, New York, pp 125-131, 1994.
- [16] M. Muhlmann-Diaz and J. Bedford, "Breakage of human chromosomes 4, 19 and y in g0 cells immediately after exposure to gamma-rays," *International journal of Radiation Biology*, vol. 65, pp. 165–173, Jan 1994.
- [17] G. Folle, W. Martínez-López, E. Boccardo, and G. Obe, "Localization of chromosome breakpoints: implication of the chromatin structure and nuclear architecture," *Mutation Research*, vol. 404, pp. 17–26, Jan 1998.
- [18] J. Yunis, M. Kuo, and G. Saunders, "Localization of sequences specifying messenger rna to light-staining g-bands of humans chromosomes," *Chromosoma*, vol. 61, pp. 335–344, Jan 1977.
- [19] W. Martínez-López, G. Folle, G. Obe, and P. Jeppesen, "Chromosome regions enriched in hyperacetylated histone h4 are preferred sites for endonuclease-and radiation-induced breakpoints," *Chromosome Research*, vol. 9, pp. 69–75, Jan 2001.

CHAPTER IV

CYTOGENETIC ANALYSIS OF INTERPHASE CELLS FROM RADIATION-INDUCED AML CASES WITH LOSS OF *PU.1* THROUGH 3D-FISH.

INTRODUCTION

4.1-Background

An early and prerequisite event for radiation-induced acute myeloid leukemia (AML) in CBA mice is loss of one copy of the *PU.1* gene, and this results from a large deletion on mouse chromosome 2⁽¹⁻⁵⁾. The breakpoints for the deletions occur primarily in a proximal breakpoint cluster (pbc) and a distal breakpoint cluster (dbc) surrounding *PU.1* gene^(6,7). C57BL/6 mice do not develop AML either spontaneously or after radiation exposure⁽⁸⁻⁹⁾. To investigate whether the breakpoint clusters within these regions is consequence of nuclear arrangement of the regions, we measured the proximity of labeled BAC-probes hybridized within the breakpoint cluster regions of chromosome 2 in bone marrow cells of radiogenic AML-sensitive CBA/CaJ and resistant C57BL/6J mice.

In this way, we proposed to determine whether a difference in regional proximity of the breakpoint cluster regions might explain the difference in susceptibility of these strains to radiation-induced AML.

However, as reported in chapter 2, we found no difference in interphase distances between pbc and dbc BAC-probes between both the sensitive and resistant strain.

Interestingly, however, in virtually every cell measured, the interphase domain of one of the chromosome 2 homologs was appreciably larger or more open than the other, along with the linear and triangular organization of the markers within the large and small domain respectively.

This suggested the possibility that the *PU.1* gene was preferentially deleted on one as opposed to the other chromosome 2 domain, again because of the difference in the architecture of the two homologs in the interphase nuclei.

To this end, I examined leukemic cells from 10 independent radiation-induced AMLs to determine whether the deletion occurred randomly or preferentially in the large or small domains.

4.2-Hypothesis

Beforehand, I assumed that the small domain, which presented the closer distance of the breakpoint clusters compared to the large domain, may have a greater possibility to

be involved in mis-rejoining events to produce the deletion of the minimal deleted region (mdr).

Therefore, that preconception lead us to test the following hypothesis:

The deletion of the PU.1 gene in radiation-induce AML cases occurs preferentially within the small or more condensed chromosome 2 territories due to its chromatin organization.

4.3-Specific Aims

Specific Aim 1: Provide cytogenetic characterization of radiation-induced AML cases with respect to the markers chosen to visualize proximal and distal breakpoint clusters along with *PU.1*. Assuming a clonal evolution of the disease in the mouse model, by the time when an AML is fully developed. Descendant of the original altered stem or progenitor hematopoietic cell must have an over-represented cell population that carries the characteristic aberration usually seen in radiation-induced AML samples.

Specific Aim 2: Determine whether the intact chromosome 2 presented distances that represent the small or the large domain within these samples through the measurements of the breakpoint clusters distance.

4.4-Experimental Approach

The logical question arising from the previous data is related to the possibility of a bias toward a preferential deletion in one homolog of chromosome 2 that leads to the development of AML. A characteristic feature of radiation-induced AML in CBA/CaJ mice is a deletion of only one copy of the *PU.1* gene⁽¹⁻⁷⁾ located in the minimal deleted region (mdr).

However, the question remains:

What is the *PU.1* copy preferentially deleted? Is the *PU.1* copy from the small or large domain?

To address this question we examined interphase cells from several independently induced AMLs that arose after irradiation of CBA mice. These AML cases were originated in different mice after exposure to gamma-irradiation, and *PU.1* loss had been previously confirmed by Dr Peng in this lab⁽¹⁰⁾.

The cells were from enlarged spleens and represented a mixture of cells, perhaps with more than one genetic change within sub-populations, but all had one change in common: the *PU.1* deletion.

Considering that these AML cases are not evident until almost 400 days, the cell population predominating within the sample might be a clonal representation of the most successful secondary mutation or genetic alteration that resulted in the largest growth advantage eventually resulting in the full development of a lethal AML.

This is one consideration that would have to be taken into account in the interpretation, because even though a deletion may occur in the original initiated cell in either the large or the more compact chromosome 2 domain, the many intervening cell generations (30 or so) necessary to produce an AML containing a billion or so cells (2^{30}) may gradually shift the initial characteristic architectural features of these domains.

Several authors^(3,5,6,11,12), such as, Rithidech et al. 1995; Bouffler et al. 1997; Finnon et al. 2002; and Kanda et al.2008, Cox et al. 1991, have shown that the progression of the disease is compatible with the hypothesis of “clonal evolution” of cells carrying mutations that leads to the progression of the AML.

The typical mutation is the deletion in chromosome 2 within the cyto-bands 2D-2E producing the loss of the *PUI* gene of only one homolog.

Through the use of chromosome 2 painting and BAC-probes we visualized the chromosome domains and the different organization of these BAC-probes markers within interphase cells showing either an open or closed configuration of the chromatin with the consequent short or long distance of the breakpoint clusters within the domains.

The clear reference provided by the differential chromatin configuration of both chromosome 2 homologs could play a key role in the determination of the preferential deletion (if any) of the *PUI* gene located in the minimal deleted region from either the small or the large domain.

4.5-Materials and Methods

4.5.1-Mice and Treatment

All the CBA/CaJ mice used in these experiments were from Jackson laboratory; the mice age at the time of the treatment were between 8 to 14 weeks of age at the time of irradiation.

The irradiation treatments were performed with a ^{137}Cs γ -ray source (J. L. Shepherd Model 81-14) irradiator, as described by Weil and co-workers 2009^(10,13). Doses delivered were 1, 2, or 3 Gy.

After irradiation treatment, mice were kept until they showed symptoms of AML or reached ~800 days of age at the vivarium at Colorado State University (CSU)⁽¹³⁾.

4.5.2-Cells

AML Infiltrated Spleens

Samples were obtained from mice that were diagnosed with AML presenting a high frequency of *PU.1* loss in the harvested cells.

The cells were fixed with the classical fixation protocol of (3:1) acetic acid : methanol as described previously⁽¹⁰⁾.

These cells, each from several mice with AML were supplied by Dr. Peng in this laboratory.

8016 Cell Line^(7,14,15)

8016 is a radiation-induced AML cell line derived from C3H mouse strain and it carries a deletion (del2C3-F2) in the *mdr* region in one copy of chromosome 2. The cell line was grown in culture with MEM plus 12% serum fetal bovine. The cells were then fixed and dropped on slides to perform 3D-FISH and measure distances between *pb*-*db*.

4.5.3-Bacteria Artificial Chromosome Clones and Fluorescence In Situ Hybridization.

The Bacterial Artificial Chromosomes (BAC) clones were selected and ordered from the BACPAC resources center (<http://bacpac.chori.org/>).

0.5 ul of each labeled BAC-probe was applied at a concentration of about 1 ng/ul to the slides. The slides were cover-slipped and sealed with rubber cement.

Co-denaturation of probes and target DNA occurred at 80°C in hybridization mix (proprietary solution designed to optimize hybridization of multiple probes) for 5 minutes followed by incubation at 37°C overnight.

The coverslips were removed and the slides washed in 50% formamide/2X SSC at 43.5°C for 5 minutes followed by 3 washes in 2X SSC at 43.5°C for 5 minutes to remove any mismatched probe. The slides were counterstained with DAPI (4',6-diamidino-2-phenylindole, dihydrochloride) in an anti-fade solution, cover-slipped, and sealed. Probe hybridization was visualized using a 3D-deconvolution, and 3D reconstruction softwares.

Measurements were performed using a combination of softwares such as ImageJ Software (<http://rsbweb.nih.gov/ij/index.html>-NIH), Autoquant software (Media Cybernetics, inc; Bethesda, MD) and Metamorph (Molecular Devices, Sunnyvale, CA).

4.6-Results

4.6.1-Chromosomal Domains and BAC-Markers Organization

Ten mice were selected for interphase analysis of AML cells harvested from infiltrated spleens of these mice. The cells harvested contained a high frequency of hemizygous loss of the *PU.1* gene that range within 89% to 99% of the scored cells⁽¹⁰⁾.

All normal cells were represented by the corresponding chromosomal territory (chromosome paints) in interphase along with the presence of markers representing proximal and distal breakpoint clusters (pbc and dbc) and the *PU.1* gene as well.

Therefore, a *normal cell* is represented for two chromosome 2 domains containing all three markers within each domain as shown in Figure 4.1.

The random production of damage in either the breakpoint clusters and/or mdr may lead to illegitimate repair of the chromosomal DNA resulting in variable outcomes based on the length and location of the deleted region.

These cells that carries different aberrations will be referred as “*variant cells*” within each cell sample.

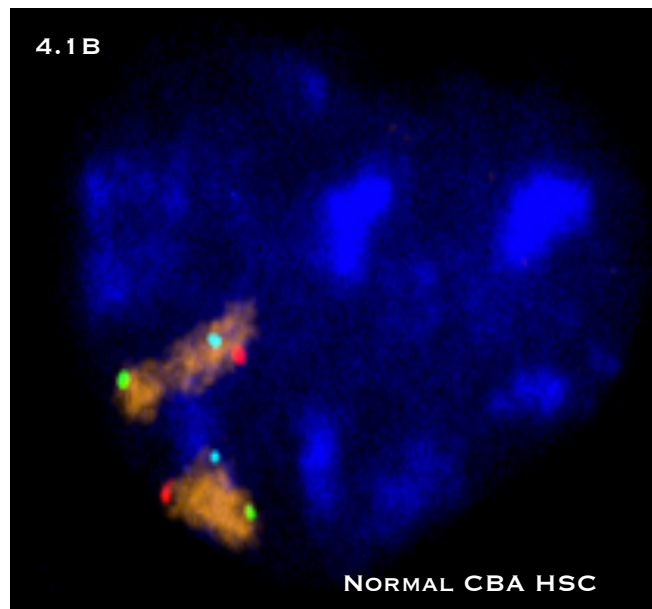
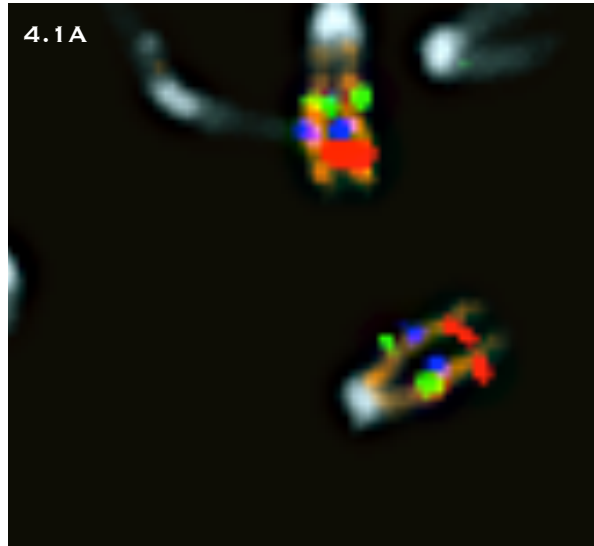


Figure 4.1: Normal hematopoietic progenitor cell. A-Chromosome 2 in a metaphase cell and B-interphase cells. Green (Spectrum green): proximal breakpoint cluster (pbc); Red (Spectrum red): distal breakpoint cluster (dbc); Cyan (DEAC): *PU.1* gene; Orange (Alexa 648): chromosome 2 paints.

Then, the cell population that carries deletions may replicate and at some point after further changes, not all of which are known, the progeny of the initiated cell presumably gains a selective growth advantage over the normal cells becoming the over-represented cell population that leads to the development of leukemia, as a result of the characteristic clonal expansion of the malignant cells.

Our analysis of interphase nuclei showed a wide range of variant cells within each individual sample case.

Thus, in general terms, within a given mouse AML sample analyzed, one phenotype was represented in high frequency compared to “variant” cells present at lower frequency within the same sample.

Then, as mentioned before, one chromosome 2 domain in every interphase cell always contained all three markers, while the other homolog, showed several sized deletions. Thus, based on the presence or absence of markers within the chromosomal domain resulting in combinations of markers remaining within the deleted domain is referred as the “*dominant deleted cell.*”

Therefore, the following list enumerates the classification of cases based on the combination of markers deleted and frequency observed in this study:

1. In four out of ten mouse AML cases (40%) the deletion was large enough to involve all three BAC-probes (pbc/PU.1/dbc). The deletion of the three markers shows that the deletion bearing chromosome has lost a large DNA region of at least 60 Mb.

The large deletion resulted in a smaller (~120 Mb) deleted chromosome 2 with no markers present within the chromosomal domain (Figure 4.2). The frequencies of this phenotype in these four AML mice cases were: M3364= 63.5%; M3208= 66.7%; M3286= 60%; and M3272= 59%. Where the MXXX represents the mouse coded sample number.

Taken these four cases together showed an average of this phenotype of 62.3%; therefore, about 38.7% were “variant” cells. Presumably the breakpoints were outside the markers used which were at about the midpoint of the cluster regions.

2. Three AML cases (30%) showed a high frequency of deletions that included two of the BAC-probes used as markers.

These cases showed the absence of both *PU.1* gene and *dbc* markers, and the presence of only one *pb*c (proximal marker) in the resulting short chromosome 2 after deletion (Figure 4.3).

The frequency of this phenotype within these three cases were: M3576= 27%; M3189= 82%; and M3269= 68%.

The average value taken all the cases together was: 59%. Presumably the one breakpoint was outside the *pb*c and one inside the *dbc* BAC marker.

The size of the deletion in these cases may be at least ~30 Mb since the distance between *PU.1* gene and *dbc* was ~30 Mb.

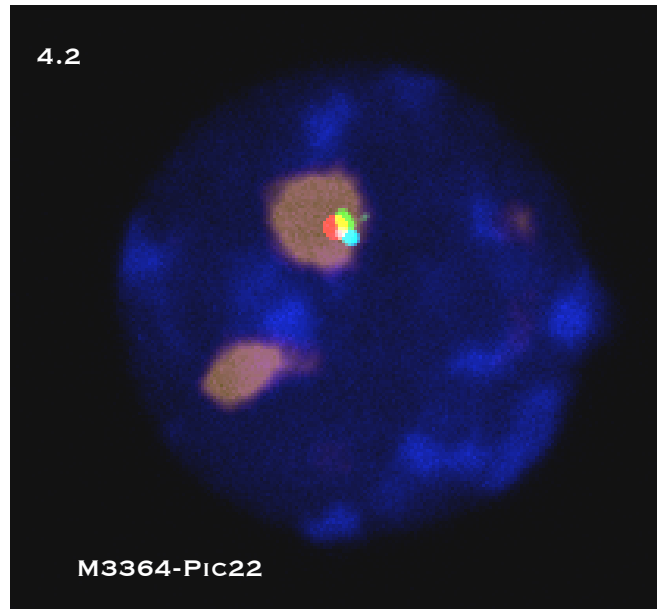


Figure 4.2: The most frequent phenotype found in 4 AML cases; one domain with all markers and the other with none.

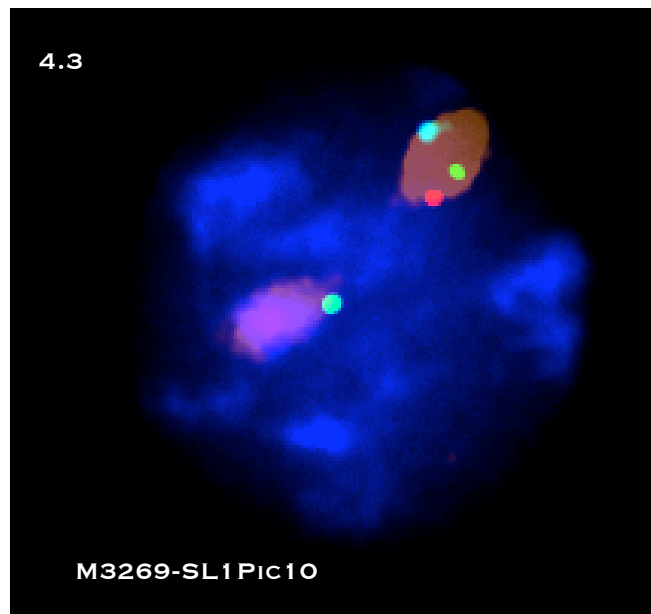


Figure 4.3: The second most frequent phenotype found in three AML cases; one complete domain and the other with deleted *PU.1* and *dbc* markers.

3. Furthermore, one case (10%) had only dbc (distal marker); therefore, *PU.1* and pbc were deleted.

The rearrangement within these cells showed that the deletion has occurred between *PU.1* gene and pbc, representing a deletion of ~30 Mb long toward the centromere (Figure 4.4).

The frequency of this phenotype was $M3416 = 53.7\%$.

The deletions that occurred in categories 2 and 3 above involving *PU.1*-dbc; and *PU.1*-pbc were about the same length as far as the linear DNA distance, but in category 2 the interacting regions were distal (toward the telomere) while in category 3 the two interacting regions were proximal (toward the centromere).

4. One AML case among the ten (10%) showed *PU.1* deletion only, representing the smallest deletion in this study.

This rearrangement showed the deletion within the limits of the minimal deleted region (mdr), resulting in the exclusion of pbc (proximal marker) and dbc (distal marker) markers from the rearrangement (Figure 4.5).

As a consequence, the deleted homolog showed presence of both pbc and dbc probes within the cells after the deletion. The frequency of this phenotype was $M3512 = 85\%$.

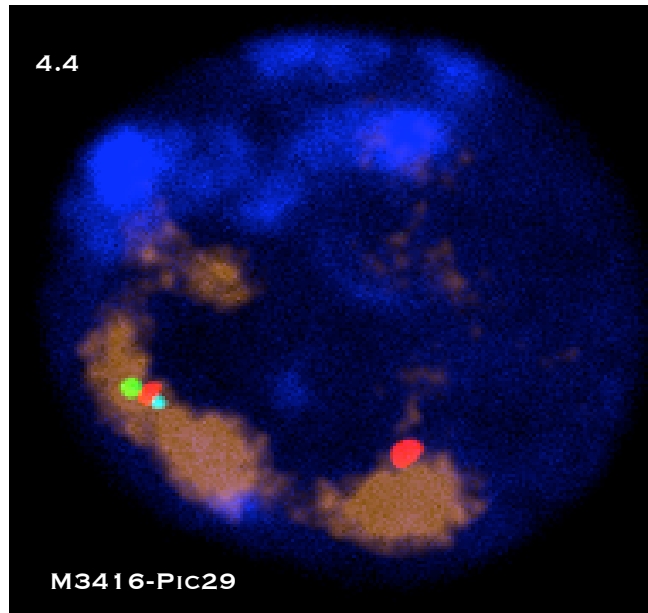


Figure 4.4- Phenotype found in one case; one normal domain and the other with deleted PU1 and pbc.

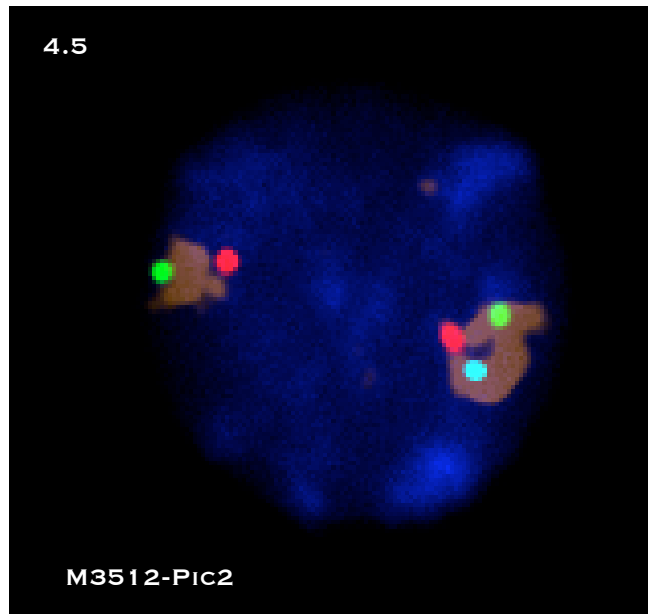


Figure 4.5- one case only with the typical deletion of one PU1 copy involving only the minimal deleted region.

5. The final AML case of the ten (10%) showed two principal sub-population phenotypes in almost the same proportion. One sub-population showed cells in which only one chromosome 2 domain was present with all three BAC markers and no other chromosome 2 domain (chromosome 2 monosomy). The other sub-population possessed cells in which one chromosome 2 domain had all three markers while the other domain had none, so the deletion breakpoints were outside the markers we used for the pbc and dbc region.

This is the only case that showed two sub-population cell populations in a proportion of almost 1:1. The frequencies of these phenotypes were M3250= 52% of cells showed only 1 domain with all markers and 41% showed 2 domains; one of them with all markers and the other homolog with no markers (Figure 4.6). However, there were a high proportion of cells that showed an unscorable rearrangement due to the difficult interpretation. Usually, the feature of these cells were multiple copies (up to four) of the proximal breakpoint cluster markers and an un-organized domain with sometimes multiple copies of the other markers or deletions in both domains.

6. 8016 cell line: The characteristic deletion of the cells is a small deletion that only involved PU.1. Thus, the deleted homolog contained the two clusters: pbc and dbc; with an extremely high (98%) frequency of this phenotype in the sample analyzed. The distances of the clusters in the intact homolog were in 50.91% of cells less than 1.79 μm and 49.09% of the cells for distances $\geq 2 \mu\text{m}$ (Figure 4.7).

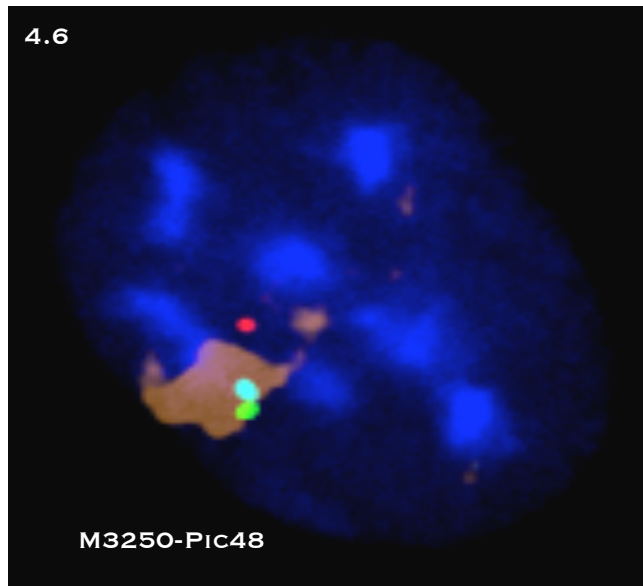


Figure 4.6: Case M3250 with 2 phenotypes equally represented one showing only one complete domain and the other showing 2 domains with one chromosomal domain without markers.

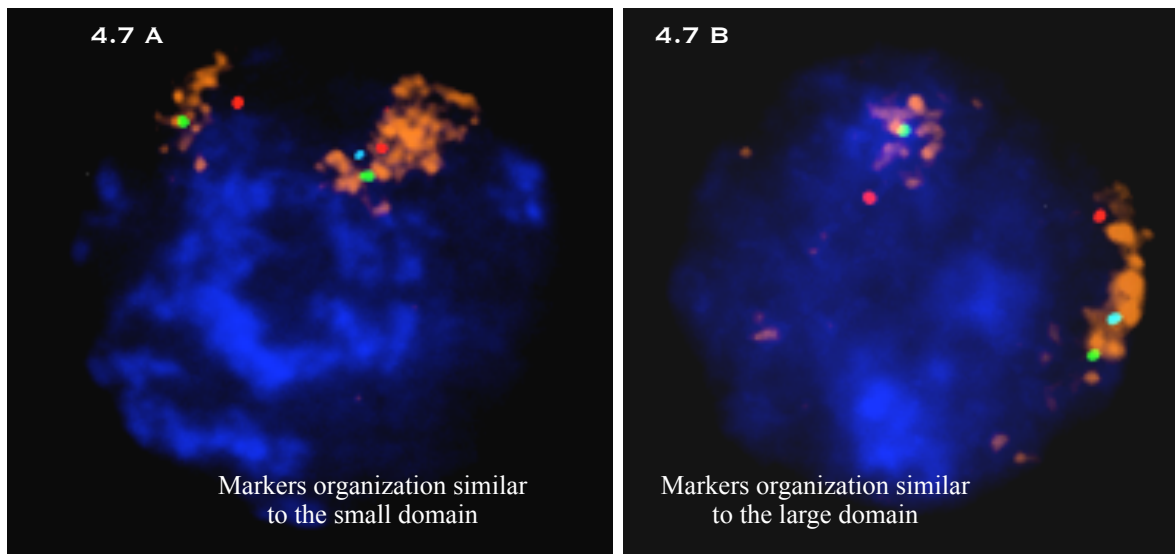


Figure 4.7: Cell line 8016: typical deletion of one PU1 copy involving only the minimal deleted region. A-Example for small domain. B-Example for large domain.

This implies an equal presence of both the small and large domain within the sample.

Generally, the chromatin of the deleted chromosome 2 territory was expanded and unorganized when compared with normal non-irradiated cells.

Normal non-irradiated cells showed that the small domain was compact or closed, containing the three markers forming a triangular organization and filling the whole chromosomal domain. In contrast, the large domain showed an elongated shape with the markers located along the elongated domain running as a relative straight alignment from centromere to telomere.

In contrast, the non-deleted chromosome in the AML samples never showed the characteristic shapes of either small or large domain but rather had extended domains that were expanded within the interphase nucleus.

Thus, viewing the domains strictly with whole chromosome paintings, the disorganization was visually apparent, but looking strictly at the arrangement of *pb*, *PU.1*, and *db* markers the triangular configuration characteristic of the compact domain in normal cells was still evident, as was the alignment of the markers within the large domain.

In general terms, the small domain in AML samples was found to be in triangular organization of the markers but located in a portion of the expanded chromosomal domain.

Large domain distances were mostly in an expanded chromosomal territory where the markers form the alignment.

This distortion or deviation from the “normal” markers organization within the chromosomal territories was evident in every cell of the AML samples analyzed.

The expansion of the chromosomal domains was clear in both the deleted and the non-deleted homolog within these AML cells.

Moreover, some of the markers appeared to be projected out of the chromosomal domain (Figure 4.8) in either the domain with the complete set of markers and/or the domain with the deletion. The most frequently projected marker was *dbc*, representing a feature never seen in normal cells. However, *PU.1* and *pbcc* were seen projected but in a lower frequency compared with *dbc* marker. This projection could represent a feature of the chromatin reorganization that may be needed for active transcription and move toward topological regions within the nuclei⁽¹⁶⁻¹⁸⁾ where the transcription levels are high; suggesting the necessity of transcription of some genes located within that DNA region.

4.6.2-Chromosomal Domain Preferentially Deleted

Since the organization of the chromosomal domains in these samples was not strictly comparable with normal cells in the features as described above; therefore, the distances between *pbcc* and *dbc* of the domain that remained intact with all the markers were used, due to the tendency of the markers to keep the relative position between them despite the organizational change of the chromatin observed in the preliminary data.

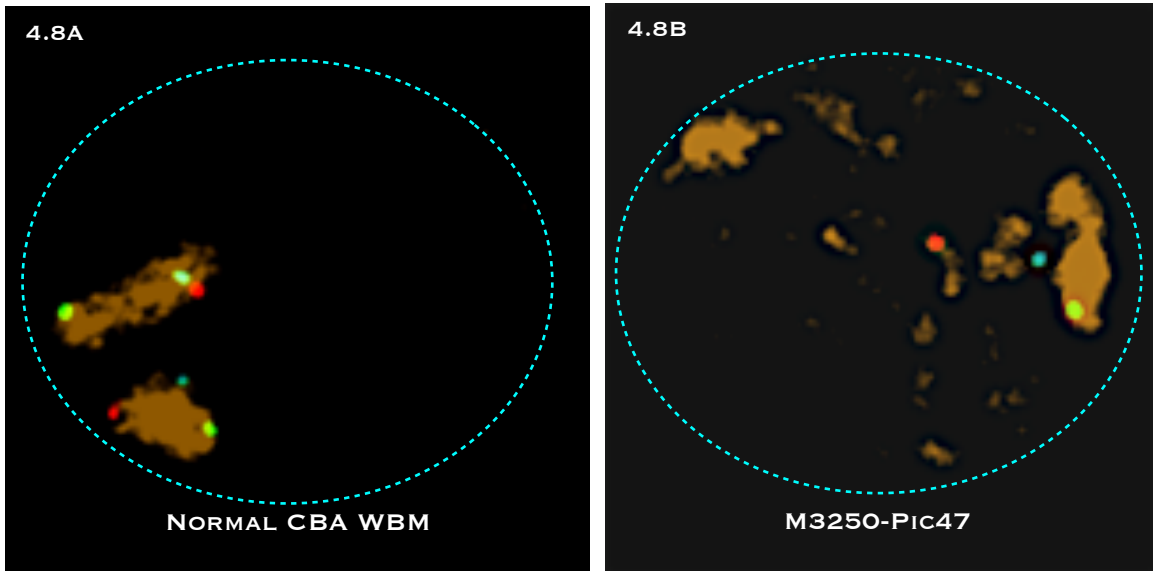


Figure 4.8: Unirradiated vs Irradiated (AML) cells. A- Unirradiated cell showing the chromosomal domain and the normal organization of the markers within each domain. B- Irradiated cell from AML samples where the remaining domain is no organized. It is visible the projection of the dbc outside of the chromosomal domain.

In normal non-irradiated cells both distances of the clusters and organization of the domain were correlated. Thus, the small domain was correlated with the triangular organization of the markers, whereas the large domain was correlated with the linear organization of the markers.

Since the chromosomal territory organization is altered in radiation-induced AML cells that develop after irradiation, we decided to use the organizational feature of the markers, which tends to remain either triangular or linear whether the cells are normal or AML.

Numerically, both domains were defined from the measurements done of the breakpoint clusters in normal bone marrow interphase cells.

We have shown in chapter 2 that the average distance between the pbc-dbc markers within the small domain was 1.2 μm , and in the large domain the average distance was 2.4 μm .

Therefore, these two averages were defined as our reference points to determine whether the chromosome 2 that remains with all markers is either the small or large domain. If for example, the remaining domain with all the markers is judged to be the small or compact domain, then the deletion must have occurred in the other or large domain.

Additionally, consideration was given concerning the fact that there was distribution of distances about the mean.

Thus, the upper limit cutoff for the distances between markers within the small domain was arbitrarily taken to be a distance less than 2 μm .

For the large domain I set a cutoff whereby any distance greater than 2 μm will be considered as large domain. Therefore, we were expecting measurement distributions that either range within $1.2 \pm (1 \text{ SD}) \mu\text{m}$ or within $2.4 \pm (1 \text{ SD}) \mu\text{m}$ to define both small and large domain respectively.

Of course, this bimodal distribution would have an overlapping region where the values obtained will not allow us to identify whether it is a small or large domain.

Therefore, the overlapping regions correspond to values that can belong to either domain and ranges from 1.8 μm to 2 μm .

For this reason, the upper limit for the small domain at 1.79 μm , and the lower limit for the large domain at 2.0 μm were re-established (Figure 4.9). Using this criterion, distances between the markers (pbc-dbc) were measured and used to determine which domain was present with all the markers within the samples of cells. Therefore, following that criterion, the deleted domain was the domain not present in the cell.

After analyzing ten AML samples, the distribution of distances between pbc and dbc showed that a high number of cells retained the domain containing the breakpoint clusters with distances $\leq 1.79 \mu\text{m}$ corresponding to the small domain.

Eight of the mouse AML cases (80%) showed that 64% to 84% of the measurements were within the reference values for the small domain.

However, there were two mouse AML cases (M3189 and M3250) where the proportion were not the same found in the first eight cases.

M3189 had a bigger proportion, 62.23% of measurements, with values representing the large domain.

Theoretical Determination of Small and Large Domains

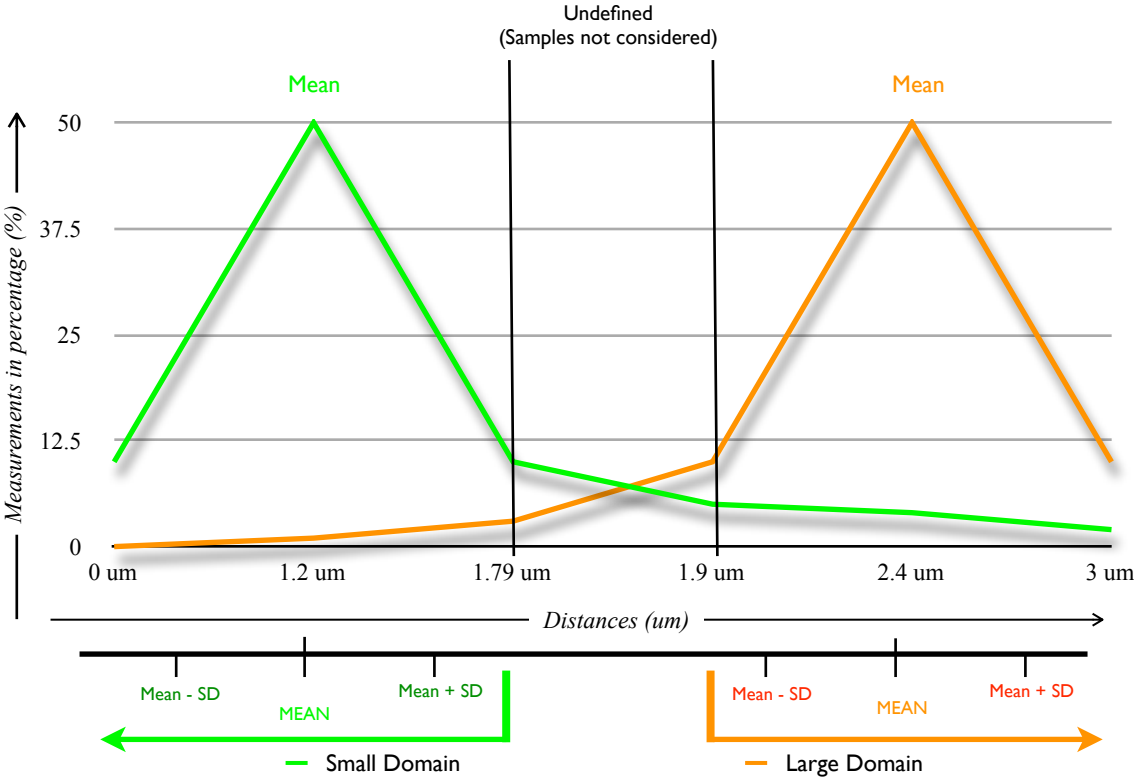


Figure 4.9: Determination of reference values to define small and large domains based in distances between pbc and dbc.

Meanwhile in M3250 the proportion observed was 55% for the small domain and 45% for the large domain.

Figure 4.10 shows the proportion of distances fitting into either the small or large domain of each AML case analyzed.

Finally, in order to compare the proportions obtained from AML cells the cell line 8016 was included in this study.

The proportions found within this phenotypically homogenous population were 50.91% presented distances ≤ 1.79 μm and 49.09% were ≥ 2.0 μm .

Thus, the cell populations of eight AML cases carry the complete small chromosome 2 domain suggesting that the deletion occurred from the large domain or that the cells carrying deletion within the large domain may have been the most successful and repopulated bone marrow after IR treatment.

However, the proportions obtained from the cell line 8016 does not fit with the idea that deletion of the large domain is the most frequent event occurring in radiation-induced AML, or the most successful event for the development of AML.

This radiation-induced mouse AML cell line has undergone many more generations or cell population doublings so it is unknown whether the domain size distributions may change after prolonged growth in culture.

With the analysis of the 8016 cell line and compared with the other AML samples analyzed led us to the question of whether there is a dynamic reorganization of the chromatin is occurring or not in radiation-induced AML.

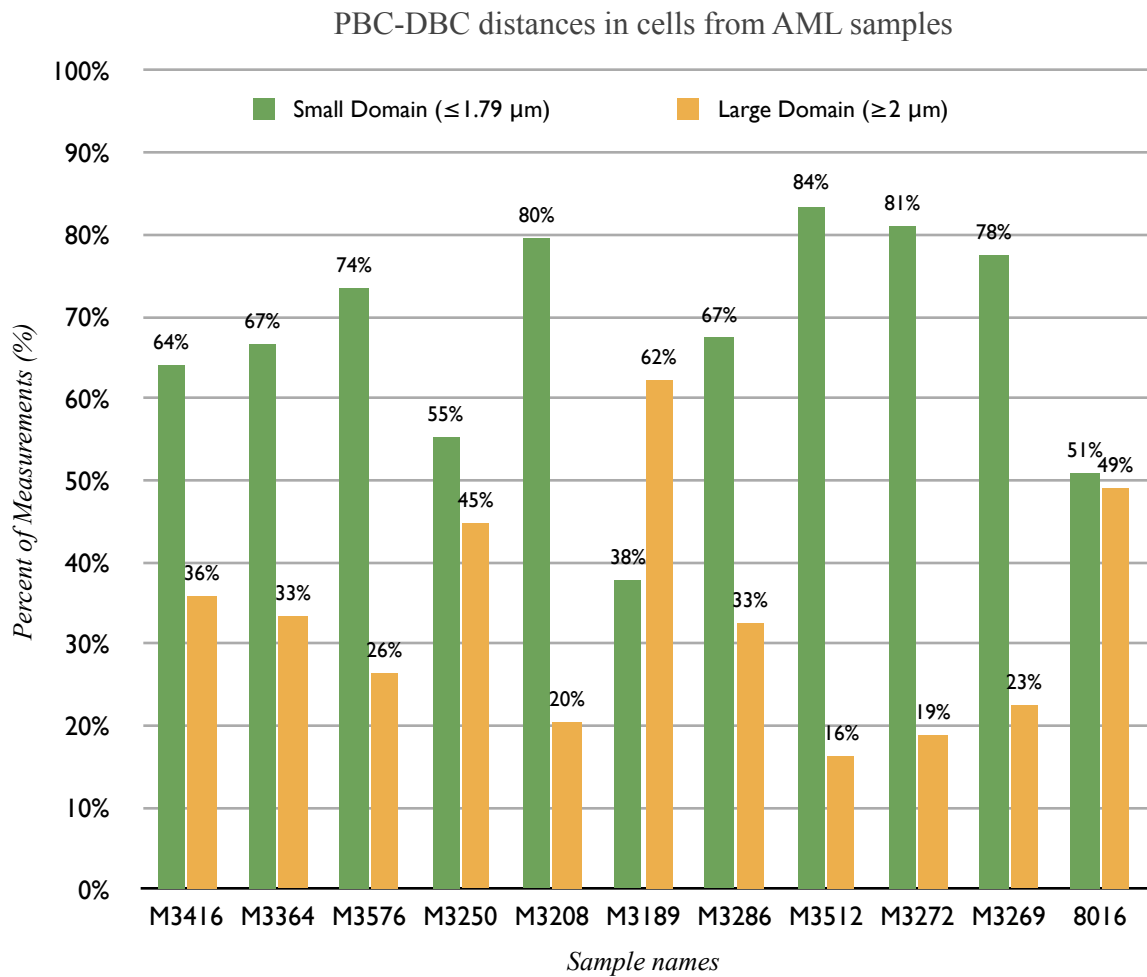


Figure 4.10: Histogram showing the distribution of measurements done within cell samples of each AML case and the cell line 8016. Green bars show the percentage of measurements which values were $\leq 1.79 \mu\text{m}$. Yellow bars show the percentage of measurements which values were $\geq 2 \mu\text{m}$.

4.7-Discussion

4.7.1-Interphase Cells: Dominant deleted cells in each sample cells

After radiation exposure all mice were maintained until they developed AML.

AML samples from these mice carried cells with a high frequency of *PU.1* gene deletion in one copy of chromosome 2.

The time courses for these mice until they were euthanized and diagnosed with AML were:

Dose: 1 Gy: 481 days. (1 case: M3416)

Dose 2 Gy: between 454-693 days. (4 cases: M3208, M3576; M3364; and M3250)

Dose 3 Gy: between 288-707 days. (5 cases: M3512; M3269; M3272; M3189 and M3286)

In spite of the different radiation doses given, the dose did not appear to have an influence on the preferential deletion of the large or small domain or in the appearance of variant cells.

Basically, there is nothing that we can correlate with the dose applied to the mice, except regarding the frequencies of mice that developed AML.

In other words, as concluded long ago, radiation-induced cancer behaves as a stochastic process whatever the initiating step is the same for all doses and only the frequency of occurrence of this initiating step and the probability of inducing the cancer that increases with dose.

The analysis of interphase cells in radiation-induced AML samples showed that within each sample there was a deleted cell described by the different combinations of markers lost on chromosome 2 and this occurred in high frequency among the AML cells. Variant cells among the AML cells from a particular animal occurred in a much lower frequency.

However, I did not find the same phenotype over-represented in all the cases. This fact suggest that there could be more than one genotype change leading to AML development without regard of how large the deletion is within chromosome 2, such that the only feature shared between the samples was the *PU.1* deletion.

The large deletion involving the three markers (pbc-*PU.1*-dbc) was the most frequent, being present in cells of four cases. In addition, three cases presented a phenotype where the deletion involved two do the markers: *PU.1* and dbc. Thus, we have 70% of the cases presenting these 2 phenotypes.

It is important to notice that the proportion of the phenotype with the deletion in *PU.1* and proximal marker did not appear very frequently (only 1 case) in comparison to 3 cases with the alternative deletion (*PU.1* and dbc). This may suggest that cells having deletions of the proximal regions are not very successful or that the deletion in the proximal region is less frequent.

Furthermore, within each sample the variant phenotypes observed showed phenotypes that in other cases are not variants but the over-represented phenotype (see appendix #).

Another feature related with chromosomal domains observed was that variant phenotypes showed the presence in interphase but not in metaphase of one, two, three or four copies of chromosome 2 and once again with variable combination of markers within the different domains.

Chromatin damage produced by gamma-irradiation generates DNA-DSBs randomly within the cells; then after DNA damage is repaired (either well repaired or mis-repaired) within the surviving cells sub-populations appear with other changes.

The evolution of these sub-populations will lead to the appearance and accumulation of more mutations that may at the end give an advantage, over the normal and other pre-leukemic cells, leading to a high proportion of this sub-population within the bone marrow.

It is known that, in fact, a point mutation in the other allele of *PU.1* is very frequently involved^(16,19). However, not only is DNA damage produced, but there are also epigenetic changes that occurred within the cells and could play an important role in leukemogenesis acceleration, increasing the mutation rate conferring genomic instability to the cells.

The loss of methylation is an event that may prove to be important in shape maintenance of chromosomal domains and loss of gene regulation.

In the current study an apparent loss of organization of the chromosomal domains was evident since the domain viewed by whole chromosome painting that kept the markers representing distances from either large or small domain never showed the same shape observed in the control non-irradiated cells.

However, the arrangement of the markers seems to be similar since I still was able to observe the triangular or linear arrangement of the markers may be due to the fixed location of some DNA region attached through their matrix attachment regions (MARs) to the nuclear matrix.

4.7.2-Domain Preferentially Deleted (Revisited)

The measurements done within the intact chromosome 2 from AML samples showed a high proportion of cells with distances between the clusters that represented the small domain from normal BM cells. Therefore, deletion of chromosome 2 occurred mainly in a nonrandom fashion because the large domain was preferentially deleted in 8 out of 10 cases in an average proportion of ~74% considering all 8 AML cases.

By making the assumption that the large domain was deleted it may suggest a greater susceptibility of the homolog that showed the features described for the large domain.

As a possible parallel, the similarities in conformation between active and inactive X-chromosomes compared with the large and small domain respectively, in chromosome 2 may suggest that the difference in organization may lead to a difference in transcriptional activity in the two homologs.

An initial assumption was that there may be no dynamic reorganization of the chromosomal domain after exposure to radiation.

Therefore, the observed domain without the deletion should be the same domain that was present before the treatment.

However, differences observed in these cells, such as the non conservation of the domains shapes (small and large), projection of markers outside the domain and the observation within two cases where the proportion was different from the majority, made us think about a possible dynamic reorganization of the chromatin as part of the radiation-induced leukemogenic process.

An interesting point arising from these observations is related to what happens within bone marrow cells from irradiated mice that did not get AML, or how about non irradiated mouse (with *PU.1* deletion) that get AML.

Could the domain organizations be different due to the radiation? If there were no such changes it would imply that the AML process resulted in the domain structure differences and not to the radiation.

M3250 (2 Gy) showed presence of about 55% small domain and 45% large domain; and M3189 (3Gy) 38% small domain and 62% large domain.

A proportion of 53% of cells showed the small domain and 47% of the cells showed the large domain in the cell line 8016 as well.

Explanation for the proportions found in those samples leads to more questions than answers.

Is there a dynamic rearrangement that leads to a reorganization of the chromatin to a progressive malignancy incompatible with the life of the mice?

Are the measurements reflecting the initial events where the large domain was deleted due to the radiation track? Or do the measurements show the results of the chromatin reorganization after clonal evolution within the mouse? Does this reorganization occurring only within the mouse microenvironment or could it happens in vitro as well? Could the time after irradiation have any influence in the results that we obtained from the samples? These questions are difficult to answer but they are driving us to new experimental approaches that will allow us to understand the mechanisms underlying radiation-induced AML.

4.8-Conclusions

Assuming a non dynamic reorganization of the chromatin within the radiation-induced AML samples, there appeared to be a trend toward a preferential deletion of the large domain. Therefore, our hypothesis of preferential deletion of the small domain was incorrect for this study.

The initial hypothesis was based on the loop formation of the chromatin where the two breakpoint clusters could come close enough to produce an illegitimate rejoin after the DSB formation. Indeed, the proximities of the clusters within the small domain were much closer than the proximities of the clusters from the large domain; however, this closer proximity within the small domain does not confer any bias or predisposition for the aberration formation.

The deletion in the large domain may suggest that a mechanism through which the deletion is not the result of proximity resulting from a simple loop formation as assumed previously.

Additionally, the different marker arrangement phenotypes that are present in the AML samples so not always involved the three markers in exactly the same way. As a result, again assuming a non dynamic reorganization of the chromatin and that the deletion occurred due to the radiation, we could hypothesize the existence of more than one chromatin loop that involved *pbcr-PUL1* and *PUL1-dbc*. Consequently, at least two tracks will be needed to be able to yield the large deletion (containing all the markers) but only one track to produce the deletion of the minimal deleted region (this model will be discussed in chapter 6).

Furthermore, *dbc* appears to be more sensitive to radiation^(6,20,21) due to the high frequency of deletion found in this study.

Finally, the observations that suggested a dynamic reorganization of the chromatin within the radiation-induced AML might lead to new lines of research to answer new questions leading to understand the events occurring in the radiation-induced leukemogenic process.

References

- [1] I. Hayata, M. Seki, K. Yoshida, K. Hirashima, T. Sado, J. Yamagiwa, and T. Ishihara, "Chromosomal aberrations observed in 52 mouse myeloid leukemias," *Cancer Research*, vol. 43, pp. 367–373, Jan 1983.
- [2] I. Hayata, "Partial deletion of chromosome 2 in radiation-induced myeloid leukemia in mice.," *Progress and Topics in Cytogenetics[PROG. TOP. CYTOGENET.]*. ..., Jan 1984.
- [3] S. D. Bouffler, E. I. Meijne, D. J. Morris, and D. Papworth, "Chromosome 2 hypersensitivity and clonal development in murine radiation acute myeloid leukaemia," *Int J Radiat Biol*, vol. 72, pp. 181–9, Aug 1997.
- [4] G. Breckon, A. Silver, and R. Cox, "Radiation-induced chromosome 2 breakage and the initiation of murine radiation acute myeloid leukaemogenesis," *Journal of Radiation Research*, vol. 2, pp. 248–256, Jan 1991.
- [5] R. Kanda, S. Tsuji, Y. Ohmachi, Y. Ishida, and N. Ban, "Rapid and reliable diagnosis of murine myeloid leukemia (ml) by fish of peripheral blood smear using probe of pu. 1, a candidate ml tumor suppressor," *Molecular Cytogenetics 1:22*, Jan 2008.
- [6] R. Finnon, J. Moody, E. Meijne, J. Haines, D. Clark, A. Edwards, R. Cox, and A. Silver, "A major breakpoint cluster domain in murine radiation-induced acute myeloid leukemia," *Molecular Carcinogenesis*, vol. 34, no. 2, pp. 64–71, 2002.
- [7] A. Silver, J. Moody, R. Dunford, D. Clark, and S. Ganz, "Molecular mapping of chromosome 2 deletions in murine radiation-induced aml localizes a putative tumor suppressor gene to a 1.0 cm region homologous to human chromosome segment 11p11–12," *Genes Chromosomes and Cancer*, vol. 24, pp. 95–104, Jan 1999.
- [8] J. Storer, "Effect of aging and radiation in mice of different genotypes," *Birth Defects Orig Artic Ser*, vol. 14, pp. 55–70, Jan 1978.
- [9] F. Darakhshan, C. Badie, J. Moody, M. Coster, R. Finnon, P. Finnon, A. A. Edwards, M. Szluinska, C. J. Skidmore, K. Yoshida, R. Ullrich, R. Cox, and S. D. Bouffler, "Evidence for complex multigenic inheritance of radiation aml susceptibility in mice revealed using a surrogate phenotypic assay," *Carcinogenesis*, vol. 27, pp. 311–8, Feb 2006.

- [10] Y. Peng, N. Brown, R. Finnon, C. Warner, X. Liu, P. Genik, M. Callan, F. Ray, T. Borak, and C. Badie, "Radiation leukemogenesis in mice: Loss of pu. 1 on chromosome 2 in cba and c57bl/6 mice after irradiation with 1 gev/nucleon 56fe ions, x-rays or gamma-rays. part i. experimental observations," *Radiation Research*, vol. 171, no. 4, pp. 474–483, 2009.
- [11] K. Rithidech, V. Bond, E. Cronkite, and M. Thompson, "Hypermutable of mouse chromosome 2 during the development of x-ray-induced murine myeloid leukemia," *Proceedings of the National Academy of Sciences*, vol. 92, pp. 1152–1156, Jan 1995.
- [12] R. Cox, G. Breckon, A. Silver, W. Mason, and A. George, "Chromosomal changes: Radiation sensitive sites on chromosome 2 and their role in radiation myeloid leukaemogenesis in the mouse," *Radiation and Environmental Biophysics*, vol. 30, no. 3, pp. 177–179, 1991.
- [13] M. M. Weil, J. S. Bedford, H. Bielefeldt-Ohmann, F. A. Ray, P. C. Genik, E. J. Ehrhart, C. M. Fallgren, F. Hailu, C. L. R. Battaglia, B. Charles, M. A. Callan, and R. L. Ullrich, "Incidence of acute myeloid leukemia and hepatocellular carcinoma in mice irradiated with 1 gev/nucleon56fe ions," *Radiation Research*, vol. 172, pp. 213–219, Aug 2009.
- [14] S. Pazzaglia, L. Pariset, S. Rebessi, and A. Saran, "Somatic cell hybrids for high-density mapping of chromosome 2 breakpoints in radiation-induced myeloid leukemia cell lines from inbred mice," *Molecular Carcinogenesis*, vol. 27, pp. 219–228, Jan 2000.
- [15] T. Hirouchi, T. Takabatake, K. Yoshida, Y. Nitta, M. Nakamura, S. Tanaka, K. Ichinohe, Y. Oghiso, and K. Tanaka, "Upregulation of c-myc gene accompanied by pu.1 deficiency in radiation-induced acute myeloid leukemia in mice," *Experimental Hematology*, vol. 36, pp. 871–885, Jul 2008.
- [16] N. Mahy, P. Perry, and W. Bickmore, "Gene density and transcription influence the localization of chromatin outside of chromosome territories detectable by FISH," *Journal of Cell Biology*, vol.159, pp. 753-763, Dec 2002.
- [17] K. Meaburn, T. Misteli, and E. Soutoglou, "Spatial genome organization in the formation of chromosomal translocations," *Seminars in cancer biology*, vol. 17, pp. 80–90, Jan 2007.
- [18] N. Mahy, P. Perry, S. Gilchrist, and R. Baldock, "Spatial organization of active and inactive genes and noncoding dna within chromosome territories," *Journal of Cell Biology*, vol. 157, pp. 579–589, May 2002.

- [19] W. D. Cook, B. J. McCaw, C. Herring, D. L. John, S. J. Foote, S. L. Nutt, and J. M. Adams, "Pu.1 is a suppressor of myeloid leukemia, inactivated in mice by gene deletion and mutation of its dna binding domain," *Blood*, vol. 104, pp. 3437–44, Dec 2004.
- [20] E. Meijne, A. Silver, S. Bouffler, D. Morris, E. W. van Kampen, S. Spanjer, R. Huiskamp, and R. Cox, "Role of telomeric sequences in murine radiation-induced myeloid leukaemia," *Genes, Chromosomes and Cancer*, vol. 16, pp. 230–237, 1996.
- [21] S. Bouffler, "Involvement of telomeric sequences in chromosomal aberrations," *Mutation Research*, vol. 404, pp. 199–204, Jan 1998.

CHAPTER V

GENETIC ANALYSIS OF THE GENOMIC IMPRINTING INFLUENCE AS POSSIBLE EXPLANATION FOR THE DELETION OF ONE COPY OF *PU.1* AFTER IONIZING RADIATION.

INTRODUCTION

5.1.1-Analogies Between Mouse Chromosome 2 and X-chromosome.

In chapter 3 of this dissertation the visualization of chromosome 2 territories showed similarities in conformation and organization of the chromatin as had been reported by others with the X-chromosomes in mammalian females.

The small and large domains of mouse chromosome 2 homologs displayed features similar to the inactive (Xi); and the active (Xa) copies of the X-chromosome respectively.

We do not know whether differences in the functional activities of the large and small domains of chromosome 2 might also show some similar differences as well. Beyond the transcriptional activity differences for the X chromosomes, many other observations bearing on the relationship between structure and function of chromatin within the interphase nucleus was well established a connection.

The actively transcribed regions of DNA have been shown to exist in an “open” conformation allowing accessibility for the transcription machinery⁽¹⁻⁷⁾.

The inactive regions tend to exist in a “closed” conformation since these regions are not actively transcribed but sequestered away from transcription making its chromatin more compact and inaccessible to the transcriptional proteins⁽⁸⁾.

Within the context of the X-chromosome, Dietzel⁽⁹⁾ and co-workers in 1999 has demonstrated a clear relationship between structure/organization and function in Xa and Xi homologs.

Differences were shown in the three dimensional interphase distances between probe markers compared between two genes within the Xa and Xi domains.

The different distances between the genes reflected a different chromatin organization related to transcriptional activity and the regulation to the level of chromatin topology occurred as a result of hiding the inactive copy of a gene away from the transcriptional process within the Xi domain.

The DNA inactivation mechanism of Xi and the genomic imprinting of genes are related and show the same result: regulation of gene expression.

The mechanism through which the inactivation of the X chromosome and the inactivation of imprinted genes is similar, but the only difference is that imprinting works in specific regions of chromosome, while the X chromosome inactivation involve almost all the chromosome.

5.1.2-Genomic Imprinting

One characteristic of the regulation occurs through genomic imprinting, which has been shown to appear in clusters, linking multiple genes for regulation under the imprinted region for a coordinated regulation of a determined chromosomal domain⁽¹⁻⁹⁾.

The X-chromosome inactivation shares this mechanism involving imprinted regions, where X-chromosome has an inactivation control center⁽¹⁰⁾ and imprinted regions have imprinting centers or imprinting control regions (ICR)^(1,2).

Thus, genomic imprinting may be an important factor that could affect the organization and architecture of the chromosomal domain.

Additionally, data compiled by the Medical Research Council Harwell⁽¹¹⁾ described imprinted regions within mouse chromosome 2⁽¹¹⁻¹⁶⁾; along with another fifteen imprinted chromosomes. Gene regulation through genomic imprinting is defined by the uniparental expression of a determined gene or gene cluster⁽¹⁻¹⁶⁾.

Thus, the genes or regions under imprinting express only one of the two allelic copies, either maternal or paternal. Intrinsically, by definition an “imprinted” gene is the inactive or silent copy inherited from one of the parents⁽¹⁻¹⁷⁾. From the viewpoint of chromatin structure, a transcriptionally active or inactive region is related to the condensation or decondensation of the chromatin and in turn is intimately associated with both DNA and histone modifications⁽¹⁷⁻¹⁸⁾.

DNA methylation is considered the landmark of genomic imprinting and is a heritable modification that typically occurs by the covalent addition of methyl groups to

cytosine residues in CpG dinucleotide sequences (CpG-islands)⁽¹⁻²⁰⁾. Cytosine methylation occurs specifically in the imprinting control region (ICR), which is a regulatory center for the regional control of imprinting or imprinted expression⁽¹⁻²¹⁾.

In addition, this methylation is species and tissue-specific and it is associated with DNA silencing⁽²²⁾.

The main histone modification related to genomic imprinting is acetylation of histone H4, which induces important remodeling of the chromatin within the interphase nucleus.

Acetylation is a reversible modification that is regulated by histone acetyltransferases (HATs) and histone deacetylases (HDACs).

The acetylation of the H4 histone decreases the affinity of this histone for the DNA resulting in a relaxed DNA.

In the opposite case, when the histone H4 is deacetylated, the resulting events are related to DNA methylation, histone H1 activation, chromatin condensation, and gene silencing^(26,28).

As shown in figure 5.1, genomic imprinting is expressed in the adult animal, however, during gametogenesis the imprinting pattern is erased and re-established by the end of the gametogenesis. Thus, an adult mouse carries both maternal and paternal imprinting but during gametogenesis that imprinting is erased; then the imprinting is re-established as either maternal imprinting in females or paternal imprinting in males during gamete maturation. Thus, it is possible to reconstitute the whole genomic imprinting in the offspring after fertilization.

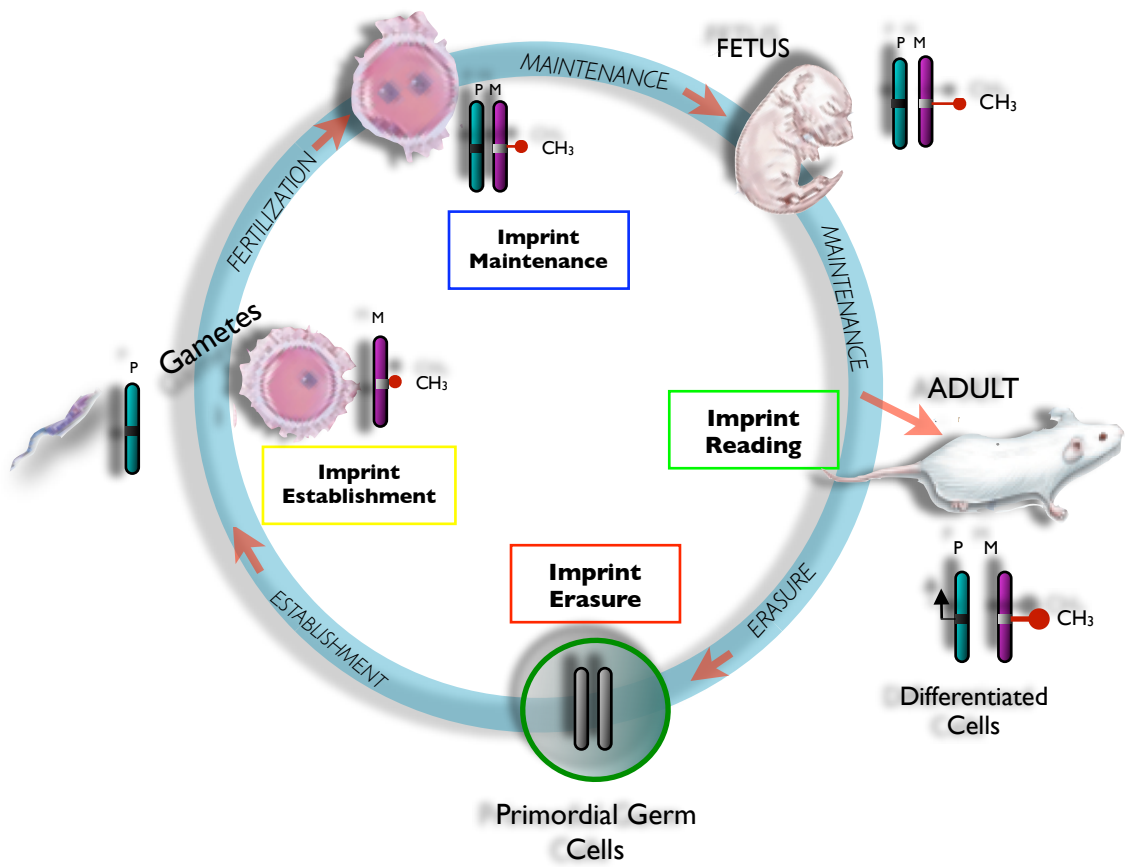


Figure 5.1: Genomic Imprinting cycle in mice.

There is no available information about the *PU.1* region in terms of genomic imprinting, but it is known that most of chromosome 2 shows imprinting.

However, it is mainly the proximal and distal regions of chromosome 2 that are imprinted^(11,14) but there is no data associated to genomic imprinting in the minimal deleted region or *PU.1*.

To explore and test the possible effect of the genomic imprinting on the structure and organization of the chromatin in both small and large domain from mouse chromosome 2, I used a different mouse model that allowed us to differentiate the parental origin of each chromosome 2 inherited after fertilization for the hybrid offspring (F1) obtained from crosses between a C3H/HeNCrl and Tirano/EiJ mouse strain.

The latter has a translocation involving chromosome 2 and 8 which allows tracking of a paternal or maternal chromosome 2.

As mentioned in chapter 1; the C3H/HeNCrl mouse strain is sensitive to AML induction after radiation treatment. In addition, chromosome 2 within this mouse model is radiosensitive.

An example of this is the leukemia cell line 8016 generated after radiation treatment showing the typical deletion of *mdr* in one copy of chromosome 2.

The other mouse strain used, Tirano/EiJ sub-strain Rb(2.8)2Lub, carries a Robertsonian translocation between chromosome 2 and 8 which, as mentioned above, is the cytogenetic marker that facilitates the visualization of chromosome 2 that belongs to this mouse strain.

5.2-Hypothesis

Thus, the work hypothesis tested was:

The domain structure is due to the influence of genomic imprinting; thus, by analyzing the chromosomal domains from C3H, it must show either small or large conformation in association to its parental origin (paternal or maternal copy).

5.3-Specific Aims

Specific Aim 1: The first aim was to generate hybrid mice from crosses between Tirano females with C3H males and Tirano males with C3H females with the consequent derivation of offspring that carries the C3H/HeNCrI chromosomes of either paternal or maternal origin respectively.

Specific Aim 2: Determination of the small and large domain in interphase bone marrow cells from offspring F1 (Tirano/EiJ ♀ x C3H/HeNCrI ♂) and from F1 (C3H/HeNCrI ♀ x Tirano ♂) by measuring the distance of the breakpoint clusters within C3H/HeNCrI chromosome 2 domain.

The detection of chromosome 2 from each mouse strain was possible due to the cytogenetic features of the mouse strains.

The use of both mouse strains, Tirano/EiJ sub-strain Rb (2;8) 2Lub and C3H/HeNCrI, made possible to follow the maternal and paternal chromosome 2 in a hybrid F1 (offspring), due to the Robertsonian translocation (2;8) that belongs to the Tirano/EiJ mouse strain.

As shown in figure 5.2, the karyotype of the hybrid offspring (F1) shows a metacentric chromosome (2;8) from the Tirano strain, while the other homolog is the typical acrocentric derived from C3H/HeNCrI.

Metaphase cells from the bone marrow from these hybrids show hybridization markers for the proximal and distal breakpoint cluster regions (pbc and dbc) in the acrocentric chromosome 2 from C3H/HeNCrI; and chromosome 8 marker in the metacentric chromosome 2 from the Tirano/EiJ mouse strain.

Therefore, this enables us to determine parental origin of each chromosome 2 in the offspring (F1) obtained.

The analysis of C3H/HeNCrI chromosome 2 domains was performed in interphase cells; therefore, the association of the chromosome 8 marker with one domain and not the other was important to determine what domain belong to C3H/HeNCrI mouse strain.

This mouse model used in this experiments facilitated the identification of the parental origin of each homolog giving us a tool to determine whether the genomic imprinting plays a role in the differential organization of both homologs and the preferential deletion of only one copy of chromosome 2 after radiation exposure.

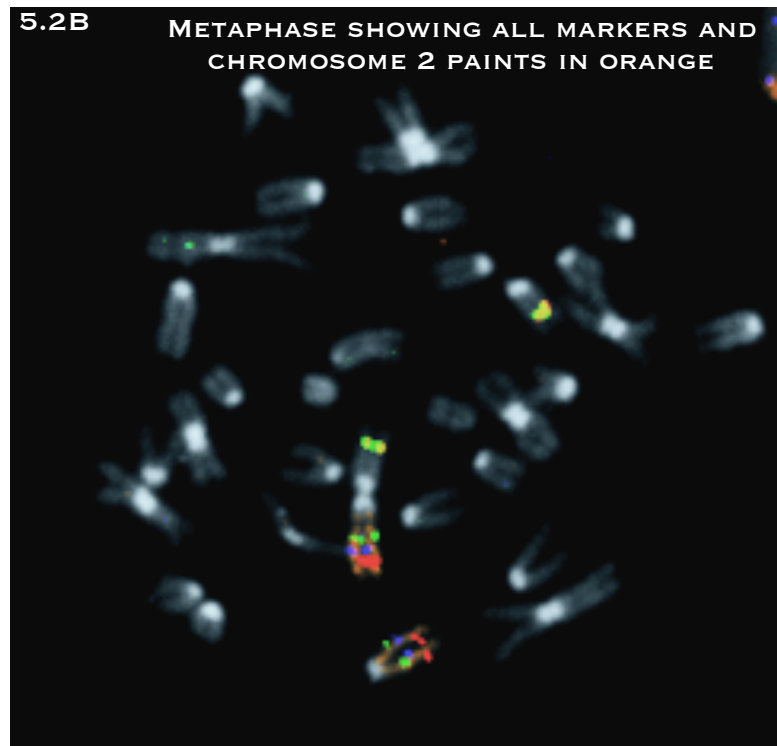
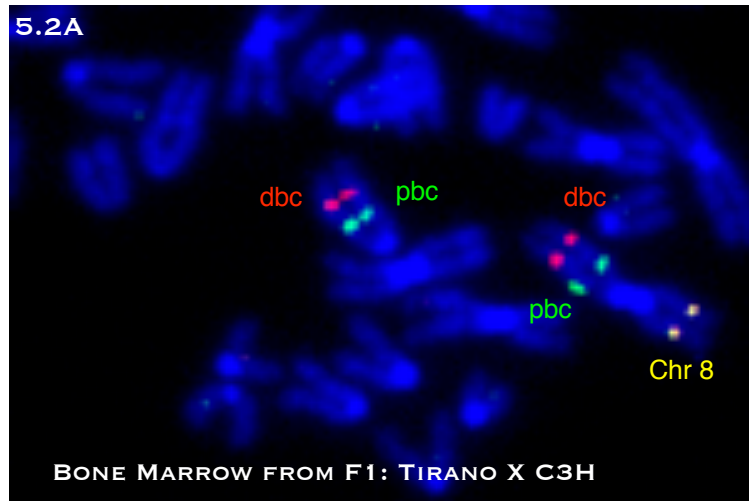


Figure 5.2: A) Metaphase showing chromosome 2 from Tirano/EiJ and C3H/HeNcrI in F1 Hybrid bone marrow cells. B) Another metaphase cell showing all markers used.

5.4-Experimental Approach

The transcriptional status of *PU.1* gene throughout the hematopoiesis is highly regulated and becomes up-regulated or down-regulated depending on the fate of the specific hematopoietic stem cell (HSC)⁽²³⁻²⁵⁾.

In addition, one more level of complexity in the regulation is conferred by the existence of genomic imprinting in several regions of chromosome 2. It is well known since 1986 when Cattanach et al.⁽¹²⁻¹⁴⁾ described the distal region of mouse chromosome 2 as imprinted.

In spite of more research is needed to detect other imprinted regions within chromosome 2, new genes have been discovered in the proximal and central region of chromosome 2.

Since genomic imprinting is produced in clusters, it may be likely that the linkage group could involve a large region of chromosome 2 in the regulation through imprinting. Within chromosome 2 there are eleven imprinted genes already described as shown in Figure 5.3. In addition, the figure 5.3 shows the location of the markers used for the distance measurements of the breakpoint cluster and *PU.1*. Nine of the imprinted genes are in the distal region within the distal breakpoint cluster and two in the proximal region of the chromosome 2 without involving proximal breakpoint cluster.

From these 11 imprinted genes, five are maternally expressed and six of them are paternally expressed.

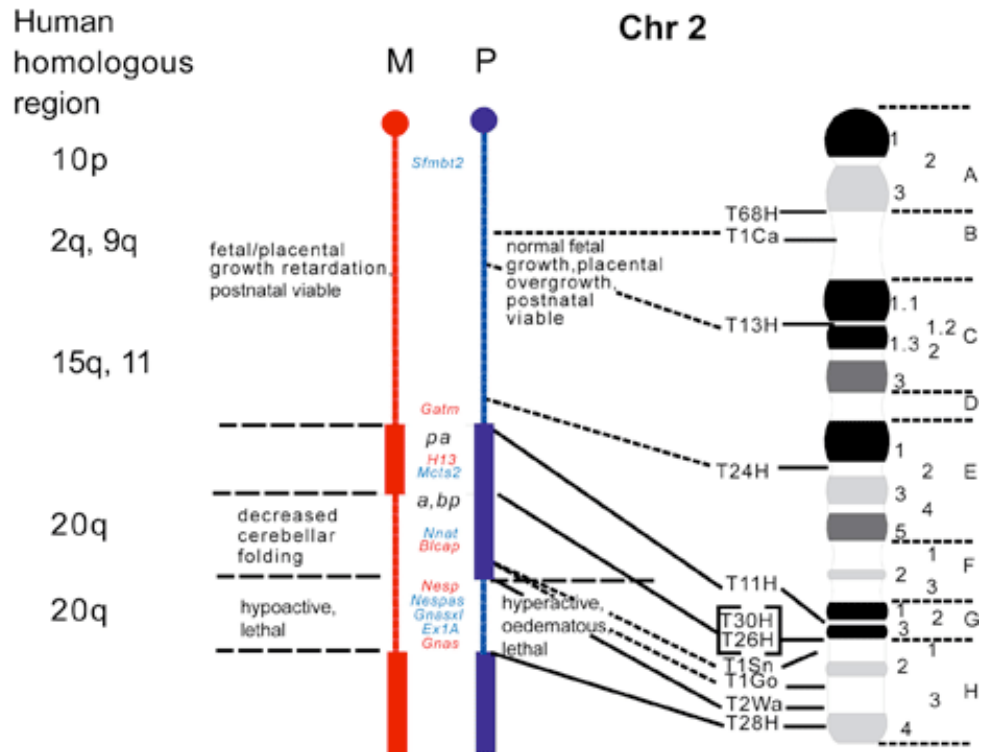


Figure 5.3: Imprinting map from mouse chromosome 2, idiogram and human homologous regions. Data from MRC Harwell.

Cox et al. in 1991⁽²⁶⁾ used the concept of genomic imprinting trying to explain the causes of the deletion of only one copy of chromosome 2.

The possible explanations for the preferential gene loss they provided were:

- A Differential mutability of maternally or paternally imprinted regions.
- B Imprinted differences in suppressor gene activity that favors the loss of the most active gene copy.

However, it is difficult to determine which homolog is the maternal or paternal copy⁽²⁶⁾.

Most of genetic studies on genomic imprinting have been done using mice with balanced translocations used to produce uniparental disomies and reveal the effect of parental origin^(12,26,27).

Mice carrying Robertsonian (Rb) translocations occur in nature and for this particular experiment the use of Tirano mouse strain sub-strain Rb(2.8)2Lub, was a useful tool for identification of the parental origin of chromosome 2.

This Rb(2.8) generates a cytogenetic distinct metacentric chromosome that differs from the rest of the acrocentric complement⁽²⁸⁾.

As shown in Figure 5.4 below, the crosses between Tirano/EiJ Rb(2.8)2Lub and C3H/HeNCrl generated offspring (F1) that were heterozygote for this specific cytogenetic marker with the corresponding paternal and maternal copy of chromosome 2 from C3H.

From these F1 mice, I proceeded to determine the domain size within the interphase cells from bone marrow keeping track on the paternal and maternal origin.

Crosses Design to C3H/HeNCrI Chromosome 2 from Maternal and Paternal Origin

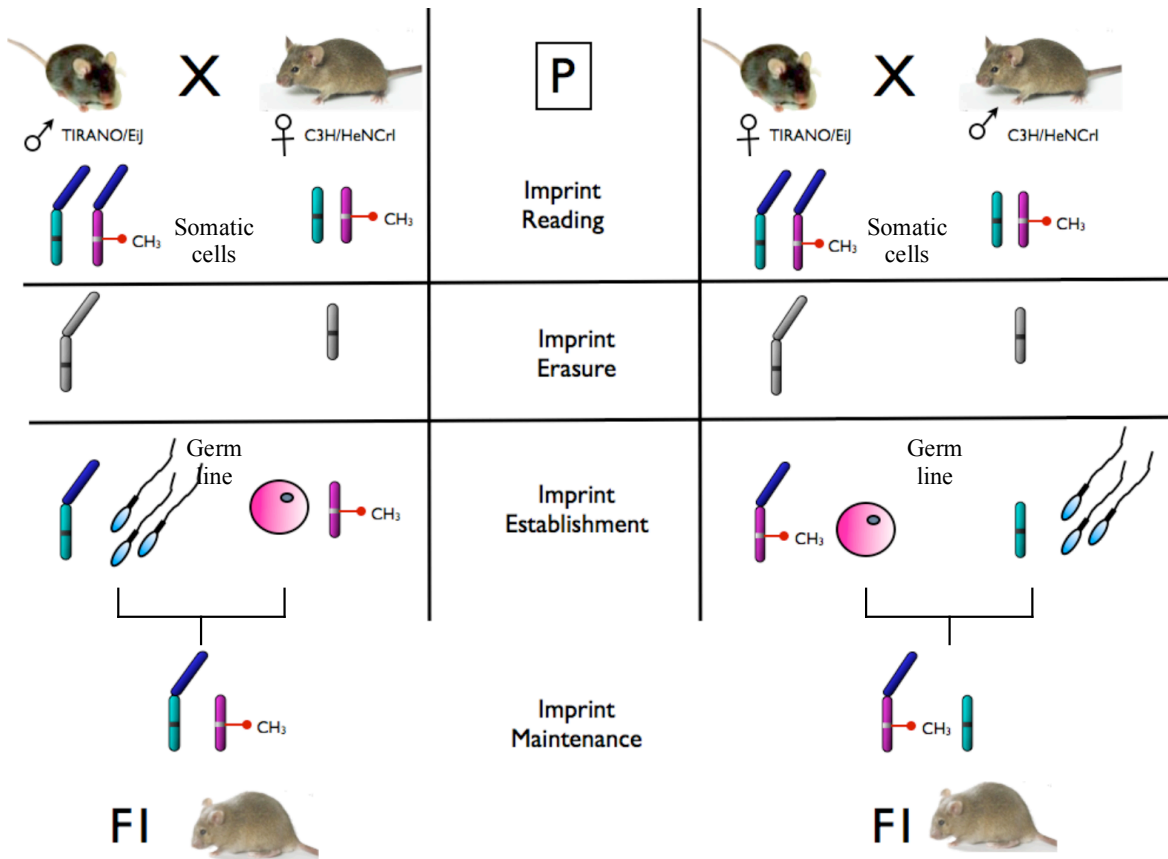


Figure 5.4: Offspring (F1) from the crosses Tirano/EiJ male X C3H/HeNCrI female; and Tirano/EiJ female X C3H/HeNCrI male; in addition, the expected genetic constitution considering the corresponding theoretical epigenetic modification.

In other words, if the close and open configuration of the chromatin that we saw in the interphase is due to the genomic imprinting, we should be able to determine its parental origin.

Thus, I expect to observe that the most active copy of chromosome 2 shows an open conformation; therefore, a high proportion of cells would be expected to be associated with the large domain derived from either the maternal or the paternal copy (but not in both) of C3H/HeNCr1 chromosome 2 domain.

Conversely, the less active copy of chromosome 2 should be transcriptionally more silenced and with a closed or more condensed conformation of the chromatin; in other words, a high proportion might be expected to be associated with the small domains.

In addition, the high proportion of either small or large domain has to be present in either copy of chromosome 2, maternal or paternal, but not in both.

The question to answer first was whether the small or large domains conformation of the chromatin is influenced by the parental origin of chromosome 2 or whether it is a random event and there is no influence of the parental origin of the chromosome.

Taking into consideration where the loss of *PU.1* occurs more frequently, I felt it may be possible to define if there is any parental influence in both the chromatin configuration and organization of the markers; consequently the result could suggest that the preferential copy deletion is influenced from either maternally or paternally inherited chromosome 2 after irradiation treatment.

5.5-Materials and Methods

5.5.1-Mice

C3H/HeNCrl and Tirano/EiJ

All C3H and Tirano/EiJ mice used in this experiment were obtained from Jackson laboratory (Bar Harbor, Maine 04609 USA) (<http://www.jax.org/index.html>).

The hybrid (F1) were bred in the laboratory animal resources (L.A.R) here at CSU. The mating was carefully followed in consideration to produce mice where the mother was a C3H/HeNCrl for one group that I called C3H_(Mat), and another group where the father of the offspring was a C3H/HeNCrl and it was called C3H_(Pat).

Therefore, I used the first generation (F1) of these crosses to perform the experiment.

5.5.2-Cells

Whole bone marrow (BM)

The femurs were obtained from the mice and the bone marrow was flushed out with a 5 ml syringe and a 30-gauge needle.

The collected bone marrow in PBS was then centrifuged at 1,000 rpm and resuspended in 8 ml of 7.5 mM KCl and 1.5 ml trypsin-EDTA. The addition of trypsin dissolved the connective tissue characteristic from the bone marrow tissue to obtain a cleaner fixation to perform 3D-FISH. After incubation at 37C the sample was filtered through a 40 um

mesh cell strainer mesh to reduce debris and cell clumps and thus obtain a cleaner cell suspension preparation.

The cell suspension was then fixed with methanol: acetic acid glacial (3:1). The cell suspension was then dropped onto the slides which were then air-dried and aged for at least 3 days before further processing.

5.5.3-BAC-clones, FISH, and image acquisition.

The Bacterial Artificial Chromosomes (BAC) clones were selected and ordered from the BACPAC resources center <http://bacpac.chori.org/> as described in chapter 3.

In these experiments I used the following BAC clones: RP23-90A5 for pbc, RP23-409P4 for dbc, and RP23-263H8 for the minimal deleted region. Furthermore, clone RP23-325K19 was added to visualize mouse chromosome 8. As described in previous chapters a whole chromosome 2 paint was used as well to identify the chromosome 2 domains. DNA was isolated and purified using alkaline lysis and according to instructions accompanying the QIAGEN filter Plasmid Maxi kit (Qiagen, Valencia, CA) used. The labeling of each BAC was made using a nick translation kit (Roche Applied Science, Indianapolis, IN). The fluorochromes used to label the DNA were: green-dUTP (green for pbc), red-dUTP (red for the dbc) from Abbott Molecular (Abbott Park, IL); DEAC (PerkinElmer, Waltham, MA) (Cyan for mdr); and green-dUTP and red-dUTP (Yellow for chromosome 8 marker).

Finally, whole chromosome 2 paint was biotin-labeled (Star-FISH®, Cambio, Cambridge, UK) and was visualized with Streptavidin-Alexa-647 (Invitrogen, Carlsbad, CA).

A solution containing 0.5 ul of each labeled BAC-probes was applied at a concentration of about 1 ng/ul to the slides. The slides were cover-slipped and sealed with rubber cement.

Co-denaturation of probes and target DNA occurred at 80°C in hybridization mix (proprietary solution designed to optimize hybridization of multiple probes) for 5 minutes followed by incubation at 37°C overnight.

The coverslips were then removed and the slides washed in 50% formamide/2X SSC at 43.5°C for 5 minutes followed by 3 washes in 2X SSC at 43.5°C for 5 minutes to remove any mismatched probe.

The slides were counterstained with DAPI (4',6-diamidino-2-phenylindole, dihydrochloride) in an anti-fade solution, cover-slipped, and sealed.

Three dimensional deconvolution, reconstruction and distance measurements of the breakpoint clusters were performed as described in previous chapters using a combination of software such as ImageJ Software (<http://rsbweb.nih.gov/ij/index.html> - NIH), Autoquant software (Media Cybernetics, inc; Bethesda, MD) and Metamorph (Molecular Devices, Sunnyvale, CA).

5.6-Results

Bone marrow cells image stacks were 3D deconvoluted and reconstructed as previously described in chapter 2 of this dissertation.

The analysis of the interphase cells considered the positioning of the BAC markers used within the chromosomal domain to recognize chromosome territories that belong to either C3H/HeNCr1 or Tirano/EiJ mouse strain in F1 cells.

Additionally, as shown in figure 5.5 the marker for chromosome 8 was key to identify the translocated chromosome 2 in interphase cells.

The measurements of the physical distances between the breakpoint clusters only within the C3H/HeNCr1 chromosomal domain showed the BAC-markers organization and chromosome 2 territories in both the maternal and paternal copies in the different offsprings.

The chromosomal domains within these samples are not comparable to the domains shape found in CBA/CaJ and C57BL/6J.

Indeed, the domains were not similar to the described small and large domain described in previous chapters. However, the organization of the BACs were mostly identical to the organization found in the small domain.

The triangular organization and close distance (between 0-1.79 μm) of the markers was found in high proportion of C3H/HeNCr1 domains analyzed.

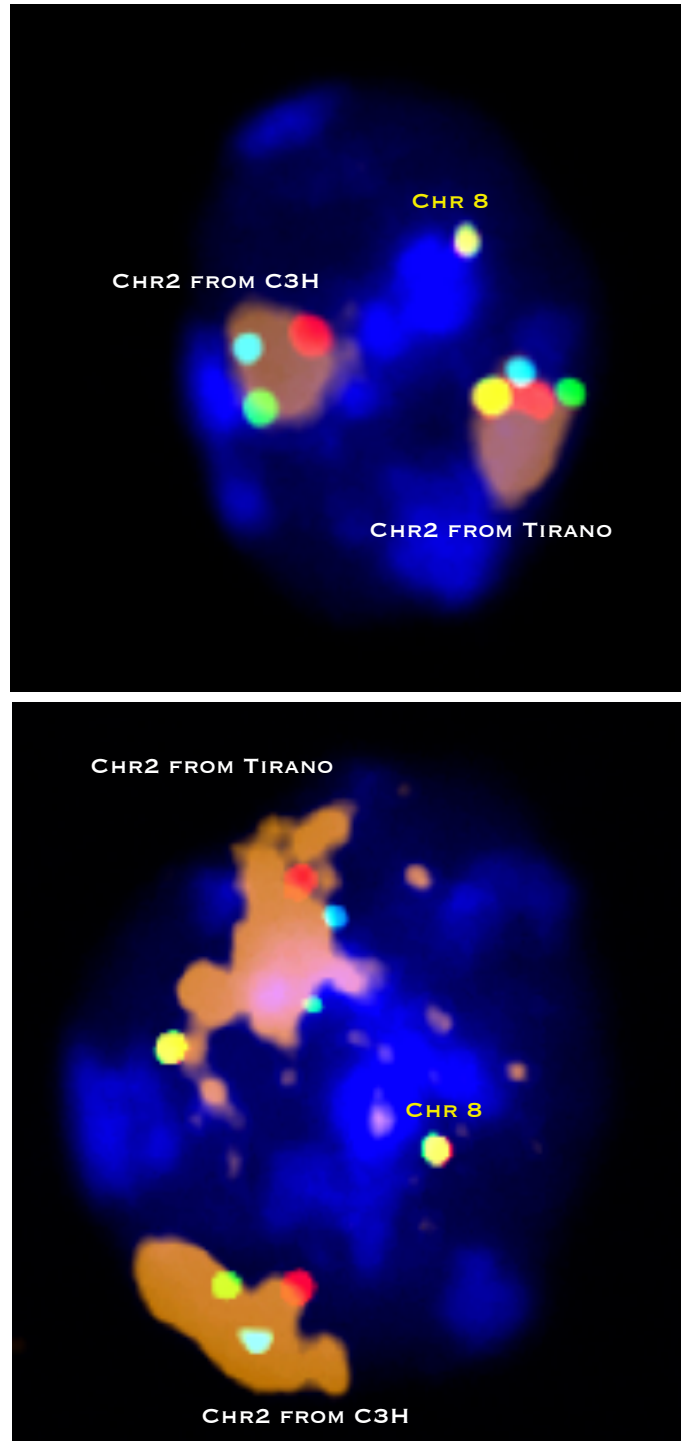


Figure 5.5: Interphase cells from F1: tirano X C3H showing one normal chromosome 2 from C3H and the translocated chromosome 2 from the Tirano strain. Orange: chr 2 domain; green: proximal breakpoint cluster; Cyan: PU.1; red: distal breakpoint cluster; and yellow: chromosome 8 marker.

The distribution of distances in the maternal C3H/HeNCRl domains showed two peaks in the histogram showed in figure 5.6, where one peak (30%) was within the range 1.2-1.59 um.

While the second peak (27%) was within the range 0.4-0.79 um. The average value for this group of measurements was $C3H_{(Mat)} = 1.26$ um and a standard deviation of 0.54 um.

On the other hand, as shown in figure 5.7, the paternal C3H/HeNCRl domain showed a similar distribution of breakpoint cluster distances compared to the distribution within the maternal domains.

Thus, the C3H/HeNCRl paternally derived chromosome 2 domain showed two peaks; one peak (32%) was within the range 1.2-1.59 um and the second peak (23%) was within 0.4-0.79 um range.

Finally, the average for this group was $C3H_{(Pat)} = 1.19$ um and a standard deviation of 0.58 um.

As shown in figure 5.8, the comparison between $C3H_{(Pat)}$ and $C3H_{(Mat)}$ showed identical breakpoint clusters distributions for both paternal and maternal copies.

The distribution of measurements within $C3H_{(Pat)}$ contains ~74% of these measurements falling within the range 0.4-1.59 um; and ~10% of the measurements were bigger than 2 um.

In comparison, within the maternal $C3H_{(Mat)}$ about 72% of the measurements were between 0.4 and 1.56 um, and only ~9% of the measurements were larger than 2 um.

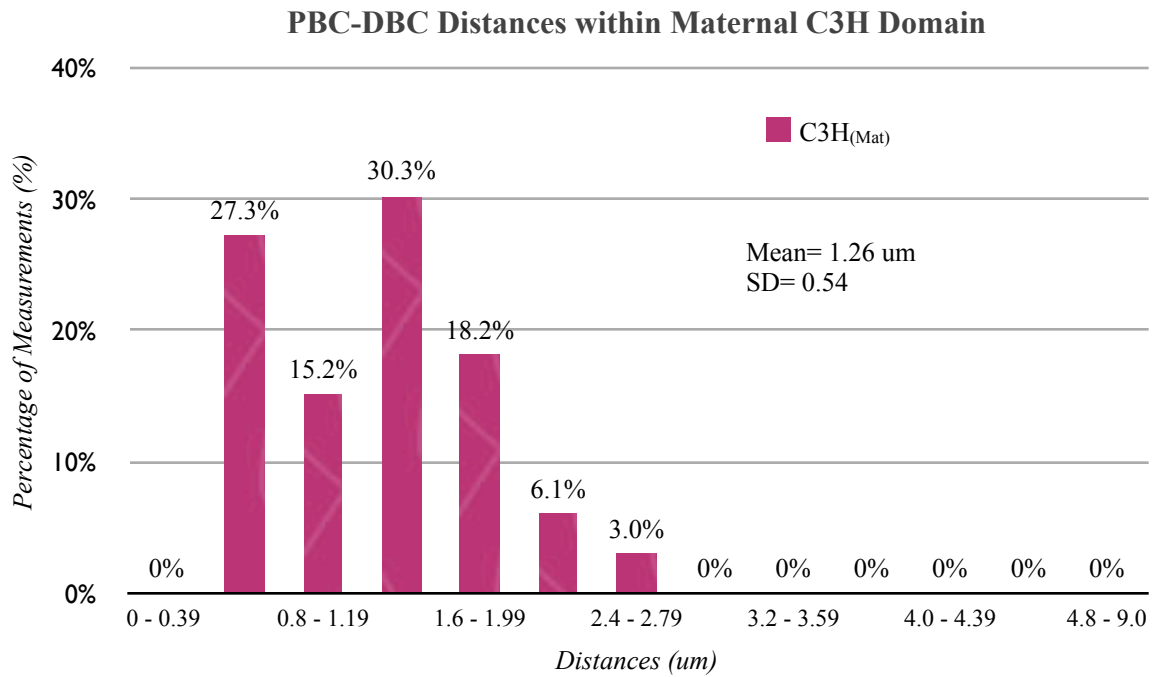


Figure 5.6: Histogram showing the distances distribution of breakpoint clusters within C3H_(Mat)

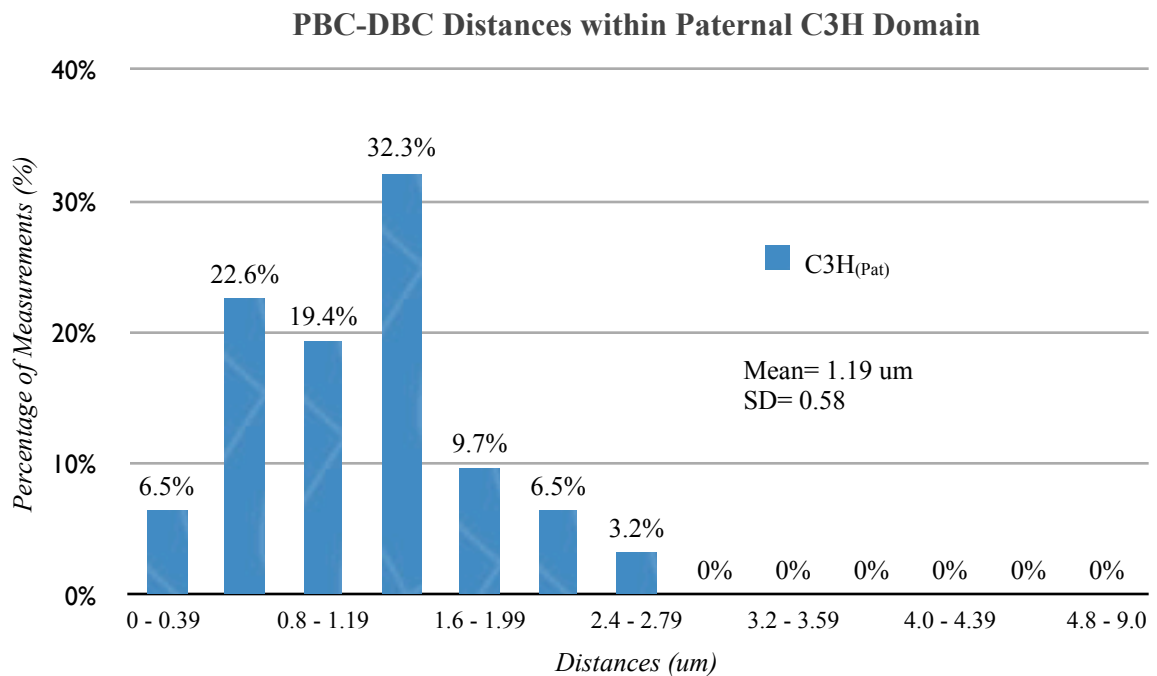


Figure 5.7: Histogram showing the distances distribution of breakpoint clusters within C3H_(Pat)

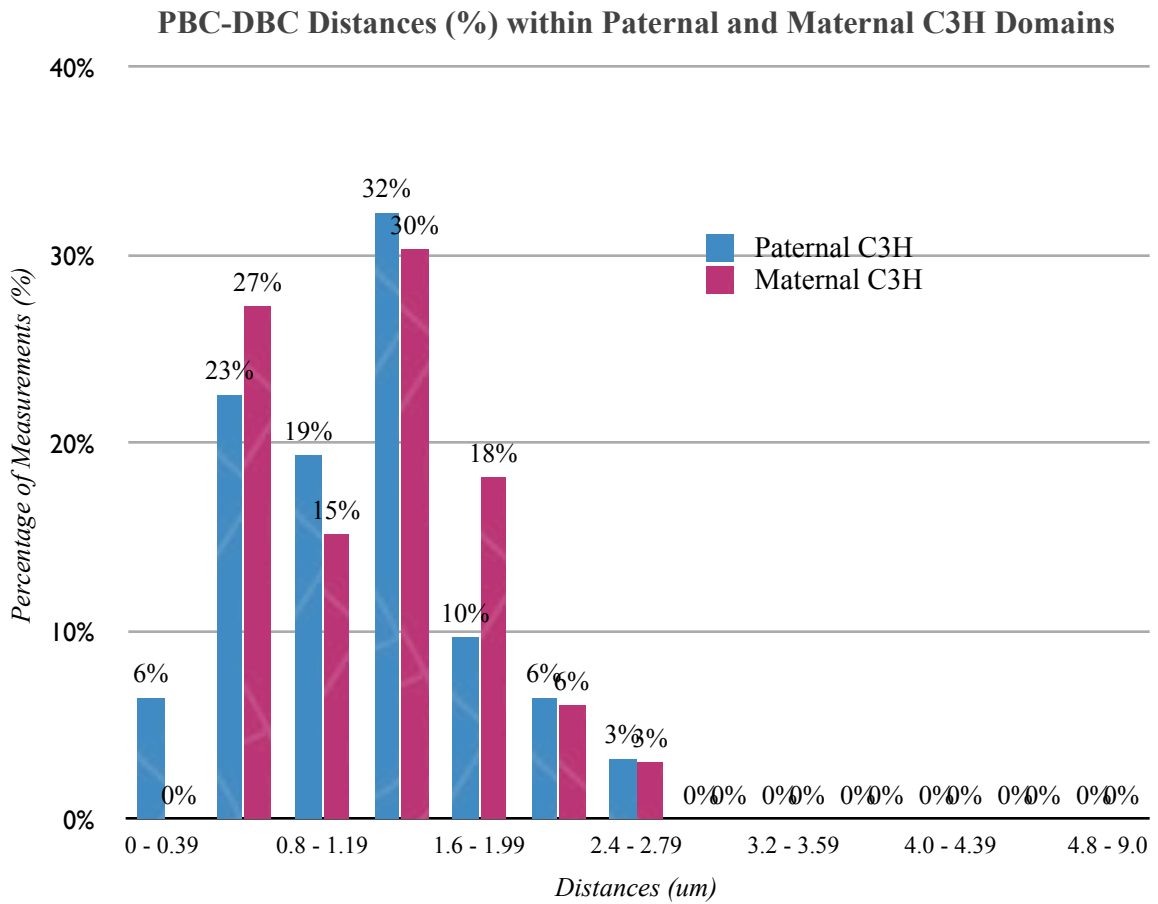


Figure 5.8: Comparison of distances distribution between C3H_(Mat) and C3H_(Pat).

5.7-Discussion

The idea behind the experimental approach was that inactive and imprinted region of DNA have both histone and DNA modifications that affect the organization and architecture of the chromatin as seen in X-chromosome inactivation in mammalian females.

However, the inactive X-chromosome is an extreme case where almost the whole chromosome is inactive. The same is not true in the imprinted mouse chromosome 2.

As mentioned above, imprinting in chromosome 2 is more complex than X-chromosome inactivation because within chromosome 2 the inactivation is partial or not total.

This partial inactivation is evident because there are regions with genes that are paternally expressed and other regions of maternally expressed genes within the same homolog.

In this case it is known that specific locations within the nucleus exist where genes being actively transcribed are located in close proximities to those that are silenced.

As an example, Dietzel et al. in 1999, showed that the distances between two genes were related to the transcriptional activity of the genes within the X-chromosomes.

ANT 2 (adenine nucleotide translocase 2) is an active gene only in X_a, but ANT 3 is expressed in both X_a, and X_i.

Thus, the three dimensional distances of the 2 genes within X_a were closer than the distances of the same genes in X_i.

The inactive copy of ANT 2 appeared located in the interior of Xi; in contrast, the active copy of ANT 2 and both active copies of ANT 3 were located in a more peripheral location.

This suggested a topological influence of the gene expression regulation. The same situation is seen in imprinted chromosomes, where the imprinted genes are grouped in determined location away from the genes that are actively transcribed⁽²⁹⁻³¹⁾.

The influence of the Robertsonian translocation in the final organization of the whole genome or even within the translocated chromosome 2 is unknown. Therefore, we do not know the influence of the translocated chromosome in the context of the whole chromatin organization.

I observed that the distances of the breakpoint clusters within C3H domains showed the same distances distribution in both maternal and paternal copy without showing any difference in organization of the markers.

As shown in figure 5.9, considering the cluster marker distance differences discussed in previous chapters, the measurements of the clusters within C3H_(Mat) and C3H_(Pat) showed that 85% and 84% of the measurements respectively, were less than 1.79 μm .

These values established as a reference for the small domain.

While for the large domain (values bigger than 2 μm) was observed in 10% of the measurements for C3H_(Pat) and 9% for C3H_(Mat).

The rest of the measurements falls into the region of undetermined domain values (ranged between 1.8 to 1.99 μm

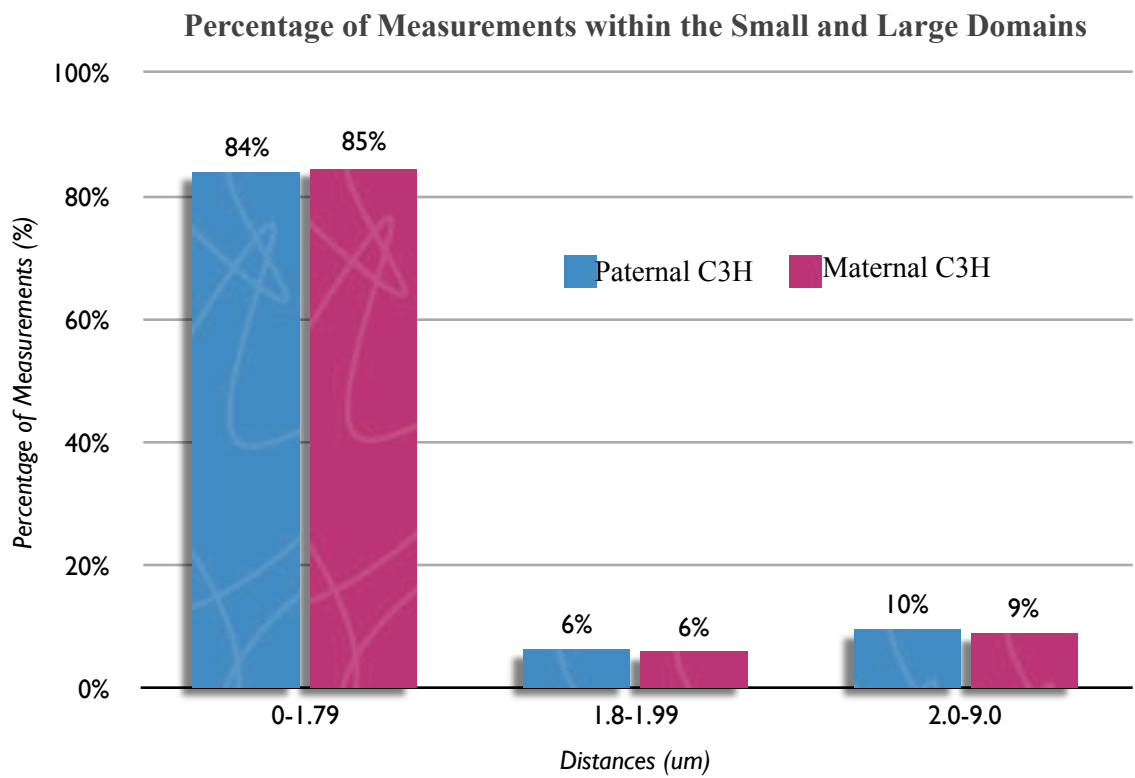


Figure 5.9: Comparison of distances distribution between C3H_(Mat) and C3H_(Pat).

5.8-Conclusions

The experimental data showed no evidence of any influence in the chromosomal domain conformation in relationship to the genomic imprinting occurring in mouse chromosome 2. The influence of genomic imprinting on the conformation of the chromosomal domains cannot be demonstrated based on the difference expected for the maternal and paternal copy of chromosome 2 within interphase cells.

All chromosome 2 domains from C3H/HeNCrl showed breakpoint clusters distances and organization of the domains similar to the small domain in both maternal and paternal copies.

Therefore, I concluded that the suggested preferential deletion of the large domain does not seem to be influenced by genomic imprinting. Consequently, genomic imprinting does not influence the conformation and organization of the chromatin in the small and large domain in mouse chromosome 2 within the mouse model used in these experiments.

References

- [1] M. Bartolomei and S. Tilghman, "Genomic imprinting in mammals," *Annual Reviews in Genetics*, vol. 31, pp. 493–525, Jan 1997.
- [2] W. Reik and J. Walter, "Genomic imprinting: parental influence on the genome," *Nat Rev Genet*, vol. 2, pp. 21–32, Jan 2001.
- [3] H. Albiez, M. Cremer, C. Tiberi, L. Vecchio, L. Schermelleh, S. Dittrich, K. Küpper, B. Joffe, T. Thormeyer, J. von Hase, S. Yang, K. Rohr, H. Leonhardt, I. Solovei, C. Cremer, S. Fakan, and T. Cremer, "Chromatin domains and the interchromatin compartment form structurally defined and functionally interacting nuclear networks," *Chromosome Research*, vol. 14, pp. 707–33, Jan 2006.
- [4] N. Mahy, P. Perry, and W. Bickmore, "Gene density and transcription influence the localization of chromatin outside of chromosome ...," *Journal of Cell Biology*, vol. 159, pp. 753–763, Dec 2002.
- [5] F. Recillas-Targa, "Dna methylation, chromatin boundaries, and mechanisms of genomic imprinting," *Archives of Medical Research*, vol. 33, no. 5, pp. 428–438, 2002.
- [6] R. Oakey and C. Beechey, "Imprinted genes: identification by chromosome rearrangements and post-genomic strategies," *Trends in Genetics*, vol. 18, pp. 359–366, July 2002.
- [7] A. P. Feinberg and B. Tycko, "The history of cancer epigenetics," *Nat Rev Cancer*, vol. 4, pp. 143–53, Feb 2004.
- [8] R. Eils, "Three-dimensional reconstruction of painted human interphase chromosomes: active and inactive x chromosome territories have similar volumes but differ in shape and surface structure," *Journal of Cell Biology*, vol. 135, pp. 1427–1440, Dec 1996.
- [9] S. Dietzel, K. Schiebel, G. Little, P. Edlmann, G. Rappold, R. Eils, C. Cremer, and T. Cremer, "The 3d positioning of ant2 and ant3 genes within female x chromosome territories correlates with gene activity," *Experimental Cell Research*, vol. 252, no. 2, pp. 363–375, 1999.
- [10] S. Duthie, T. Nesterova, and E. Formstone, "Xist rna exhibits a banded localization on the inactive x chromosome and is excluded from autosomal material in cis," *Human Molecular Genetics*, vol. 8, pp. 195–204, Jan 1999.

- [11] C. Williamson, A. Blake, S. Thomas, C. Beechey, J. Hancock, B. Cattanaach, and J. Peters, 2009. *MRC Harwell, Oxfordshire*. World Wide Web Site - Mouse imprinting data and references - http://www.har.mrc.ac.uk/research/genomic_imprinting/
- [12] B. M. Cattanaach, "Parental origin effects in mice," *Journal of embryology and experimental morphology*, vol. 97 Suppl, pp. 137–50, Oct 1986.
- [13] B. Cattanaach and C. Beechey, "Autosomal and x-chromosome imprinting," *Development*, vol. 108, no. Supplement, p. 63, 1990.
- [14] B. Cattanaach, C. Beechey, and J. Peters, "Interactions between imprinting effects in the mouse," *Genetics*, vol. 168, no. 1, pp. 397–413, 2004.
- [15] C. Williamson, C. Beechey, D. Papworth, S. Wroe, C. Wells, L. Cobb, and J. Peters, "Imprinting of distal mouse chromosome 2 is associated with phenotypic anomalies in utero," *Genetics Research*, vol. 72, no. 03, pp. 255–265, 1998.
- [16] J. Peters, S. F. Wroe, C. A. Wells, H. J. Miller, D. Bodle, C. V. Beechey, C. M. Williamson, and G. Kelsey, "A cluster of oppositely imprinted transcripts at the gnas locus in the distal imprinting region of mouse chromosome 2," *Proc Natl Acad Sci USA*, vol. 96, pp. 3830–5, Mar 1999.
- [17] T. Watanabe, A. Yoshimura, Y. Mishima, and Y. Endo, "Differential chromatin packaging of genomic imprinted regions between expressed and non-expressed ...," *Human Molecular Genetics*, vol. 9, pp. 3029–3035, Jan 2000.
- [18] E. Platonov and D. Isaev, "Genomic imprinting in epigenetic of mammals," *Russian Journal of Genetics*, vol. 49, pp. 1030–1042, Jan 2006.
- [19] K. Robertson, "Dna methylation and human disease," *Nat Rev Genet*, vol. 6, pp. 597–610, Aug 2005.
- [20] L. Lande-Diner and H. Cedar, "Silence of the genes—mechanisms of long-term repression," *Nat Rev Genet*, vol. 6, no. 8, pp. 648–654, 2005.
- [21] M. Constancia, G. Kelsey, and W. Reik, "Resourceful imprinting," *Nature*, vol. 432, pp. 53–57, Jan 2004.
- [22] S. da Rocha and A. Ferguson-Smith, "Genomic imprinting," *Current Biology*, vol. 14, pp. 646–649, Jan 2004.

- [23] R. Fisher and E. Scott, "Role of pu. 1 in hematopoiesis," *Stem Cells*, vol. 16, pp. 25–37, Oct 1998.
- [24] A. Dakic, L. Wu, and S. Nutt, "Is pu. 1 a dosage-sensitive regulator of haemopoietic lineage commitment and ...," *Trends in immunology*, vol. 28, pp. 108–114, Jan 2007.
- [25] Y. Li, Y. Okuno, P. Zhang, and H. Radomska, "Regulation of the pu. 1 gene by distal elements," *Hematopoiesis*, vol. 98, pp. 2958–2965, Jan 2001.
- [26] R. Cox, G. Breckon, A. Silver, W. Mason, and A. George, "Chromosomal changes: Radiation sensitive sites on chromosome 2 and their role in radiation myeloid leukaemogenesis in the mouse," *Radiation and Environmental Biophysics*, vol. 30, no. 3, pp. 177–179, 1991.
- [27] M. Hitchins and G. Moore, "Genomic imprinting in fetal growth and development," *Expert Reviews in Molecular Medicine*, vol. 4, no. 11, pp. 1–19, 2004.
- [28] R. Schulz, L. A. Underkoffler, J. N. Collins, and R. J. Oakey, "Nondisjunction and transmission ratio distortion of chromosome 2 in a (2.8) robertsonian translocation mouse strain," *Mamm Genome*, vol. 17, pp. 239–47, Mar 2006.
- [29] J. LaSalle and M. Lalande, "Homologous association of oppositely imprinted chromosomal domains," *Science*, vol. 272, pp. 725–728, May 1996.
- [30] K. Teller, I. Solovei, K. Buiting, B. Horsthemke, and T. Cremer, "Maintenance of imprinting and nuclear architecture in cycling cells," *Proc Natl Acad Sci USA*, vol. 104, pp. 14970–5, Sep 2007.
- [31] L. Riesselmann and T. Haaf, "Preferential s-phase pairing of the imprinted region on distal mouse chromosome 7," *Cytogenet Cell Genet*, vol. 86, pp. 39–42, Jan 1999.

CHAPTER VI

GENERAL DISCUSSION AND CONCLUSIONS

INTRODUCTION

6.1-Deletions and Breakpoint Clusters Distance Measurements

While the mechanisms of radiation-induced leukemogenesis are not well understood, some features have been established using mouse models. One interesting outcome from such studies is the observation of large variation among mouse strains in genetic predisposition and sensitivity to develop acute myeloid leukemia (AML) after radiation exposure. Cytogenetic features have become an important tool that associates specific chromosomal aberrations and the development of AML. The deletion of a specific region of mouse chromosome 2 is observed in a very high proportion of all radiation-induced AML samples.

Loss of *PU.1* gene, located within a minimal deleted region (mdr), and a point mutation detected in the second allele of this gene appears as prerequisite for AML development.

It has been suggested that the deletion of the *mdr* in mouse chromosome 2 is due to the mis-repair of initial DNA damage or lesion caused after the initial exposure to a leukemogenic dose of radiation.

Most studies⁽¹⁻¹⁰⁾ reported to date are focused on cytogenetic data from total bone marrow cells without focusing on the subsets known as progenitor and hematopoietic stem cells, likely to be the actual target cell population from which AML develops. Therefore, in the present study, the analysis was also performed in isolated hematopoietic stem cells to test the initial hypothesis that proposed a close distance of the breakpoint clusters to account for a higher frequency of deletions in chromosome 2 in the regions surrounding the *PU.1* gene.

There are two important factors to be considered: one is the time when the breaks surrounding the deletions are produced and second is the physical distance where the breaks are produced.

So, the probability to produce at least two DNA-DSBs needed to form the breaks required for an exchange in a time interval short enough to allow an interaction between them increase with the dose, because more breaks are formed at a given time. Second, we have to consider the physical proximity where this two DNA-DSB are produced within the nucleus. Thus, the closer the broken-ends are of each other the greater are the chances to interact between them. Therefore, if these regions are in close proximity before the DSBs are produced, there might be a higher probability of mis-rejoining between these DSBs generated by the radiation exposure.

The spatial arrangement of genes and chromosomes within the nucleus is nonrandom but organized in a tissue-dependent manner that generates a tissue-specific pattern. The architecture and organization of the chromatin in every tissue determine what set of genes will be sharing positions or locations within the nucleus to be actively transcribed or actively silenced⁽¹¹⁾. For instance, the set of genes that are needed and actively transcribed within the corresponding spacial organization in the nucleus of an epithelial cell are different from those needed in a blood cell. Therefore, the most likely partners available for mis-rejoining after rupture of DNA would be expected to differ for different cell types.

As an example, in human chronic myeloid leukemia (CML), several authors⁽¹¹⁻¹³⁾ showed that the partners genes (ABL in human chr9 and BCR in human chr22) implicated in the development of CML were in close proximity in blood cells but not in epithelial cells. Additionally, Kozubek in 1997 showed⁽¹⁴⁾ that in lymphocytes the distances between ABL and BCR genes were in very close proximity (0.2 and 0.3 μm) in about 8% of the sample cells, suggesting that the proximity of those genes in that fraction of cell may account for the oncological transformation.

However, what distance is considered “close proximity” concerning the distances in which chromosome breaks may interact to form exchanges.

Based in some early studies⁽¹⁴⁻²³⁾, the resulting free ends formed after the production of chromosome breaks may interact if they are formed within perhaps around 0.1 to 1.0 μm of each other. This large range of interaction implies that there are some movements of the free ends to be able to interact between them. Therefore, two regions are considered

in proximity (likely to interact) if they are at a distance less than 1 μm . Larger distances are considered to be less favorable for an interaction between the formed broken ends.

Another comparative data from Kozubek showed⁽¹⁴⁾ the same percentage (~8%) of cells displayed very close proximity of c-MYC gene (human chromosome 8) and IgH gene (human chromosome 14) in B-lymphocytes. This proximity (0.2-0.3 μm) appeared to bias the production of the translocation between those chromosomes that are necessary for the induction of Burkitt's lymphoma⁽¹⁴⁾ in humans. Further suggestions implicated that the interphase distance is an important factor for the predisposition of this aberrant rearrangement that lead to the development of the disease.

By comparison, the proportion of cells examined in my research showed that 6.8% of HSCs and 5.7% of WBM from CBA/CaJ showed proximal and distal breakpoint clusters within a distance range of 0-0.4 μm from each other.

Consequently, this observation leads to the question of how many cells presenting close proximities of the breakpoints are enough to be likely to result in a radiation-induced deletion that could evolve into a cancer cell.

As perviously mentioned, a paper published by Nikiforova⁽²⁴⁾ and co-workers in 2000 was the driving force that suggested the approach taken in this dissertation concerning the possible influence of the proximity of radiation-induced breakpoints in cells on the yield of chromosomal rearrangements. They reported data about radiation-induced thyroid cancer in which there was a correlation between a close proximity in thyroid cells of the two loci whose rearrangement is essential for the development of human thyroid cancer. H4 and RET genes are in very close proximity in normal thyroid

cells showing a closer distance than expected based in a random separation of two loci tethered on a DNA molecule free to move about by Brownian motion. In a high proportion of cells (about 35% of cells) the distance was less than 0.2 μm , when the expected separation was much larger.

In mammary epithelial cells the separation was similar to expectations. The proportion of mammary epithelial cells having this close proximity of loci followed expectation. Radiation-induced tumor development in human thyroid cells(25) shows a recurrent inversion in chromosome 10 that leads to an mis-rejoining between the RET gene and H4 gene; despite the linear distance between these two genes being known to be about 30 MB apart.

Therefore, the argument presented by Nikiforova and her co-workers is that if a high proportion of cells have two breakpoint regions in close proximity there would be a higher proportion of cells that might have the required rearrangement than would be the case in other cell types where there is no close proximity in the vast majority of cells.

Based on that model, it was felt that perhaps the same mechanism could lead to the rearrangement that occurs in mouse chromosome 2, resulting in loss of the *mdr* in CBA/CaJ bone marrow cells that are susceptible to radiation-induced AML, whereas there might not be a high proportion of such cells with the close proximity in C57BL/6J mice that do not develop either spontaneous or radiation induced AML. Results of the present study; however, showed no difference between interphase distances of the proximal and distal breakpoint cluster region markers used for CBA/CaJ compared to the C57BL/6J mouse bone marrow cells; suggesting that the difference in sensitivity to develop AML is

not related to the physical distance of the breakpoint clusters. Alternatively, we investigated the possibility that the sensitivity difference could be related to other factors such as epigenetic changes in chromosome 2 or apoptotic rate and microenvironment influence as discussed below.

While the comparison of distances between the breakpoint cluster regions associated with radiation-induced deletions in chromosome 2 within interphase bone marrow, HSCs, and fibroblast cells from CBA/CaJ and C57BL/6J mouse strain did not bear out the expectation discussed above, the resulting measurements did yield the following very interesting and unexpected result. The distances between the clusters showed a clear bimodal distribution that suggested differences in chromatin organization within each homolog of a given cell. One homolog, presented a close proximity of breakpoint clusters with average values in whole bone marrow cells of 1.24 μm and in HSCs of 0.95 μm , while within the other homolog, the data has shown an average distance in whole bone marrow of 2.4 μm and HSCs of 2.11 μm , suggesting that within this homolog the possibility of interaction is less likely to occur because the distance is larger. Therefore, this result would suggest that it may be less likely for the potential DNA breaks to be able to participate in the process of mis-rejoining between the breakpoint clusters in that homolog. Although, actual direct measurement data on the homolog in which the deletion occur are not available, if we considered that the mdr deletion occurs predominantly in one homolog, this might well be happening in the homolog that presented the closer distances of the breakpoint clusters even when we were expecting an average of 0.2 μm of distance between the cluster regions.

Based on the results, we would suggest the possibility that this difference in the expected average distances of the breakpoint cluster regions could give us a closer proximity within the small domain if further experiments were carried out in which the whole length of the clusters were marked using 10 BAC-probes to cover the entire proximal breakpoint cluster (10 MB) and 3 BAC-probes for distal breakpoint cluster (3 MB). With this higher 1Mb resolution visualization of the clusters may accurately display the actual distances of the potential breakpoints.

Thus, in this way it may be possible to find a more accurate picture of the chromatin configuration in that region and perhaps the average distance between breakpoint clusters within the small domain would then reveal the closer proximity expected originally.

6.2-Chromatin Conformation

As already mentioned, chromatin conformation has an important role in the organization and location of the breakpoint clusters within each homolog in interphase cells. The observation of a differential organization in chromosome 2 domains led us to think about differences in the configuration and architecture of the chromatin in interphase. The domain of one chromosome 2 homolog is smaller or more condensed than the other showing a closer proximity of clusters, leading us to expect a bias in the probability of a radiation-induced deletion occurring in the small domain but not in the large domain due to greater likelihood of interaction between the breaks to form a

deletion. This possible association was the basis for carrying out the measurements to begin with. The analysis of AML samples showed a high proportion of cells (in average ~74% of cells in eight out of ten AML cases analyzed) in which the non-deleted domain actually displayed features of the small domain; suggesting that the large domain in those cells was deleted in contradiction to the expected deletion occurring predominantly in the small domain.

At this point, however, we still cannot discard this option entirely because we do not know whether one domain or the other was actually more frequently deleted immediately after the initial exposure to radiation. Further, the cells analyzed in ten AML samples had a considerable amount of variant cells and one dominant deleted cell sub-population that was present in high proportion. Only one cell sample, cell line 8016, showed a homogeneous population with 98% of cells showing the same deletion, with 1 out of 58 cells showing a variant cell feature.

Several studies^(3-7, 25-33) have failed to show evidence of an initial clonal expansion of the leukemia cells but instead showed an initial production of a wide variety of aberrations suggesting that some additional mutations may be required to transform the pre-leukemic cells to the fully transformed leukemogenic state where the mutated cells may acquired a proliferative advantage over the normal cell population. However, the proliferative advantage acquired by the mutant cells was not experimentally demonstrated here.

It would appear that only the concept of clonal expansion can explain the presence of certain clones with *mdr* deletion in a high proportion in cell samples from a mouse with a fully developed AML. This raises the following questions. First, if there is clonal

expansion of the pre-leukemic cell that acquired the mutation, is the mutation present in the HSCs or progenitor cells population? Second, if chromosome 2 deletion is the initial event; then; is the other allele mutation, present in a high frequency right after radiation exposure?

The LOH analysis⁽³³⁾ performed by Rigat et al 2001, in (CBA/H X C57BL/6) F1 bone marrow progenitor stem cells (short- and long-term repopulating cells) demonstrated that the frequency of LOH in chromosome 2 after 3 Gy gamma-ray total body irradiation was not different from any other region in chromosomes not involved in radiation-induced AML.

This analysis showed that the proportion of LOH within the *mdr* in chromosome 2 was not produced in a higher frequency compared with other regions in chromosomes 4, 11 and 14, which are not involved in radiation-induced AML.

The LOH analysis was done in cells obtained from short-term and long-term clonogenic assays performed both “*in vivo*” and “*in vitro*” as follows:

After whole body irradiation, bone marrow was collected and two procedures were carried out:

- 1) *In vitro*: cells were cultured in petri dishes for 8 to 11 days (colony formation)
- 2) *In vivo*: cells were transplanted into an irradiated recipient mouse for 11, 20, 30 and 120 days. Then, at each time point BM was collected, the cells were pooled, using a fraction of cells to cultured them (*in vitro*) and the other fraction was transplanted in another recipient mouse to obtain spleen colonies (*in vivo*).

The results of the analysis showed no high frequency of LOH within mdr in chromosome 2 compared with any other region mentioned above in 8, 11, 20, 30, and 120 days after transplantation⁽³³⁾.

Therefore, it is possible that the initial events occurring after irradiation may not be only the characteristic deletion of chromosome 2, but a dynamic evolution of the stem cell compartment in the bone marrow. This, along with a radiation-induced unstable genome could lead to changes that may provoke malfunction and transformation of the normal HSC to pre-leukemic and leukemic cells. Along with the chromosome 2 deletion a dynamic evolution includes changes and selection of those changes that may provide growth advantages.

Several lines of research suggested^(5,11,34-36) that irradiation treatment triggers a dynamic reorganization of the genome leading to the characteristic features found in mice that have developed AML several months after treatment.

Qualitative and quantitative observations from the analysis of interphase nuclei performed in this study displayed a unique feature within chromosome 2 domains. Both homologs presented a different organization when compared to each other in normal non-irradiated cells. Although, we do not know the significance of the this differential organization of the chromatin within each domain, certainly it can be used as reference tool (Figure 6.1) to answer questions that may arise from these experiments. For example, is this different organization of the domains a reflection of a different organization that influences the radiosensitivity of that region? Is there a preferential deletion of one of the chromosome 2 domain in radiation-induced AML?

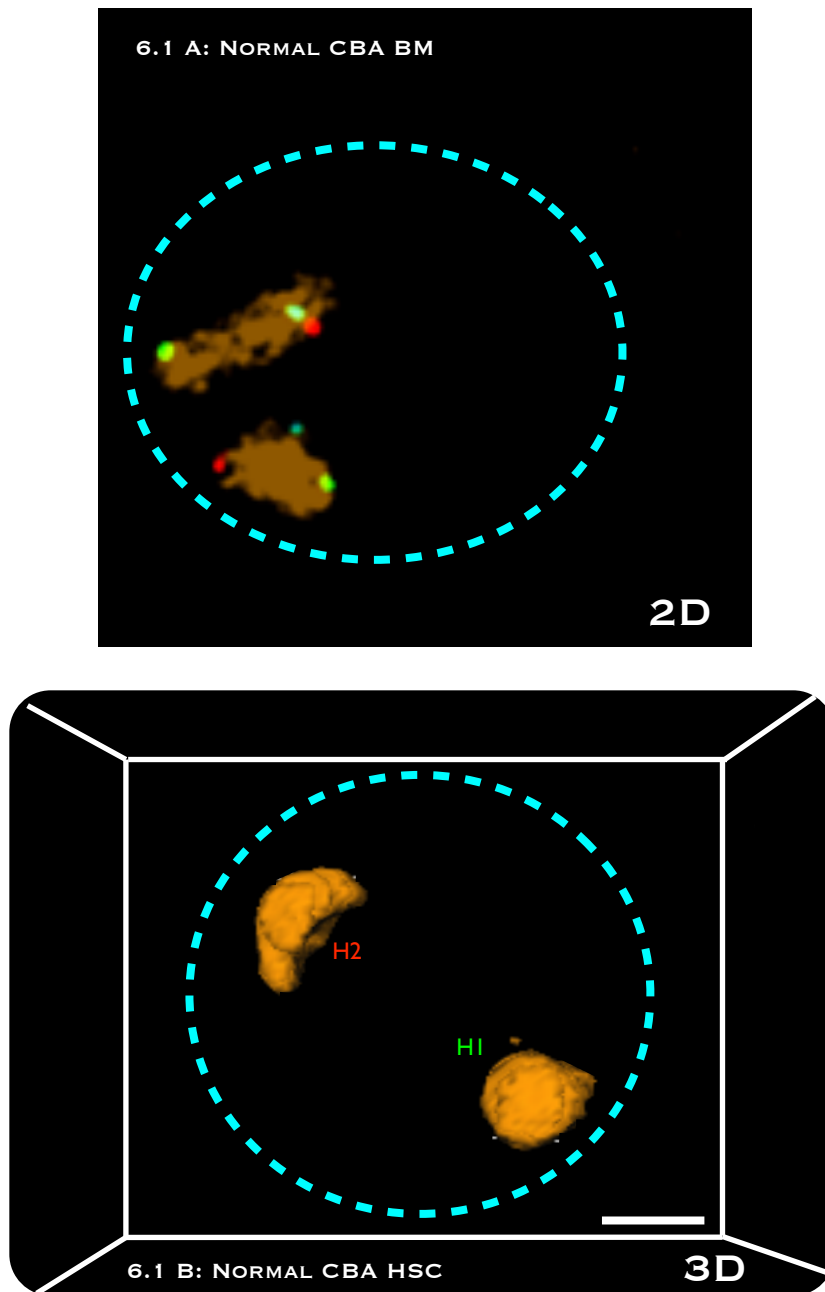


Figure 6.1: Small (H1) and large (H2) chromosome 2 domains.. A: normal bone marrow cell in 2D. B: Normal CBA HSC in 3D. The chromosomal territories are labeled with whole chromosome painting-(Alexa-647 labeled probes). *PUI* in DEAC; *dbc* in Spectrum red and *pbc* in Spectrum green.

Is the organization of each domain maintained after the radiation exposure? Is this different organization of the domains related or independent to gene expression regulation such as genomic imprinting?

Genomic imprinting is conceptually important since the organization of the chromatin is different within the two homologs that are regulated through imprinting. Thus, it was suggested that the influence of genomic imprinting may bias the occurrence of the deletion toward the non-imprinted (or active) copy⁽³⁷⁾.

LaSalle in 1997, provided some evidence of temporal and spatial association of two loci (Prader-Willi syndrome and Angelman syndrome) paternally and maternally imprinted respectively in normal human cells⁽²²⁾. The typical association between the imprinted copies was distorted due to the loss of the imprinted status of PWS or AS locus in the cells of the respective patients. They demonstrated that a reorganization of the chromatin was related to the disease.

The present study did not showed an association of the chromatin conformation of the domains, either small or large, with the parent of origin. The result of the experiments showed no influence of the genomic imprinting in the chromatin organization in the mouse model used. At this point, however, we cannot reject completely the influence of the genomic imprinting. Imprinted genes are themselves grouped themselves within the nucleus but we do not know how dominant could that feature be within the context of the overall nuclear architecture. However, the data suggest that deletion nearly always occurred in one copy of *PU.1*, leaving still the unanswered question of whether the chromatin conformation has some influence in the deletion of only one *PU.1* copy.

The analysis of AML samples performed gave some clues and opened more question about the characteristic of the radiation-induced AML, but the observations and data were obtained from animals that fully developed AML and it did not involve any proof of an event, such as *mdr* deletion, that could have occurred initially on IR exposure time.

A comparison between the chromosome 2 domains in both normal non-irradiated and radiation-induced AML samples showed a change in the organization of the chromatin that may be related to changes caused by the IR instead of changes provoked by the deletion in chromosome 2.

In addition, the wide spectrum of aberrations (specifically referred to the different combination of markers deleted) found with the markers used to label the breakpoint clusters and *PU.1* showed that deletions of different sizes are compatible with the development of AML in agreement with previous studies.

The most frequent deletion found within the samples in this study was a large deletion that involved [*pb*, *PU.1*, and *db*] in one homolog and was present in 4 out of 10 AML cases (with an average of 62.3% of cells that carry that mutation). The second most frequent deletion involved one copy of *PU.1* and *db* in 3 out of 10 AML cases (with an average of 59% of cells that carry that mutation). In agreement with others, there is no evidence that the most frequent deletion [*PU.1*, *pb*, *db*] will guarantee the outgrowth of these cells in the fully developed AML, suggesting the requirement of additional mutations for the development of AML.

The most frequent deletion found was *PU.1*-*dbc*-*pb*; however, this deletion appeared in low frequency in other sample cells that bear high frequency of other deletions such as, for example, deletions of *PU.1*-*dbc*. Therefore, the observation suggests that some additional mutations are needed, besides the deletion, to favor the outgrowth of a determined cell that carries a specific deletion that always involve *PU.1*, and that cells retaining one copy of *mdr* will potentially form AML.

The analysis of these samples was made based on the idea of determining whether the *mdr* deletion occurred within the small or large domain.

However, despite the conclusion that suggested that the deletion occurred frequently within the large domain of chromosome 2, it seems likely to be the result of a dynamic reorganization of the chromatin instead.

The unorganized architecture of the chromosomal domain and the projection of some of the markers outside the chromosomal territories showed evidence of the chromatin perturbation in irradiated cells when compared with normal unirradiated cells.

There also might be other changes, such as epigenetic changes and expression profile changes, within the cells that may occur and that could play an important role in leukemogenesis, perhaps, by accelerating the mutation rate resulting in genomic instability within the cells after exposure. Thus, the increased yield and accumulation of mutations during the latency period could lead to gaining the conditions needed to develop AML.

This is a complex process that involves more aspects and factors that go beyond the focus of this research but it is important to consider the overwhelming data to expand the

concepts and explore future directions. Epigenetic changes, apoptosis, and the microenvironment effects appear to represent important factors to be involved in chromosomal aberration formation, development and evolution of radiation-induced AML, and sensitivity to radiation-induced AML.

6.3-Epigenetic Changes Occur After Ionizing Radiation

The radiation exposure not only affects the physical structure of the DNA but also function and regulation efficiency of different genes. Epigenetic changes such as loss of methylation patterns⁽³⁸⁻⁴¹⁾, and change in gene expression profile^(31,42) are the most relevant alteration associated with cancer.

Under the notion of “multi-stage mechanism⁽⁴³⁻⁴⁵⁾ of carcinogenesis”⁽⁴⁴⁻⁴⁶⁾, radiation is known as a potent “initiator” of the carcinogenic process, however, it is not known what mechanism underlies the initiation step. Trosko^(47,48) in 1989 and 1990, referred as initiated cell to an irreversible or stable conversion of a normal stem or progenitor cell into a “pre-malignant” cell. This pre-malignant cell has the inability to differentiate but keeps its ability of division.

The interesting implication of the premalignant cell definition is that ionizing radiation may produce changes in normal stem cells at the DNA level (translocations and deletions) and may be more important at the epigenetic level producing a wide genome

demethylation leading to genomic instability setting up the pre-malignant phenotype due to inactivation, activation and/or deregulation of important genes.

In general, the trend of normal cells show an increase in the methylation status during the differentiation pathway. On the other hand, radiation-induced leukemia cells have shown an hypomethylated status compared to normal hematopoietic cells⁽³⁹⁻⁴¹⁾.

Giotopoulos and co-workers in 2006 reported differences of methylation pattern after total body irradiation of AML-sensitive CBA mouse strain and AML-resistant C57BL/6 mouse strain. Hypomethylation levels are detected in bone marrow cells from CBA mice 10 to 14 days after 3 Gy X-rays irradiation.

However, this hypomethylation was not detected in C57BL/6 mice after the same time, showing a return to control levels of wide genome methylation. Cellularity levels reached control levels after 10 to 14 days after irradiation due to the intense HSCs cycling to recover a homeostatic level of cells after the cell death produced by the radiation. This data suggest that AML-sensitive mouse strains can develop AML due to the persistence of hypomethylated pre-malignant cells. Meanwhile, AML-resistant mouse strain eliminates all hypomethylated cells after treatment, even long time after exposure (see below), however, there is no mechanism described. Comparatively, methylation profiles of radiation-induced AML samples showed the same degree of hypomethylation as the irradiated samples analyzed 14 days after irradiation treatment⁽³⁹⁾.

The analysis of the radiation-induced AML cases done in this study showed an unorganized conformation of the chromosome domains compared to normal non-irradiated samples. However, there no evidence of whether this lack of organization of

the chromatin is due to the radiation exposure or to the development of AML. Furthermore, the loss of wide genome methylation could be important as a probable cause for the loss of organization of the chromosomal domains in irradiated cells.

In addition, Trosko in 2005 suggested that an initiation inducer such as radiation could block the asymmetrical cell division of a stem cell producing and increase in stem cell population through symmetrical division, blockage of differentiation, maintaining immortality and resistance to apoptosis. This observation could be, again, a consequence of the methylation pattern erasure caused by radiation, turning off the differentiation chances of these cells.

6.4-The Role of apoptosis in Radiation-Induced AML Mouse Models: Implications in Radiation Sensitivity.

The possible explanation behind the sensitivity to develop AML observed in CBA mouse strain may be related to the efficiency in the elimination of the damaged cells.

Cell killing is one of the causes that could induce the phase of “promotion” that leads to clonal expansion of the survivor stem cells that are likely to be pre-malignant cells.

Normal bone marrow cells represent one of the most hypomethylated adult tissues and this fact is associated with the relative radiosensitivity. A comparison between different tissues and bone marrow showed as true this correlation⁽³⁷⁾. In general, radiosensitivity is related to cell death (apoptosis) as a result of the injury done into the integrity of the cells

by the radiation. Therefore, the proportion of apoptosis in response to IR is higher in hypomethylated tissues decreasing toward the more methylated (differentiated) tissues.

Several studies have demonstrated^(34,35,49-51) that for the same radiation dose CBA and C57BL/6 mouse strains showed different cell death proportions in certain cell populations.

Thus, AML-resistant mouse strain (C57BL/6), presented a greater proportion of apoptosis than the AML-sensitive mouse strain (CBA), leading to a greater cellularity reduction after irradiation.

These studies suggested that the AML-resistant mouse strain may eliminate more efficiently the damaged cells or potentially malignant cells than CBA, which result in the resistant phenotype to AML development of C57BL/6. The consequent elimination of bone marrow cells stimulate the expansion of the surviving initiated cells in CBA; while in C57BL/6 only undamaged or cells with permissible levels of damage would be expanded.

Finally, Kadhim and co-workers in 2003 reviewed the association between chromosomal instability and apoptosis in a comparison between CBA and C57BL/6 bone marrow cells. The data showed an inverse relationship between chromosomal instability and apoptosis in these strains⁽⁵²⁾. The observations obtained were that AML-resistant strain showed more apoptosis, and no genomic instability (chromosomal instability), while, AML-sensitive mouse strain showed less proportion of apoptosis and an increase in chromosomal instability following radiation exposure. In addition, the data shown provide evidence that at high doses (1-3 Gy) there is a clear inverse relationship between

apoptosis and chromosomal instability; however, the relationship is not clear at lower doses (0.1 Gy) suggesting that a more complex mechanism is activated only at higher doses (Figure 6.2). After 1Gy, they reported an increase in the proportion of cells with chromosomal aberrations and a decrease of apoptosis in CBA mice compared to control. However, the opposite is observed in C57BL/6 mice, showing a decrease of chromosomal aberration along with the increase in apoptosis proportion.

It is important to notice that the percentage of apoptotic cells in C57BL/6 at 1 day, and more interestingly, at 365 days post-irradiation was still showing a very high proportion in C57BL/6; whereas, in CBA apoptosis is almost inexistent 365 days after exposure (Table 6.1)⁽⁵²⁻⁵⁴⁾.

This fact may suggest that a lower proportion of apoptosis could enhance the chances of appearance and evolution of pre-leukemic cells in CBA; meanwhile, C57BL/6 eliminates more efficiently all potentially malignant cells, even long time after exposure.

6.5-Microenvironment, Target Cells, and Radiation Exposure

Finally, an important factor that influences the development of radiation-induced AML is thought to be the microenvironment. The stromal cells in the bone marrow (BM) are the responsible for the homeostatic regulation of the hematopoietic system. Therefore, it is logical to think that ionizing radiation will produce an alteration of the homeostatic regulation with the consequent aberrant response to the injury produced by

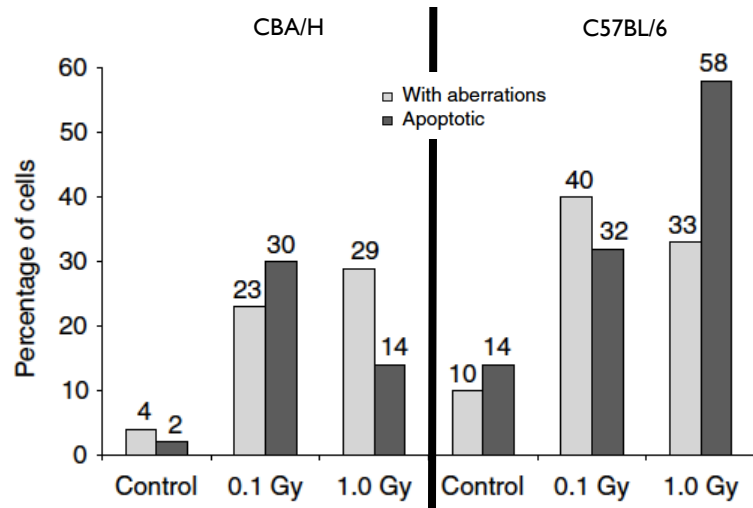


Figure 6.2: Delayed genomic instability and apoptosis determined in BM from CBA and C57BL/6. BM cells were irradiated in vitro with 0.1 and 1 Gy X-rays and chromosomal aberration (Kadhim et al 1999) and apoptosis proportion (Green et al 2001) were determined. [Kadhim 2003]

Mouse strain	γ -Ray dose (Gy)	Time post-IR (days)	% Apoptotic cells
CBA	0.1	1	8
		365	6
	3	1	19
		365	1
C57BL/6	0.1	1	14
		365	7
	3	1	70
		365	26

Table 6.1: Differences in genetic predisposition to radiation induced apoptosis. Apoptosis proportion in BM from CBA and C57BL/6 determined by Annexin V assay (Green et al 2001) 1 day and 365 days after exposure to γ -rays.

the ionizing radiation, and that could lead to a failure in the regulation of proliferation and differentiation of the HSCs as described below.

There are several observations that suggest the role and importance of the microenvironment in the progression and maintenance of AML. Lorimore in 2005 demonstrated⁽⁵⁵⁾ the influence of the microenvironment in radiation-induced genomic instability and the production of chromosomal instability in non-irradiated cells transplanted in irradiated mouse recipient. In bone marrow transplantation experiments, in vitro irradiated (with either gamma or alpha radiation) and non-irradiated BM cell from male mouse were transplanted into an irradiated female recipient. The results showed that the progeny of the irradiated BM repopulated the recipient bone marrow presenting, however, delayed cytogenetic aberrations characteristic of chromosomal instability.

Furthermore, a mixture of irradiated and non-irradiated (cells that carry a cytogenetic marker [Rt(14;15)]) showed increasingly more chromosomal aberration in the progeny of both irradiated and non-irradiated BM cells. Whereas, non-irradiated cells kept in culture (non-transplanted) showed no chromosomal aberrations in any of the time points analyzed (10, 30, 100 days post-transplantation).

The chromosomal aberrations found in the progeny of the irradiated donors can be explained as a consequence of genomic instability. However, the chromosomal aberration found in the non-irradiated donors cannot be explained through the concept of genomic instability. The observation suggested that the occurrence of chromosomal aberration could be a result of the microenvironment influence. Thus, the injury

produced into the recipient mice through IR exposure is, in some way, recorded and produced a long term response. Furthermore, other groups^(33,34,56-59) have found that the responses to IR are genotype-dependent, thus, comparing CBA and C57BL/6 mouse strains confirmed the different responses associated to each strain.

These observations showed that within the BM compartment at 6 hs and 24 hs after irradiation there is an immunological response that interacts with the BM microenvironment to produce a response to the injury produced.

Macrophages activation occurred in both mouse strains; however, this response is genotype-dependent. Thus, CBA presented a pro-inflammatory response defined as M1-like phenotype. M1-like response is characterized by the production of nitric oxide (NO) produced by the macrophages that have migrated to the BM starting a pro-inflammatory reaction within the HSCs microenvironment. This inflammatory response produces potentially damaging response.

On the other hand, C57BL/6 macrophages produce the opposite response observed in CBA, an anti-inflammatory response. This response is defined as M2-like phenotype and is characterized by the reduction of NO and the production of polyamines and proline, which act as antioxidants and stimulates tissue regeneration.

Initially, before irradiation, macrophages from both mouse strains showed M1-like phenotype; however, after irradiation, only macrophages from C57BL/6 switches to M2-like phenotype in response to IR. In addition, the gene expression profile showed ~200 genes differentially expressed⁽⁵⁴⁾.

In vitro experiments showed that there is no activation of macrophages in response to the IR, which implies that the response is a tissue response.

Further data⁽³⁴⁾, demonstrated that cytogenetic aberration was induced after exposure of clonogenic cells to conditioned media by bone marrow or bone marrow macrophages obtained from CBA, but it was not seen when exposed to conditioned media or BM macrophages from C57BL/6.

Additionally, they found that the signaling molecules implicated in CBA response were NO and TNF-alpha (major pro-inflammatory cytokine secreted by macrophages [TNF alpha can induce DNA damage, including DNA strand breaks]), which effect was reversed (less chromosomal aberration induced) by using antibodies (anti-TNF-alpha) and NO scavengers.

The modification within the microenvironment is not only made by macrophages, but the endosteal niche change and conditioned the progression and maintenance of potentially leukemic cells. Ayala in 2009, described⁽⁶⁰⁾ that there is a strong modulation of the pre-leukemic and leukemic cells by both cell-cell interaction (leukemic-stromal (fibroblast)) and through soluble factors (anti-apoptotic) that prevent apoptosis by up-regulation of Bcl-2 family proteins.

Overall, there are two main concepts leading to two major ideas; one represented for what is known as the *target cell* hypothesis where mutations in the target cell generated by ionizing radiation seems to be the main cause for radiation-induced AML.

The other idea is related to the BM microenvironment response to the radiation injury known as *untargeted cell effect* of the ionizing radiation.

These two different concepts are supported for enough evidence that can meet a common model to understand the IR effects that may cause the development of radiation-induced AML.

This dissertation was focused mainly in the target cell hypothesis and the above observations and considerations led to the main starting point for the studies described in this study.

The starting hypothesis was that the nuclear organization of chromosome 2 differs in bone marrow cells between CBA and C57BL/6 mice in such a way that the breakpoint cluster regions involved in the *PU.1* deletions are in closer proximity in the CBA bone marrow cells than in the C57BL/6 bone marrow cells.

The experimental result, while negative, led to the observation that the interphase organization of the chromosome 2 domains within the same cells was different, and have arisen the question of whether deletions of *PU.1* in radiation induced AML cells preferentially involved preferentially one or the other domain; and finally what might be the underlying cause of the different organization of the two chromosome 2 domains and even a possible dynamic reorganization of the chromatin within the radiation-induced AML cells.

All these observation can be explore in future experimental designs to deeply understand the dynamic of the chromatin after exposure to ionizing radiation, and ultimately, understand whether that dynamic is involved in radiation-induced AML.

6.6-A Model of Events Leading to Radiation-induced AML

Some important events are summarized with this hypothetical model describing what could be the pathway leading to the development of radiation-induced AML in CBA/CaJ mice.

Initially, the homeostatic state of the stem cells in the bone marrow is based on the stationary state of mostly quiescent HSCs in an adult mouse. A very small number of these cells enter to the cell cycle to maintain the proper number of cells within each compartment of the BM.

Cells have to decide whether they differentiate into multi-potential progenitor (MPP) or self-renew during the normal hematopoiesis. The homeostatic regulation involve interactions between HSCs and the stromal cells to control cell replication and differentiation and to maintain the hierarchical hematopoietic system.

After irradiation, the normal hematopoietic homeostasis is disrupted and both the HSCs cells and the microenvironment are altered. Effects of IR in the microenvironment involve aberrant responses that may affect the proper control of proliferation and differentiation of the HSCs. Secretion of cytokines and expression of membrane molecules in cells from the microenvironment is genotype-dependent and will define the destiny of the surviving HSCs.

Ionizing radiation effects within the target cells (HSCs and MPPs) will produce DNA damages leading to different types of wide genome chromosomal aberrations and

alterations in the normal epigenetic pattern, such as methylation and gene expression profile, and cell death.

The close proximity of the breakpoint clusters is an empiric requirement for the deletion of the minimal deleted region to occur. However, based in the result obtained in this research, instead of one loop formation that bring the breakpoint clusters together it may be possible a three-loop structure that bring together each breakpoint clusters closer to *PU.1*. However, to test this hypothetical configuration, it would be required a higher (1 Mb) resolution 3D FISH. Thus, the combination of rearrangement of the DNA-DSBs mis-rejoining may lead to the different phenotypes observed.

Gene expression profile is changed, since group of genes are activated after exposure to IR, some genes are differentially expressed in BM cells⁽³¹⁾ and a set of around 200 genes are differentially expressed in macrophages derived from CBA and C57BL/6⁽³⁵⁾. Additionally, epigenetic effects of irradiation implicate erasure of the regulation pattern of genes. Loss of methylation pattern leads to deregulation and/or suppression of oncogenes and tumor suppressors respectively.

Cell death has a key role in eliminating cells that carries unrepaired or misrepair damage that are lethal for the cells. An efficient elimination of potentially leukemic cells is an essential factor that is involved in the sensitivity of the different mouse strains to develop radiation-induced AML. An inefficient elimination of potentially leukemic cells allow their evolution within the mouse where this surviving cells may reorganize the chromatin to adapt to the new conditions.

The wide effect of IR is not only in the target cells but in the microenvironment that surround these cells. It is logical to think what is happening outside the target cells since the mice were exposed to a whole body irradiation.

After the exposure, an immune response to IR occurred in the bone marrow compartment with the consequent migration of immune cells (such as macrophages) will trigger a long term response. Pro-inflammatory response transform and modify the microenvironment by secreting and receiving signaling molecules, suggesting an attempt to eliminate damaged cells. However, the anti-apoptotic signals that protect HSCs appears to be favorably stronger to allow the survival of potentially leukemic stem cells (only in sensitive but not in resistant mouse strain).

The survival and evolution of the potentially leukemic stem cells is facilitated due to the interaction with the microenvironment and the inefficient elimination of the damaged cells. However, there are some cells that are heavily damaged and are eliminated through apoptosis. Considering experimental data, there is a depletion of the cell population in BM after irradiation; but the cellularity is recovered 14 days after treatment implicating an accelerated period of cycling HSCs to reconstitute hematopoiesis.

This vigorous repeated cycling cells drained out and aged HSCs with the consequent loss of its repopulating capabilities as well as enhances the replicative stress⁽⁶¹⁾ promoting aging⁽⁶²⁾ and largely increasing its mutation rates. Therefore, the latency time under this conditions allow the evolution through acquisition of the necessary additional mutations (such as the mutation in the second allele of *PU.1*) that are required for the development of radiation-induced AML.

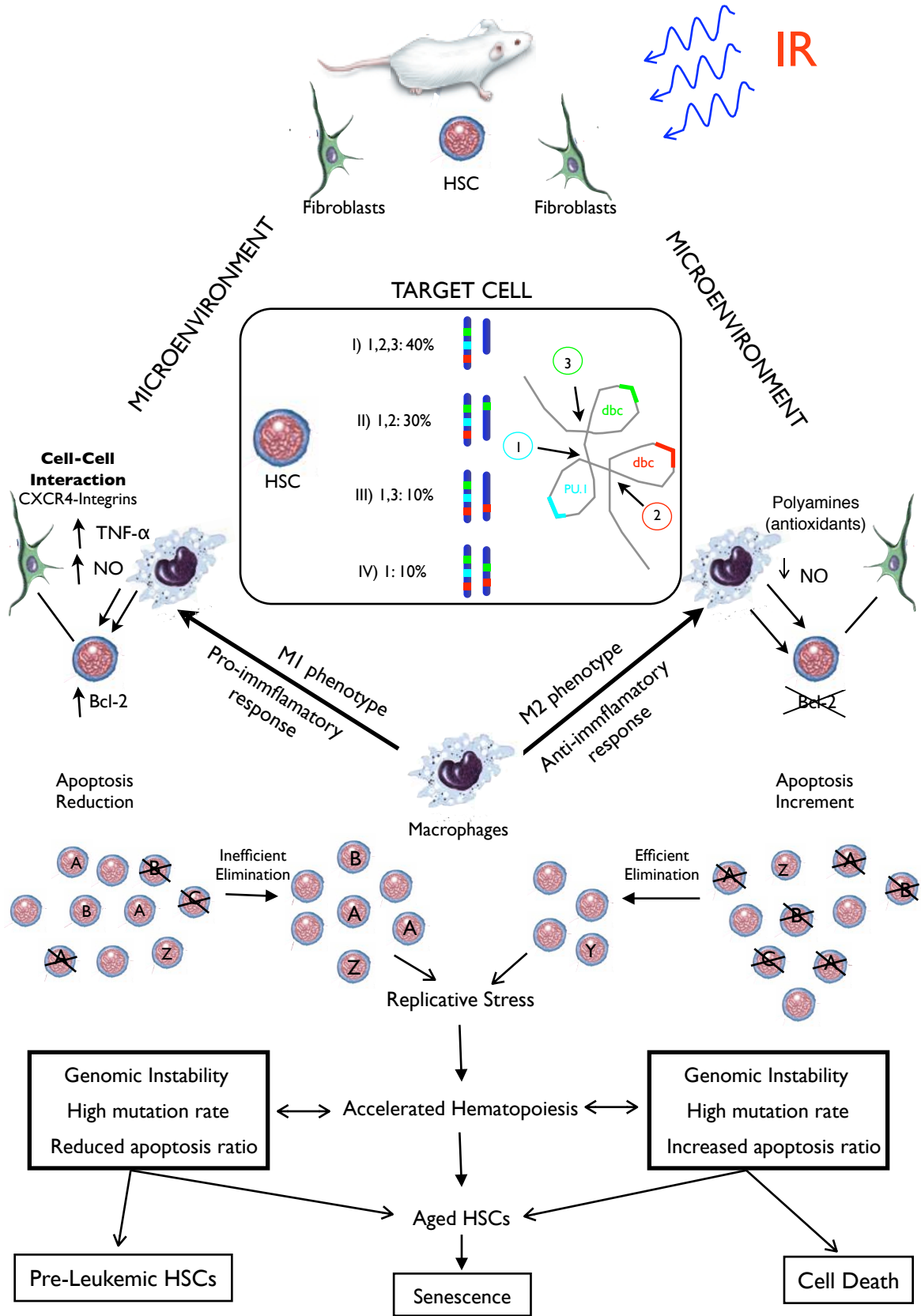


Figure 6.3: Diagram describing the model: After exposure to ionizing radiation (IR) the target cells (hematopoietic stem cells) and the microenvironment cells (fibroblasts from the endosteal compartment) are affected as well as macrophages that migrate to the bone marrow (BM) in response to the radiation. Deletions in chromosome 2 are produced in the target cells. The response of the microenvironment is strain dependent; therefore, in CBA, after macrophage migration they produce a pro-inflammatory response in the BM, while, in C57BL/6, macrophages produce an anti-inflammatory response. The response in CBA is characterized by the production of TNF α and Nitric Oxide. In addition, interaction with fibroblasts induces the production of the anti-apoptotic protein Bcl-2, leading to a reduction of the apoptotic ratio. These events are chronic throughout the leukemogenesis. On the other hand, C57BL/6 strain reduces the production of nitric oxide and increases the production of polyamines to act as antioxidant. There is no production or expression of Bcl-2 protein; therefore, the apoptotic elimination of damaged cells is more efficient than the elimination in CBA. However, in both cases the BM repopulation is obtained by exhaustive replication of the surviving HSCs, which suffer a replicative stress. As a consequence, genomic instability and an increase in the mutation rate will produce two different outcomes. In CBA, cells bearing mutations will become pre-leukemic HSCs, while cells without mutations will accelerate hematopoiesis and daughter HSCs will age and finally become senescent. C57BL/6, on the other side, produce a chronic high proportion of apoptosis to eliminate cells with mutations until the end of its life.

Some final considerations are based on the importance of the mutation rate increased under the stress caused by the radiation exposure in the target cell and the influence of the microenvironment response to IR that set up the initial conditions increasing the probability to develop leukemic cells.

Despite the fact that there is no conclusive evidence that the acquisition of the *mdr* deletion confers any proliferative advantage to the cell, the deletion of that region is increased after exposure. However, *mdr* deletion is not produced in high frequency compared to other regions not related to radiation-induced AML after exposure. Nonetheless, this is a region that may have a different and special chromatin organization in one homolog that makes it more vulnerable or sensitive to radiation, favoring the production of the deletion after radiation exposure.

6.7-General Conclusions

In summary, there is a clear difference in the chromatin organization in both chromosome 2 homolog domains in interphase cells; where the different distances of the breakpoint clusters is associated to the different organization of the homologs. In addition, the description and classification of the chromosomal territories as small and large domain is a feature that could be used for future research. The bimodal distribution of the distances showed closer distances of the breakpoint clusters within the small domain compared to the large domain suggesting the probability to be consider as the region involved in the

rearrangement that lead to the deletion. The distance between the clusters is important because the only way for an interstitial deletion can occur, it is needed to have a close proximity of the breakpoint clusters to be able to interact between them. A different conformation of the chromatin could explain the deletion in only one homolog but not in the other homolog; the utilization of the small and large domain could give some clues if the domains are analyzed short after irradiation to accurately determine whether there is any preferential deletion of small or large domain or not. It remains to be done an analysis of the nuclear matrix and the matrix attachment region that could be involved in the different conformation of the chromatin within both the small and large domain.

Despite the observation of a high proportion of cells (~74% of cells considering 8 out of 10 AML cases) that carries the small domain in radiation-induced AML samples suggesting that the deletion occurred more frequently in the large domain, this observation was made in fully developed AML samples; therefore, it is not completely related to what happened right after IR exposure but to the already evolved tumor cells.

The possibility of a dynamic reorganization of the chromatin in radiation-induced AML samples is a question that remains to be answer analyzing BM samples right after irradiation to either confirm or reject the observation that showed higher proportion of cells with the large domain deleted. The different organization did not show to be influenced by the genomic imprinting in chromosome 2; therefore, still it is not known the cause of the small and large domain organization.

The complex interaction between the bone marrow and HSCs and the response to ionizing radiation is key to identify the events leading to the development of AML.

Therefore, not only the effect of IR in the HSC (the target cell) but also in the microenvironment (non-target cells) surrounding the HSC are important to understand the factors and players involved in the onset and establishment of the conditions needed to allow the potentially leukemic cells to appear.

References

- [1] A. Upton, "Cancer research 1964: Thoughts on the contributions of radiation biology," *Cancer research*, Jan 1964.
- [2] R. Mole and D. Papworth, "The dose-response for x-ray induction of myeloid leukaemia in male cba/h mice.," *British Journal of Cancer*, vol. 47, no. 2, p. 285, 1983.
- [3] I. Hayata, "Partial deletion of chromosome 2 in radiation-induced myeloid leukemia in mice.," *Progress and Topics in Cytogenetics[PROG. TOP. CYTOGENET.]*. ..., Jan 1984.
- [4] S. D. Bouffler, E. I. Meijne, D. J. Morris, and D. Papworth, "Chromosome 2 hypersensitivity and clonal development in murine radiation acute myeloid leukaemia," *Int J Radiat Biol*, vol. 72, pp. 181–9, Aug 1997.
- [5] K. Rithidech, V. Bond, and E. Cronkite, "... chromosomal deletion in murine leukemic cells induced by radiation with different ...," *Experimental ...*, Jan 1993.
- [6] A. Silver, J. Moody, R. Dunford, D. Clark, and S. Ganz, "... localizes a putative tumor suppressor gene to a 1.0 cm region homologous to human chromosome segment ...," *Genes Chromosomes and Cancer*, Jan 1999.
- [7] R. Finnon, J. Moody, E. Meijne, J. Haines, D. Clark, A. Edwards, R. Cox, and A. Silver, "A major breakpoint cluster domain in murine radiation-induced acute myeloid leukemia," *MOLECULAR CARCINOGENESIS*, vol. 34, pp. 64–71, Jun 2002.
- [8] W. D. Cook, B. J. McCaw, C. Herring, D. L. John, S. J. Foote, S. L. Nutt, and J. M. Adams, "Pu.1 is a suppressor of myeloid leukemia, inactivated in mice by gene deletion and mutation of its dna binding domain," *Blood*, vol. 104, pp. 3437–44, Dec 2004.
- [9] Y. Peng, N. Brown, R. Finnon, C. Warner, X. Liu, P. Genik, M. Callan, F. Ray, T. Borak, and C. Badie, "Radiation leukemogenesis in mice: Loss of pu. 1 on chromosome 2 in cba and c57bl/6 mice after irradiation with 1 gev/nucleon 56fe ions, x rays or gamma-rays. part i. experimental observations," *Radiation Research*, vol. 171, no. 4, pp. 474–483, 2009.
- [10] R. Kanda, S. Tsuji, Y. Ohmachi, Y. Ishida, and N. Ban, "Rapid and reliable diagnosis of murine myeloid leukemia (ml) by fish of peripheral blood smear using ...," *Molecular Cytogenetics*, Jan 2008.

- [11] L. Parada, P. McQueen, and P. Munson, "Conservation of relative chromosome positioning in normal and cancer cells," *Current Biology*, Jan 2002.
- [12] L. Parada, S. Sotiriou, and T. Misteli, "Spatial genome organization," *Experimental Cell Research*, Jan 2004.
- [13] H. Neves, C. Ramos, M. da Silva, A. Parreira, and L. Parreira, "The nuclear topography of abl, bcr, pml, and raralpha genes: evidence for gene proximity in specific phases of the cell cycle and stages of hematopoietic differentiation," *Blood*, vol. 93, no. 4, p. 1197, 1999.
- [14] S. Kozubek, L. Ryznar, M. Kozubek, and R. G. ..., "Distribution of abl and bcr genes in cell nuclei of normal and irradiated lymphocytes," *Blood*, Jan 1997.
- [15] D. E. Lea, "Action of radiations on living cells," 2nd ed. Cambridge University Press, London, pp. 250–251, 1955.
- [16] S. Wolff, "Interpretation of induced-chromosome breakage and rejoining," *Radiation Research-Supplement 1*, pp. 453–462, 1959.
- [17] J. Roix, P. McQueen, P. Munson, L. Parada, and T. Misteli, "Spatial proximity of translocation-prone gene loci in human lymphomas," *Nature Genetics*, vol. 34, no. 3, pp. 287–291, 2003.
- [18] L. Hlatky, R. Sachs, M. Vazquez, and M. Cornforth, "Radiation-induced chromosome aberrations: insights gained from biophysical modeling," *Bioessays*, Jan 2002.
- [19] R. Sachs, A. Chen, and D. Brenner, "Review: proximity effects in the production of chromosome aberrations by ionizing radiation," *International Journal of Radiation Biology*, Jan 1997.
- [20] R. Sachs, D. Brenner, A. Chen, and P. Hahnfeldt, "Intra-arm and interarm chromosome intrachanges: tools for probing the geometry and dynamics ...," *Radiation Research*, Jan 1997.
- [21] M. Cornforth and J. Bedford, "A quantitative comparison of potentially lethal damage repair and the rejoining of interphase ...," *Radiation Research*, Jan 1987.
- [22] J. LaSalle and M. Lalande, "Homologous association of oppositely imprinted chromosomal domains," *Science*, vol. 272, no. 5262, p. 725, 1996.

- [23] A. Belmont, S. Dietzel, A. Nye, and Y. Strukov, "Large-scale chromatin structure and function," *Current Opinion in Cell Biology*, Jan 1999.
- [24] M. Nikiforova, J. Stringer, R. Blough, and M. M. ..., "Proximity of chromosomal loci that participate in radiation-induced rearrangements in human cells," *Science*, Jan 2000.
- [25] I. Hayata, "Chromosomal aberrations observed in 52 mouse myeloid leukemias," *Cancer Research*, Jan 1983.
- [26] S. D. Bouffler, E. I. Meijne, R. Huiskamp, and R. Cox, "Chromosomal abnormalities in neutron-induced acute myeloid leukemias in cba/h mice," *Radiation Research*, vol. 146, pp. 349–52, Sep 1996.
- [27] S. D. Bouffler, G. Breckon, and R. Cox, "Chromosomal mechanisms in murine radiation acute myeloid leukaemogenesis," *Carcinogenesis*, vol. 17, pp. 655–9, Apr 1996.
- [28] G. Breckon, D. Papworth, and R. Cox, "... radiation myeloid leukaemogenesis: A possible role for radiation-sensitive sites on chromosome 2," *Genes*, Jan 1991.
- [29] K. Rithidech, L. Honikel, and E. Whorton, "mfish analysis of chromosomal damage in bone marrow cells collected from cba/caj mice following ...," *Radiation and Environmental Biophysics*, Jan 2007.
- [30] D. MacDonald, E. Boulton, D. Pocock, D. Goodhead, M. Kadhim, and M. Plumb, "Evidence of genetic instability in 3 gy x-ray-induced mouse leukaemias and 3 gy x-irradiated haemopoietic stem cells," *International Journal of Radiation Biology*, vol. 77, pp. 1023–31, Oct 2001.
- [31] F. Darakhshan, C. Badie, J. Moody, M. Coster, R. Finnon, P. Finnon, A. A. Edwards, M. Szluinska, C. J. Skidmore, K. Yoshida, R. Ullrich, R. Cox, and S. D. Bouffler, "Evidence for complex multigenic inheritance of radiation aml susceptibility in mice revealed using a surrogate phenotypic assay," *Carcinogenesis*, vol. 27, pp. 311–8, Feb 2006.
- [32] E. Boulton, C. Cole, A. Knight, and H. Cleary, "Low-penetrance genetic susceptibility and resistance loci implicated in the relative risk for ...," *Blood*, Jan 2003.
- [33] B. Rigat, S. Lorimore, M. Plumb, and E. Wright, "A pcr-based clonal analysis of radiation-induced loss of heterozygosity in haemopoietic stem cells," *Leukemia*, vol. 15, no. 10, pp. 1604–1611, 2001.

- [34] S. A. Lorimore, J. A. Chrystal, J. I. Robinson, P. J. Coates, and E. G. Wright, "Chromosomal instability in unirradiated hemaopoietic cells induced by macrophages exposed in vivo to ionizing radiation," *Cancer research*, vol. 68, pp. 8122–6, Oct 2008.
- [35] P. Coates, J. Rundle, S. Lorimore, and E. Wright, "Indirect macrophage responses to ionizing radiation: implications for genotype-dependent bystander signaling," *Cancer research*, vol. 68, no. 2, p. 450, 2008.
- [36] E. Wright, "Ionizing radiation and leukaemia: more questions than answers," *Hematological Oncology-Chichester*, vol. 23, no. 3, pp. 119–126, 2005.
- [37] R. Cox, G. Breckon, A. Silver, W. Mason, and A. George, "Chromosomal changes: Radiation sensitive sites on chromosome 2 and their role in radiation myeloid leukaemogenesis in the mouse," *Radiation and Environmental Biophysics*, vol. 30, no. 3, pp. 177–179, 1991.
- [38] J. F. Costello and C. Plass, "Methylation matters," *Journal of Medical Genetics*, vol. 38, pp. 285–303, May 2001.
- [39] G. Giotopoulos, C. McCormick, C. Cole, A. Zanker, M. Jawad, R. Brown, and M. Plumb, "Dna methylation during mouse hemopoietic differentiation and radiation-induced leukemia," *Experimental Hematology*, vol. 34, no. 11, pp. 1462–1470, 2006.
- [40] J. F. Kalinich, G. N. Catravas, and S. L. Snyder, "The effect of gamma radiation on dna methylation," *Radiation Research*, vol. 117, pp. 185–97, Feb 1989.
- [41] M. Ehrlich, "Dna methylation in cancer: too much, but also too little," *Oncogene*, vol. 21, pp. 5400–13, Aug 2002.
- [42] T. Hirouchi, T. Takabatake, K. Yoshida, Y. Nitta, M. Nakamura, S. Tanaka, K. Ichinohe, Y. Oghiso, and K. Tanaka, "Upregulation of c-myc gene accompanied by pu.1 deficiency in radiation-induced acute myeloid leukemia in mice," *Experimental Hematology*, vol. 36, pp. 871–885, Jul 2008.
- [43] H. Pitot, "Factors predisposing to cancer," *Science*, vol. 17, July 1981.
- [44] J. Trosko, C. Chang, and B. Madhukar, "Modulation of intercellular communication during radiation and chemical carcinogenesis," *Radiation Research*, Jan 1990.

- [45] J. Trosko, C. Chang, B. Upham, and M. Tai, "Low-dose ionizing radiation: induction of differential intracellular signalling possibly affecting intercellular communication," *Radiation and environmental ...*, Jan 2005.
- [46] D. Hanahan and R. A. Weinberg, "The hallmarks of cancer," *Cell*, vol. 100, pp. 57–70, Jan 2000.
- [47] J. Trosko and C. Chang, "Stem cell theory of carcinogenesis," *Toxicology Letters*, Jan 1989.
- [48] J. Trosko, "The role of stem cells and cell-cell communication in radiation carcinogenesis: ignored concepts," *British Journal of Radiology*, Jan 2005.
- [49] M. Weil, C. Amos, K. Mason, and L. Stephens, "Genetic basis of strain variation in levels of radiation-induced apoptosis of thymocytes," *Radiation Research*, Jan 1996.
- [50] E. G. Wright, "Microenvironmental and genetic factors in haemopoietic radiation responses," *International Journal of Radiation Biology*, vol. 83, pp. 813–8, Jan 2007.
- [51] C. E. Mothersill, K. J. O'Malley, D. M. Murphy, C. B. Seymour, S. A. Lorimore, and E. G. Wright, "Identification and characterization of three subtypes of radiation response in normal human urothelial cultures exposed to ionizing radiation," *Carcinogenesis*, vol. 20, pp. 2273–8, Dec 1999.
- [52] M. A. Kadhim, "Role of genetic background in induced instability," *Oncogene*, vol. 22, pp. 6994–9, Oct 2003.
- [53] L. M. Green, D. K. Murray, A. M. Bant, G. Kazarians, M. F. Moyers, G. A. Nelson, and D. T. Tran, "Response of thyroid follicular cells to gamma irradiation compared to proton irradiation. i. initial characterization of dna damage, micronucleus formation, apoptosis, cell survival, and cell cycle phase redistribution," *Radiation Research*, vol. 155, pp. 32–42, Jan 2001.
- [54] M. A. Kadhim and E. G. Wright, "Radiation-induced transmissible chromosomal instability in haemopoietic stem cells," *Adv Space Res*, vol. 22, pp. 587–96, Jan 1998.
- [55] S. A. Lorimore, J. M. McIlrath, P. J. Coates, and E. G. Wright, "Chromosomal instability in unirradiated hemopoietic cells resulting from a delayed in vivo bystander effect of gamma radiation," *Cancer research*, vol. 65, pp. 5668–73, Jul 2005.
- [56] P. Coates, S. Lorimore, and E. Wright, "Damaging and protective cell signalling in the untargeted effects of ionizing radiation," *Mutation Research/Fundamental ...*, Jan 2004.

- [57] S. Lorimore, P. Coates, G. Scobie, and G. Milne, "Inflammatory-type responses after exposure to ionizing radiation in vivo: a mechanism for radiation-induced bystander effects?," *Oncogene*, Jan 2001.
- [58] E. Wright, "Ionizing radiation and secondary leukaemia: experimental approaches," *Hematology Meeting Reports (formerly Haematologica Reports)*, vol. 2, no. 15, 2009.
- [59] C. D. Mills, K. Kincaid, J. M. Alt, M. J. Heilman, and A. M. Hill, "M-1/m-2 macrophages and the th1/th2 paradigm," *J Immunol*, vol. 164, pp. 6166–73, Jun 2000.
- [60] F. Ayala, R. Dewar, M. Kieran, and R. Kalluri, "Contribution of bone microenvironment to leukemogenesis and leukemia progression," *Leukemia*, vol. 23, pp. 2233–41, Dec 2009.
- [61] N. Ban and M. Kai, "Implication of replicative stress-related stem cell ageing in radiation-induced ...," *British Journal of Cancer*, Jan 2009.
- [62] Y. Wang, B. A. Schulte, A. C. LaRue, M. Ogawa, and D. Zhou, "Total body irradiation selectively induces murine hematopoietic stem cell senescence," *Blood*, vol. 107, pp. 358–66, Jan 2006.

APPENDIX I

MEASUREMENTS OF BREAKPOINT CLUSTERS DISTANCES

NAME: David Maranon

DATE: AUG'09

QUESTIONS:

1-Are the distances between the breakpoint clusters closer in AML-sensitive mice compared to AML-resistant mice?

2-Are the distance of the breakpoint clusters similar in hematopoietic cell compare to non-hematopoietic cell type?

HYPOTHESIS:

The AML-sensitive and hematopoietic cells are expected to show closer proximity's of the clusters.

MATERIALS:

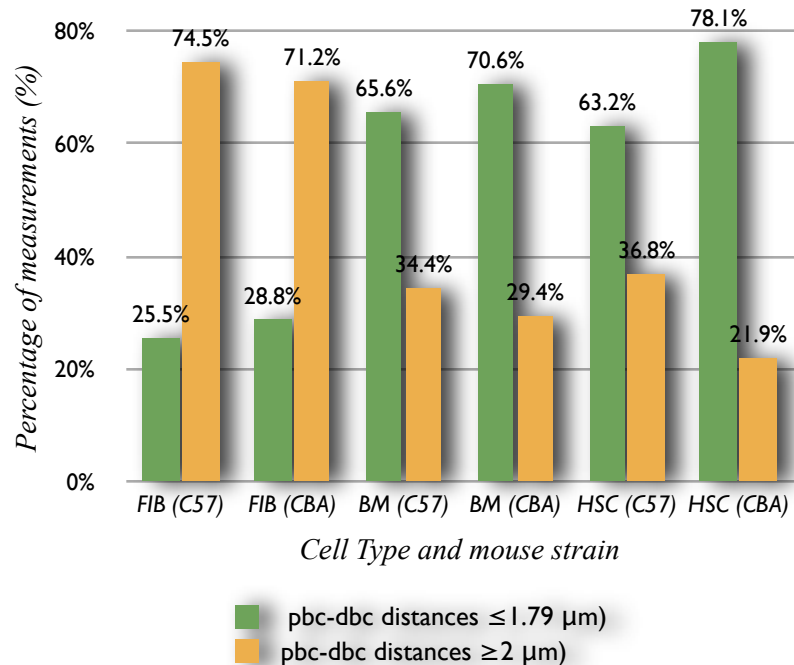
CBA/CaJ & C57BL/6 Mice: Fibroblasts, Bone Marrow, Progenitor cells

PROCEDURE:

3D-FISH with BAC-probes that shows proximal and distal breakpoint clusters; PU.1 gene and a chromosome 2 paints. The absolute physical distances was measured between the two breakpoint clusters in all cell types.

Distances	FIB C57	FIB CBA	BM C57	BM CBA	HSC C57	HSC CBA
psc-dbc distances $\leq 1.79 \mu\text{m}$	25.5%	28.8%	65.6%	70.6%	63.2%	78.1%
psc-dbc distances $\geq 2 \mu\text{m}$	74.5%	71.2%	34.4%	29.4%	36.8%	21.9%

Pbc-dbc Distances measurements $\leq 1.79 \mu\text{m}$ vs distances $\geq 2 \mu\text{m}$



Small Domain (Group H1)

CELL #	FIB (CBA)	FIB (C57)	BM (CBA)	BM (C57)	HSC (CBA)	HSC (C57)
1	0.864	0.938	0.898	1.040	1.673	0.775
2	3.039	3.551	1.206	1.613	2.849	4.059
3	1.292	0.951	0.413	0.233	0.874	1.128
4	1.395	1.177	1.208	1.742	0.798	0.440
5	1.221	1.767	1.040	1.138	0.577	1.130
6	0.702	3.060	2.224	3.807	0.862	1.082
7	2.335	1.838	0.258	0.612	1.257	1.206
8	1.304	0.891	0.896	1.428	0.987	1.345
9	1.257	2.544	0.645	0.530	0.144	0.832
10	2.899	3.891	0.617	0.530	1.092	1.991
11	3.154	1.646	0.973	1.575	1.100	1.894
12	2.260	2.345	0.530	2.049	0.065	3.695
13	1.114	1.657	0.854	2.582	0.603	1.097
14	0.200	2.536	0.400	1.519	0.459	0.669
15	3.050	5.112	0.182	0.861	0.905	0.681
16	2.115	2.576	0.996	0.945	0.802	0.949
17	1.642	2.667	1.356	1.910	0.839	0.656
18	2.095	2.464	1.618	0.841	1.542	1.221
19	2.576	2.421	3.404	2.174	0.288	0.862
20	0.416	1.168	1.648	0.802	2.168	0.144
21	4.334	0.485	2.035	0.787	0.425	0.557
22	3.570	1.270	0.938	2.026	0.678	
23	2.729	2.316	0.506	1.740		
24	1.748	1.504	1.039	2.460		
25	1.860	2.347	3.755	0.410		
26	1.760		0.498	1.154		
27	0.400			1.363		
28	1.455			1.351		
29	2.394			1.446		
30	2.426			0.233		
31				1.899		
32				0.920		
33				0.804		
34				0.465		
35				0.288		
Average	1.920	2.125	1.159	1.294	0.954	1.258

Large Domain (Group H2)

CELL #	FIB (CBA)	FIB (C57)	BM (CBA)	BM (C57)	HSC (CBA)	HSC (C57)
1	3.535	1.827	1.974	1.235	3.975	0.927
2	4.101	5.517	1.361	2.288	6.204	7.555
3	2.530	3.401	0.841	4.676	1.195	1.734
4	2.480	3.488	1.494	1.836	1.487	2.897
5	1.703	2.763	2.456	1.183	1.069	1.183
6	3.162	3.295	2.258	8.630	1.881	1.098
7	2.720	4.492	2.379	3.200	2.215	2.147
8	2.258	4.728	1.098	2.049	1.884	1.821
9	2.890	2.790	1.742	1.250	1.409	2.652
10	3.293	4.713	0.684	0.643	1.313	2.059
11	4.863	3.311	3.030	1.872	1.998	2.106
12	2.823	4.795	1.241	3.393	1.104	4.137
13	3.063	6.597	1.230	2.829	1.977	3.875
14	1.047	2.887	0.740	2.457	2.006	1.904
15	4.070	7.161	1.029	1.423	1.100	1.418
16	2.394	3.439	1.124	1.389	1.594	2.440
17	3.774	5.003	3.227	2.888	1.252	2.280
18	2.226	5.490	1.677	1.115	5.542	2.233
19	3.408	2.823	5.746	3.600	1.126	0.949
20	3.929	3.757	2.262	1.330	2.978	1.424
21	4.752	0.990	3.785	0.968	2.002	1.189
22	4.159	4.126	2.583	2.639	1.080	
23	4.338	3.994	1.415	5.035		
24	2.871	4.326	4.638	2.981		
25	2.202	5.874	9.481	2.142		
26	2.892		0.702	1.442		
27	2.318			2.049		
28	4.015			1.690		
29	3.821			1.887		
30	3.470			2.362		
31				2.063		
32				0.930		
33				1.352		
34				1.593		
35				1.442		
Average	3.17	4.06	2.32	2.28	2.11	2.287

Distances distribution in **Fibroblasts**: frequency and percentage of cells (CBA and C57)

Distances (um)	Number of Measurements [Frequency]	CBA/Cal (FIB) [H] (%)	Number of Measurements [Frequency]	C57BL/6 (FIB) [H] (%)
0 - 0.39	1	2	0	0
0.4 - 0.79	3	5	1	2
0.8 - 1.19	3	5	6	12
1.2 - 1.59	6	10	2	4
1.6 - 1.99	5	8	5	10
2.0 - 2.39	10	17	3	6
2.4 - 2.79	6	10	8	16
2.8 - 3.19	10	17	3	6
3.2 - 3.59	5	8	6	12
3.6 - 3.99	3	5	3	6
4.0 - 4.39	6	10	2	4
4.4 - 4.79	1	2	4	8
4.8 - 9.0	1	2	7	14
TOTAL	60	100	50	100

Distances distribution in **Fibroblasts**: Small (H1) and Large (H2) Domains in CBA and C57

DISTANCES (um)	CBA % (H1)	CBA % (H2)	CBA [H] %	C57 % (H1)	C57 % (H2)	C57 [H] %
AVERAGE	1.92	3.17	2.55	2.12	4.06	3.09
STANDARD DEVIATION	0.99	0.91	1.13	1.06	1.43	1.58
CELLS SCORED	30	30	30	25	25	25
0 - 0.39	3.33	0.00	1.67	0.00	0.00	0.00
0.4 - 0.79	10.00	0.00	5.00	4.00	0.00	2.00
0.8 - 1.19	6.67	3.33	5.00	20.00	4.00	12.00
1.2 - 1.59	20.00	0.00	10.00	8.00	0.00	4.00
1.6 - 1.99	13.33	3.33	8.33	16.00	4.00	10.00
2.0 - 2.39	16.67	16.67	16.67	12.00	0.00	6.00
2.4 - 2.79	10.00	10.00	10.00	24.00	8.00	16.00
2.8 - 3.19	13.33	20.00	16.67	4.00	8.00	6.00
3.2 - 3.59	3.33	13.33	8.33	4.00	20.00	12.00
3.6 - 3.99	0.00	10.00	5.00	4.00	8.00	6.00
4.0 - 4.39	3.33	16.67	10.00	0.00	8.00	4.00
4.4 - 4.79	0.00	3.33	1.67	0.00	16.00	8.00
4.8 - 9.0	0.00	3.33	1.67	4.00	24.00	14.00
TOTAL	100.00	100.00	100.00	100.00	100.00	100.00

Distances distribution in **BM**: frequency and percentage of cells (CBA and C57)

Distances (um)	Number of Measurements [Frequency]	CBA/CaJ (BM) [H] (Percent)	Number of Measurements [Frequency]	C57BL/6 (BM) [H] (Percent)
0 - 0.39	2	4	3	4
0.4 - 0.79	10	19	7	10
0.8 - 1.19	12	23	13	19
1.2 - 1.59	8	15	15	21
1.6 - 1.99	5	10	9	13
2.0 - 2.39	5	10	9	13
2.4 - 2.79	2	4	4	6
2.8 - 3.19	1	2	3	4
3.2 - 3.59	2	4	2	3
3.6 - 3.99	2	4	2	3
4.0 - 4.39	0	0	0	0
4.4 - 4.79	1	2	1	1
4.8 - 9.0	2	4	2	3
TOTAL	52	100	70	100

Distances distribution in **BM**: Small (H1) and Large (H2) Domains in CBA and C57

DISTANCES (um)	CBA (H1)	CBA (H2)	CBA [H]	C57 (H1)	C57 (H2)	C57 [H]
AVERAGE	1.16	2.32	1.74	1.29	2.28	1.79
STANDARD DEVIATION	0.88	1.92	1.59	0.78	1.49	1.28
CELL #	26	26	26	35	35	35
0 - 0.39	7.69	0.00	3.85	8.57	0.00	4.29
0.4 - 0.79	26.92	11.54	19.23	17.14	2.86	10.00
0.8 - 1.19	30.77	15.38	23.08	25.71	11.43	18.57
1.2 - 1.59	11.54	19.23	15.38	17.14	25.71	21.43
1.6 - 1.99	7.69	11.54	9.62	14.29	11.43	12.86
2.0 - 2.39	7.69	11.54	9.62	8.57	17.14	12.86
2.4 - 2.79	0.00	7.69	3.85	5.71	5.71	5.71
2.8 - 3.19	0.00	3.85	1.92	0.00	8.57	4.29
3.2 - 3.59	3.85	3.85	3.85	0.00	5.71	2.86
3.6 - 3.99	3.85	3.85	3.85	2.86	2.86	2.86
4.0 - 4.39	0.00	0.00	0.00	0.00	0.00	0.00
4.4 - 4.79	0.00	3.85	1.92	0.00	2.86	1.43
4.8 - 9.0	0.00	7.69	3.85	0.00	5.71	2.86
TOTAL	100.00	100.00	100.00	100.00	100.00	100.00

Distances distribution in HSC: frequency and percentage of cells (CBA and C57)

Distances (um)	Number of Measurements [Frequency]	CBA/CaJ (HSC) [H] (Percent)	Number of Measurements [Frequency]	C57BL/6 (HSC) [H] (Percent)
0 - 0.39	3	7	1	2
0.4 - 0.79	6	14	6	14
0.8 - 1.19	14	32	12	29
1.2 - 1.59	7	16	5	12
1.6 - 1.99	5	11	5	12
2.0 - 2.39	4	9	5	12
2.4 - 2.79	0	0	2	5
2.8 - 3.19	2	5	1	2
3.2 - 3.59	0	0	0	0
3.6 - 3.99	1	2	2	5
4.0 - 4.39	0	0	2	5
4.4 - 4.79	0	0	0	0
4.8 - 9.0	2	5	1	2
TOTAL	44	100	42	100

Distances distribution in HSC: Small (H1) and Large (H2) Domains in CBA and C57

DISTANCES (um)	CBA (H1)	CBA (H2)	CBA [H]	C57 (H1)	C57 (H2)	C57 [H]
AVERAGE	0.95	2.11	1.53	1.26	2.29	1.77
STANDARD DEVIATION	0.65	1.40	1.23	0.97	1.48	1.34
CELL #	22	22	22	21	21	21
0 - 0.39	13.64	0.00	6.82	4.76	0.00	2.38
0.4 - 0.79	27.27	0.00	13.64	28.57	0.00	14.29
0.8 - 1.19	36.36	27.27	31.82	33.33	23.81	28.57
1.2 - 1.59	9.09	22.73	15.91	14.29	9.52	11.90
1.6 - 1.99	4.55	18.18	11.36	9.52	14.29	11.90
2.0 - 2.39	4.55	13.64	9.09	0.00	23.81	11.90
2.4 - 2.79	0.00	0.00	0.00	0.00	9.52	4.76
2.8 - 3.19	4.55	4.55	4.55	0.00	4.76	2.38
3.2 - 3.59	0.00	0.00	0.00	0.00	0.00	0.00
3.6 - 3.99	0.00	4.55	2.27	4.76	4.76	4.76
4.0 - 4.39	0.00	0.00	0.00	4.76	4.76	4.76
4.4 - 4.79	0.00	0.00	0.00	0.00	0.00	0.00
4.8 - 9.0	0.00	9.09	4.55	0.00	4.76	2.38
TOTAL	100.00	100.00	100.00	100.00	100.00	100.00

Normalization Values in CBA/CaJ [Large/Small]

Cell #	CBA (FIB) Small	CBA (FIB) Large	CBA (FIB) Large Small	CBA (BM) Small	CBA (BM) Large	CBA (BM) Large Small	CBA (HSC) Small	CBA (HSC) Large	CBA (HSC) Large Small	I:I relationship	
										X	Y
1	0.864	3.535	4.09	0.898	1.974	2.20	1.673	3.975	2.38	0.00	0.00
2	3.039	4.101	1.35	1.206	1.361	1.13	2.849	6.204	2.18	1.00	1.00
3	1.292	2.530	1.96	0.413	0.841	2.04	0.874	1.195	1.37	1.50	1.50
4	1.395	2.480	1.78	1.208	1.494	1.24	0.798	1.487	1.86	2.00	2.00
5	1.221	1.703	1.39	1.040	2.456	2.36	0.577	1.069	1.85	2.50	2.50
6	0.702	3.162	4.50	2.224	2.258	1.02	0.862	1.881	2.18	3.00	3.00
7	2.335	2.720	1.16	0.258	2.379	9.22	1.257	2.215	1.76	3.50	3.50
8	1.304	2.258	1.73	0.896	1.098	1.23	0.987	1.884	1.91	4.00	4.00
9	1.257	2.890	2.30	0.645	1.742	2.70	0.144	1.409	9.77	4.50	4.50
10	2.899	3.293	1.14	0.617	0.684	1.11	1.092	1.313	1.20	5.00	5.00
11	3.154	4.863	1.54	0.973	3.030	3.11	1.100	1.998	1.82	5.50	5.50
12	2.260	2.823	1.25	0.530	1.241	2.34	0.065	1.104	17.12	6.00	6.00
13	1.114	3.063	2.75	0.854	1.230	1.44	0.603	1.977	3.28	6.50	6.50
14	0.200	1.047	5.24	0.400	0.740	1.85	0.459	2.006	4.37	7.00	7.00
15	3.050	4.070	1.33	0.182	1.029	5.64	0.905	1.100	1.21	7.50	7.50
16	2.115	2.394	1.13	0.996	1.124	1.13	0.802	1.594	1.99	8.00	8.00
17	1.642	3.774	2.30	1.356	3.227	2.38	0.839	1.252	1.49	8.50	8.50
18	2.095	2.226	1.06	1.618	1.677	1.04	1.542	5.542	3.59	9.00	9.00
19	2.576	3.408	1.32	3.404	5.746	1.69	0.288	1.126	3.91	9.50	9.50
20	0.416	3.929	9.44	1.648	2.262	1.37	2.168	2.978	1.37	10.00	10.00
21	4.334	4.752	1.10	2.035	3.785	1.86	0.425	2.002	4.71		
22	3.570	4.159	1.16	0.938	2.583	2.75	0.678	1.080	1.59		
23	2.729	4.338	1.59	0.506	1.415	2.79					
24	1.748	2.871	1.64	1.039	4.638	4.46					
25	1.860	2.202	1.18	3.755	9.481	2.52					
26	1.760	2.892	1.64	0.498	0.702	1.41					
27	0.400	2.318	5.80								
28	1.455	4.015	2.76								
29	2.394	3.821	1.60								
30	2.426	3.470	1.43								

Normalization in CBA/CaJ: RATIO (L/S) in percentage of cells

RATIO	CBA (FIB) (%)	CBA (BM) (%)	CBA (HSC) (%)
1-1.1	6.67	7.69	0.00
1.2-1.5	36.67	30.77	22.73
1.51-1.8	23.33	3.85	9.09
1.81-2.1	3.33	11.54	22.73
2.11-2.4	6.67	15.38	13.64
2.41-2.7	0.00	7.69	0.00
2.71-3.0	6.67	7.69	0.00
3.11-3.4	0.00	3.85	4.55
3.41-3.7	0.00	0.00	4.55
3.71-4.0	0.00	0.00	4.55
4.1-4.4	3.33	3.85	4.55
>4.4	13.33	7.69	13.64
TOTAL	100.00	100.00	100.00

Normalization in CBA/CaJ: RATIO (L/S): All cell types.

RATIO	CBA/CaJ Total Frequency	CBA/CaJ Total in Percent
1-1.1	4	5.13
1.2-1.5	24	30.77
1.51-1.8	10	12.82
1.81-2.1	9	11.54
2.11-2.4	9	11.54
2.41-2.7	2	2.56
2.71-3.0	4	5.13
3.11-3.4	2	2.56
3.41-3.7	1	1.28
3.71-4.0	1	1.28
4.1-4.4	3	3.85
>4.4	9	11.54
TOTAL	78	100.00

Normalization Values in C57BL/6 [Large/Small]

cell #	C57 (FIB) Small	C57 (FIB) Large	C57 (FIB) Large Small	C57 (BM) Small	C57 (BM) Large	C57 (BM) Large Small	C57 (HSC) Small	C57 (HSC) Large	C57 (HSC) Large Small	I:I Relationship	
										X	Y
1	0.938	1.827	1.95	1.040	1.235	1.19	0.775	0.927	1.20	0.00	0.00
2	3.551	5.517	1.55	1.613	2.288	1.42	4.059	7.555	1.86	1.00	1.00
3	0.951	3.401	3.57	0.233	4.676	20.10	1.128	1.734	1.54	1.50	1.50
4	1.177	3.488	2.96	1.742	1.836	1.05	0.440	2.897	6.58	2.00	2.00
5	1.767	2.763	1.56	1.138	1.183	1.04	1.130	1.183	1.05	2.50	2.50
6	3.060	3.295	1.08	3.807	8.630	2.27	1.082	1.098	1.01	3.00	3.00
7	1.838	4.492	2.44	0.612	3.200	5.23	1.206	2.147	1.78	3.50	3.50
8	0.891	4.728	5.31	1.428	2.049	1.43	1.345	1.821	1.35	4.00	4.00
9	2.544	2.790	1.10	0.530	1.250	2.36	0.832	2.652	3.19	4.50	4.50
10	3.891	4.713	1.21	0.530	0.643	1.21	1.991	2.059	1.03	5.00	5.00
11	1.646	3.311	2.01	1.575	1.872	1.19	1.894	2.106	1.11	5.50	5.50
12	2.345	4.795	2.05	2.049	3.393	1.66	3.695	4.137	1.12	6.00	6.00
13	1.657	6.597	3.98	2.582	2.829	1.10	1.097	3.875	3.53	6.50	6.50
14	2.536	2.887	1.14	1.519	2.457	1.62	0.669	1.904	2.85	7.00	7.00
15	5.112	7.161	1.40	0.861	1.423	1.65	0.681	1.418	2.08	7.50	7.50
16	2.576	3.439	1.34	0.945	1.389	1.47	0.949	2.440	2.57	8.00	8.00
17	2.667	5.003	1.88	1.910	2.888	1.51	0.656	2.280	3.48	8.50	8.50
18	2.464	5.490	2.23	0.841	1.115	1.33	1.221	2.233	1.83	9.00	9.00
19	2.421	2.823	1.17	2.174	3.600	1.66	0.862	0.949	1.10	9.50	9.50
20	1.168	3.757	3.22	0.802	1.330	1.66	0.144	1.424	9.87	10.00	10.00
21	0.485	0.990	2.04	0.787	0.968	1.23	0.557	1.189	2.13		
22	1.270	4.126	3.25	2.026	2.639	1.30					
23	2.316	3.994	1.72	1.740	5.035	2.89					
24	1.504	4.326	2.88	2.460	2.981	1.21					
25	2.347	5.874	2.50	0.410	2.142	5.22					
26				1.154	1.442	1.25					
27				1.363	2.049	1.50					
28				1.351	1.690	1.25					
29				1.446	1.887	1.30					
30				0.233	2.362	10.16					
31				1.899	2.063	1.09					
32				0.920	0.930	1.01					
33				0.804	1.352	1.68					
34				0.465	1.593	3.43					
35				0.288	1.442	5.00					

Normalization in C57BL/6: RATIO (L/S) in percentage of cells

RATIO (L/S)	C57 (Fib) (%)	C57 (BM) (%)	C57 (HSC) (%)
1-1.1	8.00	14.29	19.05
1.2-1.5	20.00	40.00	19.05
1.51-1.8	12.00	20.00	9.52
1.81-2.1	20.00	0.00	14.29
2.11-2.4	4.00	5.71	4.76
2.41-2.7	8.00	0.00	4.76
2.71-3.0	8.00	2.86	4.76
3.11-3.4	8.00	0.00	4.76
3.41-3.7	4.00	2.86	9.52
3.71-4.0	4.00	0.00	0.00
4.1-4.4	0.00	0.00	0.00
>4.4	4.00	14.29	9.52
TOTAL	100.00	100.00	100.00

Normalization in C57BL/6: RATIO (L/S): All cell types.

RATIO (L/S)	C57BL/6 Total Frequency	C57BL/6 Total in percent
1-1.1	11	13.58
1.2-1.5	23	28.40
1.51-1.8	12	14.81
1.81-2.1	8	9.88
2.11-2.4	4	4.94
2.41-2.7	3	3.70
2.71-3.0	4	4.94
3.11-3.4	3	3.70
3.41-3.7	4	4.94
3.71-4.0	1	1.23
4.1-4.4	0	0.00
>4.4	8	9.88
TOTAL	81	100.00

APPENDIX II

RADIATION-INDUCED AML (SPLEEN SAMPLES)

NAME: David Maranon

DATE: Sept'09

QUESTIONS:

Where did PU.1 deletion occurred more frequently? Was it in the small or large chromosome 2 domain? Was it random?

HYPOTHESIS:

PU.1 deletion occurs more frequently within the small chromosome 2 domain due to its compact chromatin conformation in interphase.

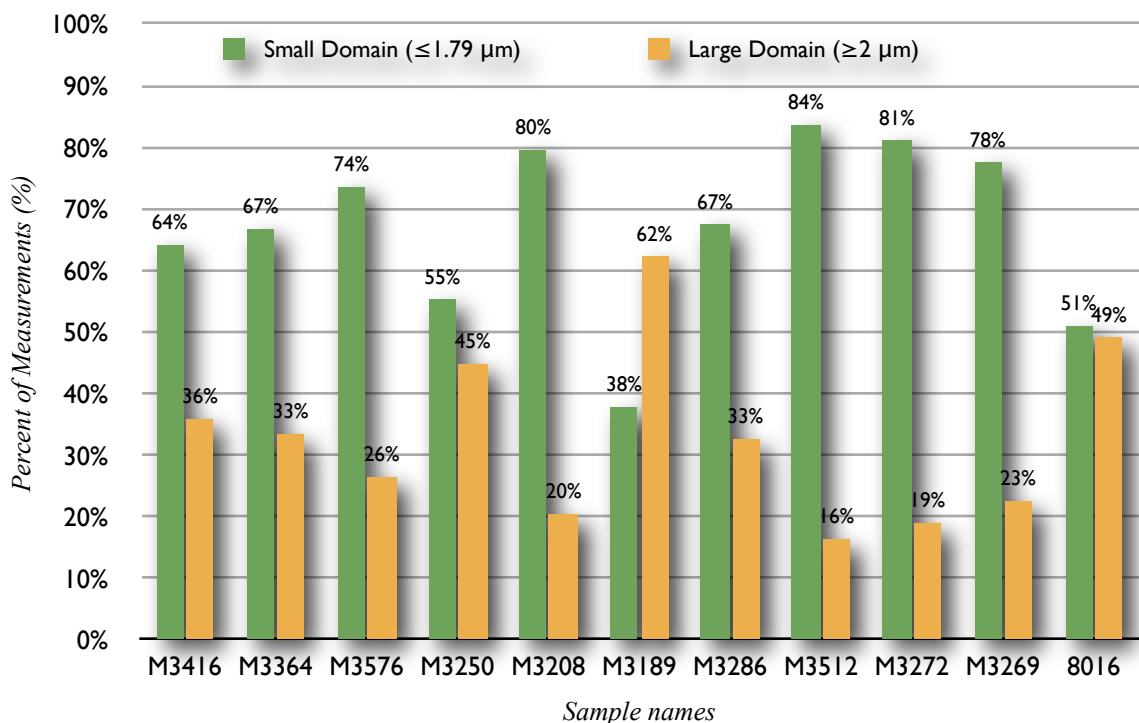
MATERIALS:

Spleen cells derived from 10 different radiation-induced AML mice and 8016 cell line.

PROCEDURE:

After γ -ray irradiation of 1, 2, and 3 Gy some mice developed AML. The mice case were selected considering high frequency of PU.1 deletion. 3D FISH was performed in the cells to measure the distances between the breakpoint clusters (pbc-dbc) to determine whether the PU.1 deletion occurred within the small or large domain.

PBC-DBC distances in cells from AML samples



AML Group: distance measurements (pbc-dbc)

Cell	M 3416	M 3364	M 3576	M 3189	M 3286	M 3512	M 3250	M 3272	M 3208	M 3269	8016 cell line
1	1.73	1.87	1.17	1.38	1.05	0.82	0.61	1.69	1.43	1.68	0.75
2	0.14	1.55	1.47	4.39	2.53	0.96	2.77	0.84	1.82	1.46	4.60
3	1.05	1.82	1.65	3.54	1.24	1.26	2.85	2.26	2.34	1.84	3.52
4	1.37	0.87	0.64	0.89	0.64	1.43	2.92	1.82	1.96	0.36	2.78
5	2.04	1.49	2.27	0.76	2.00	0.91	0.54	1.31	1.34	1.90	3.83
6	0.93	1.77	2.28	2.18	1.17	2.36	2.24	2.98	1.10	0.46	1.42
7	1.21	0.61	2.46	3.13	1.28	0.58	1.87	2.17	2.37	2.68	1.78
8	3.22	1.95	1.92	2.33	0.48	1.03	0.94	0.65	1.72	0.83	2.86
9	1.58	0.51	1.20	2.32	0.69	1.50	0.98	0.90	1.62	0.89	0.70
10	2.27	2.73	2.16	1.52	7.05	0.84	3.48	0.51	1.39	1.61	1.51
11	1.60	2.15	1.07	0.72	1.08	1.20	3.13	1.28	0.63	1.32	7.61
12	1.34	3.39	3.10	5.74	1.49	1.43	3.52	1.30	1.28	1.75	1.95
13	2.23	1.20	1.38	1.49	0.99	1.24	0.28	0.75	1.77	1.25	1.35
14	2.10	2.43	2.24	2.94	1.24	2.34	1.48	1.12	1.94	0.93	0.72
15	1.27	2.63	0.89	0.18	1.14	1.21	1.75	0.75	2.30	1.39	1.78
16	1.52	0.27	1.00	0.80	1.56	1.50	0.90	0.50	1.95	1.92	4.41
17	3.06	1.10	3.13	2.36	1.66	0.82	1.50	2.51	0.58	3.15	2.03
18	1.13	1.39	1.75	2.12	1.38	0.70	2.43	1.30	1.00	1.31	0.84
19	1.00	1.69	1.13	1.16	0.57	1.19	1.30	1.71	1.31	1.22	2.65
20	0.33	0.90	1.25	1.97	1.36	0.89	2.26	0.68	0.93	1.97	0.75
21	2.26	0.92	0.25	1.93	1.94	1.52	1.88	2.01	1.57	1.47	0.54
22	1.45	0.33	1.06	2.95	1.63	1.13	1.31	1.15	1.94	1.33	1.47
23	2.58	0.36	1.69	1.33	0.33	1.30	3.00	1.74	1.67	1.88	4.20
24	2.01	0.25	0.49	0.38	1.06	0.34	0.65	0.32	2.03	0.73	2.99
25	2.84	1.67	1.10	1.30	2.30	0.51	2.49	2.54	0.84	0.91	2.20
26	1.20	0.74	1.15	1.04	1.28	1.75	0.53	0.76	2.16	2.84	1.44
27	1.46	2.42	1.39	3.04	1.86	1.20	1.40	1.69	1.64	1.38	1.15
28	0.79	1.68	2.00	3.16	2.59	1.43	2.55	0.45	0.74	1.59	1.56
29	0.85	0.92	1.56	2.60	1.19	2.12	1.99	0.88	0.94	1.17	2.02

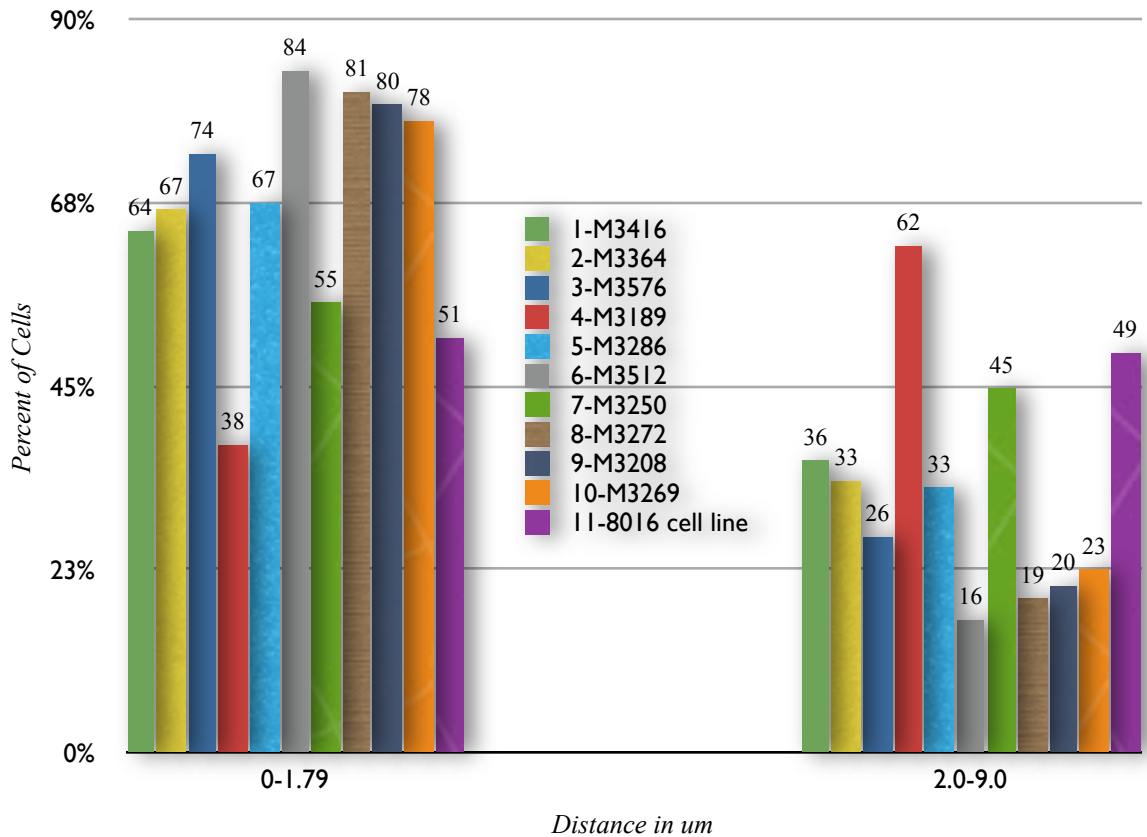
AML Group: distance measurements (pbc-dbc)

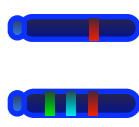
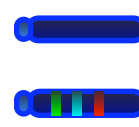
Cell	M 3416	M 3364	M 3576	M 3189	M 3286	M 3512	M 3250	M 3272	M 3208	M 3269	8016 cell line
30	3.86	1.07	1.77	1.30	1.26	1.01	1.23	0.98	1.27	2.44	2.67
31	1.86	1.94	0.78	3.25	2.36	1.57	0.45	0.82	0.78	2.47	1.74
32	0.80	0.95	1.34	1.67	1.69	0.92	3.49	1.75	1.21	0.51	1.04
33	0.18	2.44	1.16	4.63	2.36	2.99	1.51	1.89	2.14	0.67	0.79
34	3.33	0.27	1.56	2.52	0.75	2.09	2.02	2.64	0.61	2.38	4.51
35	2.30	1.15	2.32	3.93	2.53	1.25	1.33	1.62	1.05	1.12	4.34
36	2.51	2.23		2.72	0.75	1.86	3.07	0.77	1.78	1.24	1.98
37	1.05	1.73		3.19	2.01	0.94	1.89	0.85	0.98	1.13	2.43
38	1.48	2.02		1.06	0.22	2.21	0.88	1.11	1.19	1.98	1.89
39	1.46	1.26		2.24	0.46	0.65	1.29	0.43	1.79	1.54	3.55
40	0.80	1.81		1.91	2.49	0.68	1.99		1.12	2.17	3.04
41		2.65		2.89	1.68	0.75	3.54		2.81	1.94	4.26
42		2.26		4.99	1.99	1.59	1.82		1.29	1.89	0.58
43		2.42		4.19	3.13	1.60	3.84		2.89	1.33	2.94
44		2.11		2.72	2.56	1.54	0.18		1.57	3.86	1.15
45		0.39		2.92	1.85	2.84			1.25	1.24	1.42
46		1.02		2.45	2.88	1.78			0.61	0.87	1.19
47		2.52		1.37	3.27	1.83			1.56	0.93	1.62
48				1.92		0.94			2.27	2.14	0.80
49				4.09		0.88			0.74		1.42
50						0.95					2.14
51						3.21					2.20
52											2.41
53											3.27
54											1.14
55											2.60
56											0.66
57											1.33
58											2.11
59											
Average	1.78	1.68	1.49	2.80	1.90	1.55	1.90	1.29	1.45	1.68	2.11

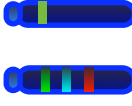
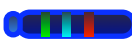
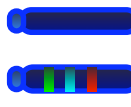
AML Group: distances from pbc to dbc distribution

Distance (um)	Global average	M 3416	M 3364	M 3576	M 3189	M 3286	M 3512	M 3250	M 3272	M 3208	M 3269	8016 cell line
0-1.79	68.75	64.10	66.67	73.53	37.78	67.44	83.67	55.26	81.08	79.54	77.50	50.91
2.0-9.0	31.25	35.90	33.33	26.47	62.23	32.56	16.33	44.73	18.92	20.45	22.50	49.09

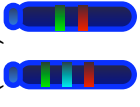
PBC-DBC distances distribution: values $\leq 1.79\mu\text{m}$ vs $\geq 2\mu\text{m}$



Case ID	Dose γ-rays	Previous notes (from Warner, C. & Peng, Y) Metaphases scoring	Feature	Variants	Results	
					Small domain	Large domain
M3416	1 Gy	lifespans= 481 days AML + Pu.1 Loss = 91% 100 Cells scored	2 Domains= 1RBG + 1(R) 29/54=53.7% 	<p>2 DOMAINS</p> <p>1 RGB + 1RB=6/54=~11%</p> <p>1 RGB + 1BG=1/54=1.85%</p> <p>1 RGB+1 (none)=1/54=1.85%</p> <p>1 cell->1 RGB+1 RGB=2/54=3.7%</p> <p>1 (1R2B2G)+ 1 2R=1/54=1.85%</p> <p>1 (2R GB)+1 (none)=1/54=1.85%</p> <p>3 DOMAINS</p> <p>1 RGB + 1 B + 1G=1/54=1.85%</p>	64.1%	35.90%
M3364	2 Gy	lifespans= 553 days AML + Pu.1 Loss = 94% 100 Cells scored	2 DOMAINS = 1RBG+1(none) 40/63= ~63.5% 	<p>2 DOMAINS</p> <p>4 cells->1 RGB+1 RGB=8/63=13%</p> <p>1 RGB + 1B=1/63=1.6%</p> <p>1 RGB + 1 (2B1G)=1/63=1.6%</p> <p>3 DOMAINS</p> <p>1 RGB + 2 (none)=1/63=1.6%</p> <p>1 RGB + 1 RB + 1 G=1/63=1.6%</p> <p>1 DOMAIN</p> <p>2 cells->1 RGB=2/63=3.2%</p> <p>1 (1R1G2B)=1/63=1.6%</p>	66.67%	33.37%

Case ID	Dose γ-rays	Previous notes (from Warner, C. & Peng, Y) Metaphases scoring	Feature	Variants	Results	
					Small domain	Large domain
M3576	2 Gy	lifespan= 547 days AML + Pu.1 Loss = 97% 100 Cells scored	<p>Ploidy variants 1 cell n=4 Pu.1=4</p> <p>2 DOMAINS 1RBG+1(G) 16/59= 27%</p> 	<p>3 DOMAINS 4 cells: 1 RGB+1(1R2G1)+1(G)=4/59=6.8% 1 RGB+1(RG)+1(2G)=1/59=1.7% 1 RGB + 1(RGB)+1(G)=1/59=1.7% 1 RGB + 1(GB)+1(2G1R)=1/59=1.7%</p> <p>4 DOMAINS 2 cells-> 2 RGB+2 (G)=4/59=6.8% 2 RGB+1(GB)+1(G)=2/59=3.4% 1 RGB+1(GR)+2(G)=1/59=1.7%</p> <p>2 DOMAINS 3 cells-> 1 RGB+1(GB)=3/59=5.1% 2 cells-> 1 RGB+1(GR)=2/59=3.4% 2 cells-> 2 RGB=4/59=6.8% 1 RGB+1(none)=1/59=1.7% 1 RGB+1(R)=1/59=1.7% 1 RGB^B+1(RGB^G)=2/59=3.4% 1 RGB^G+1(RGB^G)=2/59=3.4% 1 (1R1G2B)+1(G)=1/59=1.7% 1 (2R3G2B)+1(G)=1/59=1.7% 1 (R)+1(GB)=1/59=1.7%</p> <p>73.53%</p>	<p>26.47%</p>	
M3250	2 Gy	lifespan= 693 days AML + Pu.1 Loss = 97% 100 Cells scored	<p>1 DOMAIN=1RBG 23/44=~52%</p> 	<p>2 DOMAINS 2 cells-> 1(RGB)+1(G)=2/44 = 4.5% 1 cells-> 1(RGB)+1(RG)=1/44=2.27%</p> <p>2 DOMAINS=1RBG+1(none) 18/44= ~41%</p> 	<p>55.26%</p>	<p>44.74%</p>

Case ID	Dose γ-rays	Previous notes (from Warner, C. & Peng, Y) Metaphases scoring		Feature	Variants	Results	
		lifespans AML + Pu.1 Loss = % 100 Cells scored	Ploidy variants 1 cell n=4 Pu.1=2			Small domain	Large domain
M3208	2 Gy	lifespans= 454 days AML + Pu.1 Loss = 92% 100 Cells scored	Ploidy variants 1 cell n=4 Pu.1=2	2 DOMAINS = 1RBG+1(none) 34/51 = 66.7% 1 DOMAIN = 1RBG 13/51 = 25.5% 	2 DOMAINS 2 cells-> 1 RGB+1(B) = 2/51=3.9% 3 DOMAINS 1 RGB + 2 (none)=1/51=1.97% 1 RGB + 1 (R) + 1(none)=1/63=1.97%	79.54%	20.46%
M3189	3 Gy	lifespans= 707 days AML + Pu.1 Loss = 99% 100 Cells scored	Ploidy variants 1 cell n=4 Pu.1=2	2 DOMAINS = 1RBG + 1(G) 40/49 = 82% 	2 DOMAINS 3 cells-> 1RGB + 1(GB)=3/49=6.1% 3 cells-> 1RGB^G + 1(G)=3/49=6.1% 2 cells-> 1RGB + 1(2G)=2/49=4.1% 3 DOMAINS 1 RGB^R+1(B)+1(none)=1/49=2.05%	37.78%	62.23%
M3286	3 Gy	lifespans= 464 days AML + Pu.1 Loss = 98% 100 Cells scored	Ploidy variants 2 cell n=4 Pu.1=4	2 DOMAINS 1RBG + 1 (none) 28/47 = ~60% 	1 DOMAIN 13 cells-> 1(RGB)=13/47=28% 2 DOMAINS 2 cells-> 1(RGB^R+1(none)=2/47=4.25% 2 cells-> 1(RGB^B) +1(none)=2/47=4.25% 1 (RGB) + 1(B)=1/47=2.13% 3 DOMAINS 1(RGB)+2(none)=1/47=2.13%	67.44%	32.56%

Case ID	Dose γ-rays	Previous notes (from Warner, C. & Peng, Y) Metaphases scoring	Feature	Variants	Results	
					Small domain	Large domain
M3512	3 Gy	lifespans= 288 days AML + Pu.1 Loss = 97% 100 Cells scored	1RBG + 1 (RG)=50/59=~85% 2 DOMAINS 	1 DOMAIN 5 cells-> 1(RGB)= 5/59=~8.5% 2 DOMAINS 2 cells-> 1(RGB)+1(G)=2/59 = 3.4% 1 cell-> 1(RGB)+1(2R1G)=1/59=1.7% 1(RGB) + 1(none)=1/59 =1.7%	83.67%	16.36%
M3272	3 Gy	lifespans= 546 days AML + Pu.1 Loss = 93% 100 Cells scored	1RBG+1(none)=23/39= ~59% 2 DOMAINS 1 DOMAIN 1RBG=13/39=~33%	2 DOMAINS 1(RGB*B)+1(none)=1/39= 2.56% 1(RGB)+1(G)=1/39 = 2.56% 1RGB + 1(GB)=1/39= 2.56%	81.08%	18.92%
M3269	3 Gy	lifespans= 290 days AML + Pu.1 Loss = 89.1% 55 Cells scored	2 DOMAINS = 1RBG + 1(G) 34/50=~68% 	2 DOMAINS 8 cells-> 1(RGB)+1(BG)=8/50 = 16% 1 cells-> 1(RGB)+1(RG)=1/50=2% 1 cells-> 1(RGB)+1(2G)=1/50=2% 1 cells-> 1(RGB)+1(none)=1/50=2% 3 DOMAINS 3 cells-> 1(RGB)+1(B)+1(G)=3/50=6% 2 cells-> 1(RGB) + 1(G) + 1(none)=2/50=4%	77.5%	22.5%
8016 cell line	Immortalized (cell line) AML+ PU.1 loss = ~99% 58 cells scored		2 DOMAINS = 1RBG+1(RG) 57/58= ~98% 	3 DOMAINS 1(RGB) + 1(B) + 1(none)=1/58=~2%	50.91%	49.09%

APPENDIX III

GENOMIC IMPRINTING (TIRANO PROJECT)

NAME: David Maranon

DATE: Oct'09

QUESTION:

Is there any parental influence in the determination of “small” and “large” domain within BM interphase cells?

HYPOTHESIS:

Both “small” and “large” domains are determined by the parent of origin due to genomic imprinting.

MATERIALS AND METHODS:

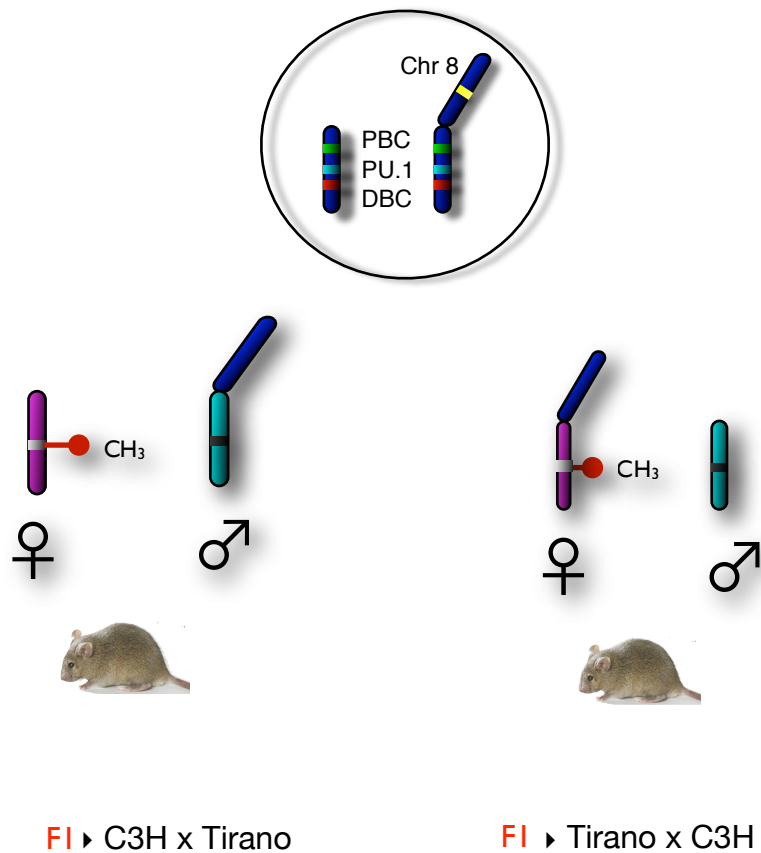
BM from F1: tirano x C3H
BM from F1: C3H x tirano

PROCEDURE:

F1 generation from crosses of C3H females with Tirano males and Tirano females with C3H males.

Bone marrow cells were obtained from the offspring (F1) from each cross.

Physical distances measurements between proximal and distal breakpoint clusters were measured within the C3H chromosomal domain from the different offspring.



pbc-dbc measurements in C3H chromosome 2

Cell Number	Tirano x C3H		C3H x Tirano
	C3H _(Pat)		C3H _(Mat)
1	1.88		0.90
2	0.73		1.09
3	1.29		1.16
4	1.2		1.25
5	0.60		1.28
6	0.51		0.51
7	2.3		0.61
8	1.27		0.48
9	0.73		1.40
10	0.95		1.30
11	0.33		0.61
12	0.75		1.98
13	1.26		1.74
14	1.41		0.72
15	1		1.77
16	1.17		0.64
17	0.20		0.62
18	1.11		1.46
19	1.82		0.62
20	1.75		0.85
21	2.54		0.41
22	1.37		1.50
23	2.28		1.7
24	1.57		1.18
25	0.98		1.92
26	1.2		2.06
27	0.91		1.39
28	1.3		2.48
29	1.44		2.18
30	0.40		1.29
31	0.50		1.38
32			1.37
33			1.65
AVERAGE	1.19		1.26
SD	0.58		0.54

Distances distribution

DISTANCES (um)	TIRANO X C3H		C3H X TIRANO	
	C3H(PAT)		C3H(MAT)	
AVERAGE	1.19		1.26	
STANDARD DEVIATION	0.58		0.54	
CELL #	31 Percentage (%)		33 Percentage (%)	
0 - 0.39	2	6.45	0	0
0.4 - 0.79	7	22.58	9	27.27
0.8 - 1.19	6	19.35	5	15.15
1.2 - 1.59	10	32.26	10	30.30
1.6 - 1.99	3	9.68	6	18.18
2.0 - 2.39	2	6	2	6.06
2.4 - 2.79	1	3	1	3.03
2.8 - 3.19	0	0	0	0
3.2 - 3.59	0	0	0	0
3.6 - 3.99	0	0	0	0
4.0 - 4.39	0	0	0	0
4.4 - 4.79	0	0	0	0
4.8 - 9.0	0	0	0	0
TOTAL	31	100.00	33	100.00

pbC-dbc Distances in C3H Chromosomes

